Finite Subdivision Rules from Matings of Quadratic Functions: Existence and Constructions

Mary E. Wilkerson

Dissertation submitted to the Faculty of the
Virginia Polytechnic Institute and State University
in partial fulfillment of the requirements for the degree of

Doctor of Philosophy
in
Mathematics

William J. Floyd, Chair
Peter E. Haskell
Leslie D. Kay
John F. Rossi

April 24, 2012
Blacksburg, Virginia

Keywords: Finite Subdivision Rules, Matings, Hubbard Trees, Combinatorial Dynamics

Finite Subdivision Rules from Matings of Quadratic Functions

Mary E. Wilkerson

(ABSTRACT)

Combinatorial methods are utilized to examine preimage iterations of topologically glued polynomials. In particular, this paper addresses using finite subdivision rules and Hubbard trees as tools to model the dynamic behavior of mated quadratic functions. Several methods of construction of invariant structures on modified degenerate matings are detailed, and examples of parameter-based families of matings for which these methods succeed (and fail) are given.

Acknowledgments

There are several wonderful, caring, and helpful people who deserve the greatest of my appreciation for helping me through this document and for my last several years at Virginia Tech:

- My family and friends, I owe you thanks for your love and support.
- Robert and the Tolls of Madness, thank you for keeping me sane by providing an outlet to help me get away from grad school every now and then.
- All of my previous mentors and professors in the VT Math Department, I can't express how far I feel that I've come thanks to the opportunities you've given me to learn and grow. Thank you all for giving me a chance and guiding me to where I am today.
- Rod, thank you for being generally awesome and more than I ever could have asked for.
- My committee, thank you for your time, effort, and care in reviewing this dissertation.
- Last but certainly not least, I owe my deepest gratitude to Dr. William Floyd for providing me with the first real challenges I ever encountered in mathematics, and for pushing me to keep going even when I was not sure that I could. I cannot thank you enough for your wisdom, understanding, unfathomable patience, and constant guidance over the last several years.

I owe this document to all of you.

Contents

List of Figures

Chapter 1

Preliminaries

1.1 Introduction

At the heart of complex dynamics is the desire to understand iterations of complex functions. Students of complex analysis typically obtain an introduction to this topic when learning to visualize how different functions map $\mathbb{C}$ to itself. Their textbooks usually illustrate a few basic examples of functions by tiling $\mathbb{C}$ and using this tiling to display which regions of the space map where. (Alternatively, for preimages, they may display which regions map to the original tiles.) Thus, at a rudimentary level, tilings of $\mathbb{C}$ are useful for visualizing basic dynamics on $\mathbb{C}$.

To gain new insights on the structures of complex maps, however, we may opt to choose more specialized tilings. If we are fortunate enough to know of invariant structures preserved by a complex map, it may be possible to build a finite tiling utilizing said structures. Then, if we investigate what happens to preimages of our map, the tiling will subdivide. Such a tiling and subdivision paired with the map between them forms a *finite subdivision rule* which records combinatorial information on the dynamics of the map [4].

Finite subdivision rules are a powerful tool in studying the complex dynamics of rational maps. Primarily, they serve to emphasize the basic structures of a map—such as critical points, invariant sets, and clarifying where regions on a space will map (as previously mentioned). However, it is also possible to start with finite subdivision rules and recover information on expansion properties of maps, in some cases even working backwards to obtain analytic maps with the same underlying structure. Finite subdivision rules may thus be utilized in complex dynamics to "discretize" analytic information, in a process which is sometimes reversible. Through using these combinatorial methods to study the dynamics of maps that yield proper subdivisions, we may gain valuable information on when analytic information can be retrieved from discrete information regarding a map, as well as further insight into how finite subdivision rules work.

The area of focus of this paper specifically is the relationship between finite subdivision rules and topological gluings of polynomials called *matings*. A primary objective in this work has been to identify and catalogue tilings for finite subdivision rules that arise from matings.

Through striving for this goal we have been able to examine the combinatorial dynamics on related families of maps, and subsequently determine factors which will guarantee whether or not a finite subdivision rule can be found for a mating of two polynomials.

In the remainder of Chapter 1, I summarize prerequisite material for examining finite subdivision rules that come from mated quadratic functions. This includes background on invariant structures of polynomials, and parameter notation that will be used to obtain matings and finite subdivision rules. The link between finite subdivision rules and matings of polynomials—as suggested by several results on rational maps—will also be discussed as an argument for the subsequent investigations in this paper.

In Chapter 2, I discuss several potential tiling constructions for finite subdivision rules that utilize pre-existing invariant structures on a suggested map. I detail the rules for construction, illustrate how they may be applied with a few examples, and prove when each of these methods will yield a tiling that can admit a finite subdivision rule. This includes a discussion on what constitutes a successful and a "failed" tiling, and parameter-based suggestions for when such cases will occur.

In Chapter 3, I place an example which has been well-discussed in the relevant literature into context with the methods and insights from Chapter 2. I also make note of a few intriguing parameter-based families of examples which arose during the cataloguing process, and prove that under certain conditions we can obtain finite subdivision rules from matings in these families. Finally, I detail the remaining notable connections between these findings and the current literature, as well as topics for future study.

We start with a discussion of invariant structures on polynomial maps.

1.2 Invariant Structures

We have informally suggested that finite subdivision rules requires a tiling, a subdivision of that tiling, and a map between the two which describes how the tiles subdivide. Thus, should we wish to develop a subdivision rule that utilizes a specific map, we should have an idea of what invariant structures on the map look like in order to devise a useful tiling. This need for investigation of invariant structures essentially demands understanding of *Julia sets*; the methods utilized later on in this paper call for the definition of structures called *Hubbard trees*.

1.2.1 Julia Sets

We utilize the definitions given in [17] to determine a Julia set:

Definition 1.1. *A collection of holomorphic maps on $\widehat{\mathbb{C}}$ is* **normal** *if every infinite sequence of maps from the collection contains a subsequence which converges locally uniformly (i.e. converges uniformly on compact subsets) to a limit.*

Definition 1.2. *Let $f : \widehat{\mathbb{C}} \to \widehat{\mathbb{C}}$ be a non-constant holomorphic mapping, and let $f^{\circ n} : \widehat{\mathbb{C}} \to \widehat{\mathbb{C}}$ be its n-fold iterate. The* **Fatou set of f, $F(f)$,** *consists of all points $z_0 \in \widehat{\mathbb{C}}$ that have an*

open neighborhood U such that $\{f^{\circ n}|_U : n \in \mathbb{N}\}$ forms a normal family on U. The complement of the Fatou set is the **Julia set of f, $J(f)$.**

In essence, the definitions yield that the Fatou set for a map f is where points iterate "nicely" and in a predicable manner, whereas the points in the Julia set for f behave more "erratically" under iteration. By definition, the Fatou set is open (for any U as found in the definition, it should be noted that $U \subseteq F(f)$), thus the Julia set is closed. In fact, the Julia set is also known to be the closure of the set of repelling periodic points. Both $F(f)$ and $J(f)$ are completely invariant under f—meaning each of these sets are fixed by f and f^{-1}.

As an alternate way to develop the Julia set in the case of polynomials we may consider the following:

Definition 1.3. *For a polynomial f, the* **filled Julia set** $K(f)$ *is given by the complement of the basin of ∞—i.e., the set of points whose forward orbit under f is bounded.*

The Julia set in the case of polynomials can also be defined as the boundary of the filled Julia set. We also have that the filled Julia set is completely invariant under f.

Example 1.4. Consider $f(z) = z^2$. On iteration, $\{|z| < 1\}$ converges locally uniformly to 0, while $\{|z| > 1\}$ converges locally uniformly to ∞. Thus, $lim_{n\to\infty} f^{\circ n}(z)$ is not a continuous function on the boundary $\{|z| = 1\}$. Since $\{f^{\circ n}\}$ are continuous functions, we cannot expect local uniform convergence to a discontinuous function—which is a concern on neighborhoods of points on the unit circle. This implies that the Julia set of f is given by $J(f) = \{z : |z| = 1\}$ and the Fatou set is given by its complement $F(f) = \{z : z \notin J(f)\}$.

Alternatively, we can note that $K(f)$ is the closed unit disk, as the collection of points $\{|z| > 1\}$ forms the basin of infinity. Since f is a polynomial, $J(f) = \partial K(f)$, so we must have that $J(f) = \{|z| = 1\}$. □

While the map in the above example yields a relatively simple geometrical figure for its Julia set, this simplicity is fairly atypical and fractal Julia sets occur much more frequently. A commonly studied grouping of Julia sets which includes the above and several other more intricate examples stems from the **Mandelbrot set**:

Definition 1.5. *Let $c \in \mathbb{C}$ and $f_c(z) = z^2 + c$. The* **Mandelbrot set**, *M, is the set of all values of c such that the forward orbit of 0 under f_c is bounded. Equivalently, the Mandelbrot set is also the set of all values of c for which the Julia set of f_c is connected. (See* [8]*.)*

Neat properties occur for values of c which allow the critical point 0 to have a periodic or pre-periodic orbit under iterations of f_c:

1. Values of c which yield a strictly preperiodic orbit for 0 under f_c are called **Misiurewicz points**. (By "strictly preperiodic" we emphasize that the forward orbit *becomes* periodic after a finite number of iterations, but never returns to the initial point.) We will refer to such f_c as **preperiodic** functions.

2. Misiurewicz points are dense in the boundary of the Mandelbrot set.

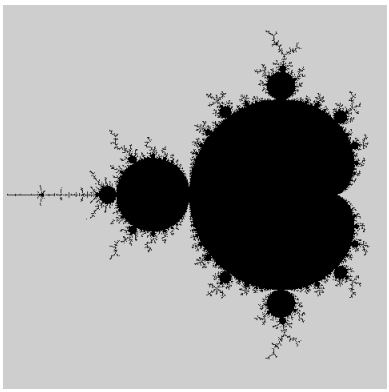

Figure 1.1: The Mandelbrot set, M. (The base graphics for this figure and many others in this paper were generated with Mandel 5.4; see [11].)

3. If c is a Misiurewicz point, f_c has a Julia set which is a **dendrite** that is simply and locally connected. (A dendrite is a locally connected nonempty compact connected metric space that contains no simple closed curves. This implies that the space has no interior and admits a possibly infinite tree-like structure.) (See [19].)

4. If the forward orbit of 0 is periodic under f_c, it returns to 0 after a finite number of iterations. We will refer to such f_c as **periodic** functions. The filled Julia sets of such f_c are also simply and locally connected, but have non-empty interior.

Since quadratic functions stemming from Misiurewicz points will be crucial to the main points in this paper, it is important that we develop a parameter system for describing them. The typical parameter convention as used above—that the "c" in f_c is given by the complex coordinate used in $f(z) = z^2 + c$—is actually not one that we will continue to use through much of this paper. We will develop the new convention in the following section on external rays.

1.2.2 External rays and parameter notation

Definition 1.6. *Let $c \in M$ and $K(f_c)$ be the filled-in Julia set of the map $f_c(z) = z^2+c$. Since $K(f_c)$ is connected, $\mathbb{C}\backslash K(f_c)$ is conformally isomorphic to the complement of the closed unit disk via some holomorphic map $\phi : \mathbb{C}\backslash K(f_c) \to \mathbb{C}\backslash\overline{\mathbb{D}}$. This map can be chosen to conjugate $z \mapsto z^2$ on $\mathbb{C}\backslash\overline{\mathbb{D}}$ to f_c on $\mathbb{C}\backslash K(f)$. (That is, $\phi(z^2) = f_c(\phi(z))$.)*

Taking the preimage of rays of the form $\{re^{2\pi it} : 1 < r < \infty\}$ under ϕ for fixed $t \in \mathbb{R}/\mathbb{Z}$ yields the **external ray of angle** *t, $R_c(t)$, on the filled Julia set $K(f_c)$. (See Figure 1.2.)*

If $K(f_c)$ is locally connected, an external ray "lands" on the Julia set at a unique point—that is, the map $\gamma_c : \mathbb{R}/\mathbb{Z} \to \mathbb{C}$ given by $\gamma_c(t) = \lim_{r\to 1^+} \phi^{-1}(re^{2\pi it})$ is well-defined. In this case, $\gamma_c(t)$ is the **landing point** *of the external ray of angle t.*[16]

Since periodic and preperiodic functions have filled Julia sets that are locally connected, external rays land on the Julia sets of these functions. An important point to note is that

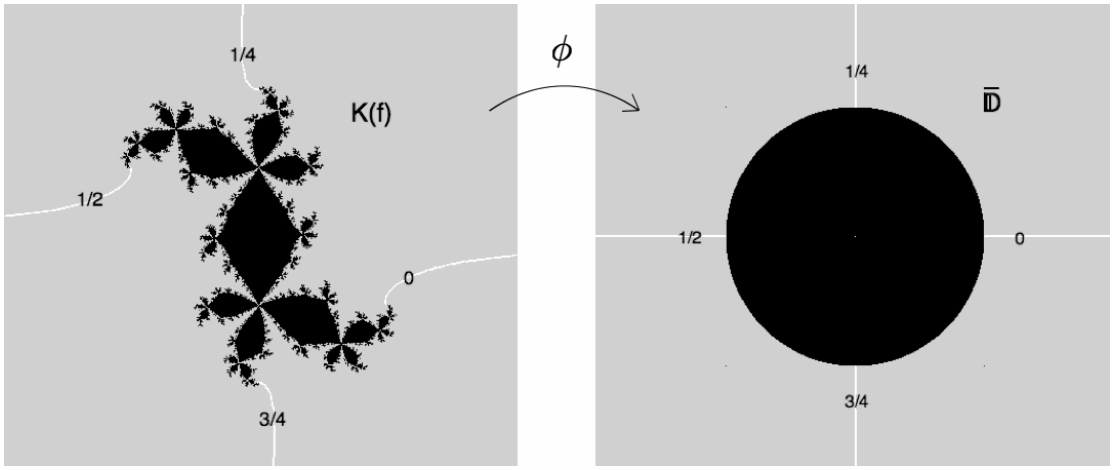

Figure 1.2: External rays on $K(f)$ come from preimages of rays on $\overline{\mathbb{D}}$ under ϕ.

the semiconjugacy $\phi(z^2) = f_c(\phi(z))$ forces the following relationship: Applying f_c to $R_c(t)$ yields $R_c(2t)$, or in other words, f_c doubles the angles of external rays on $K(f_c)$, mod 1. We can thus use this notion to determine where the landing points of rays map under iterations of f_c, since it implies that $f(\gamma_c(t)) = \gamma_c(2t)$:

Example 1.7. Consider $f_i(z) = z^2 + i$, as shown in Figure 1.3. This yields that the forward orbit of 0 under f_i is given by:

$$0 \longrightarrow \mathrm{i} \longrightarrow \text{-}1\text{+}\mathrm{i} \longrightarrow \text{-}\mathrm{i}$$

Now examine the angles of the external rays that land at each of these points, as the above mapping sequence is essentially the following:

$$\gamma(\tfrac{1}{12}) = \gamma(\tfrac{7}{12}) \longrightarrow \gamma(\tfrac{1}{6}) \longrightarrow \gamma(\tfrac{1}{3}) \longrightarrow \gamma(\tfrac{2}{3})$$

Note how we can use external rays and the angle-doubling map to model what happens to points when we iterate with f_i! $\square$

This suggests an alternate parameter notation for Misiurewicz points—instead of referring to the parameter coordinate $c \in M$, we can refer to the external angle θ of the ray that lands at c in $J(f)$. Thus, instead of referring to the function in the above example as f_i, we could refer to it as $f_{1/6}$. More generally, we write f_θ for the typical f_c. Since we can model the forward orbit of c under $f_c = f_\theta$ by examining the forward orbit of θ under the angle-doubling map, it should be noted that strictly preperiodic functions *must* be associated with rational parameter angles θ possessing an even denominator.

Douady and Hubbard define that the external angle(s) associated to the preperiodic point c on the Julia set of f_c are the same as the external angle(s) associated to a point $z = c$ on the Mandelbrot set. In other words, even though our definition of this parameter system stems from external rays on the filled Julia set, this system yields useful rays on the Mandelbrot

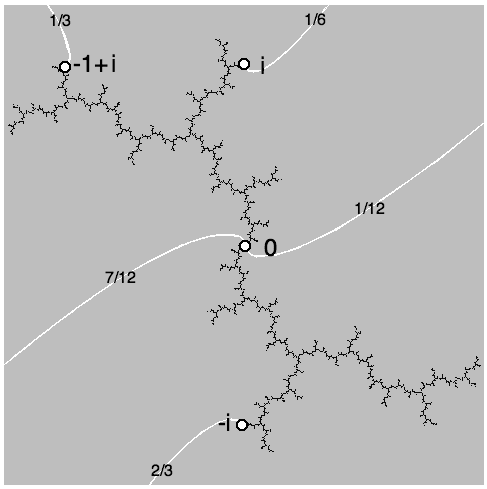

Figure 1.3: Rays on $z \mapsto z^2 + i$

set as well. We shall distinguish between these rays by referring to external rays on the Mandelbrot set as **parameter rays**.

While the above settles the nomenclature for preperiodic functions, Douady and Hubbard also included in this scheme a naming system for periodic functions as well. Periodic functions stem from parameters $c \in \mathbb{C}$ which lie at the center of connected components of $M \backslash \partial M$. (These connected subsets of M are called **hyperbolic components**.) If an angle has a forward orbit under doubling modulo 1 which mimics the forward orbit of c under $z \mapsto z^2 + c$, that angle has a parameter ray which lands at the base of the hyperbolic component for c (or $\overline{c}$) in M. (Note that we do not state that $\gamma(\theta) = c$ here: if $z \mapsto z^2 + c$ is periodic, c is contained in the interior of $K(f)$ and cannot be the landing point of any external ray.) Under our new parameter system, periodic functions must be associated with rational θ possessing an odd denominator. [7]

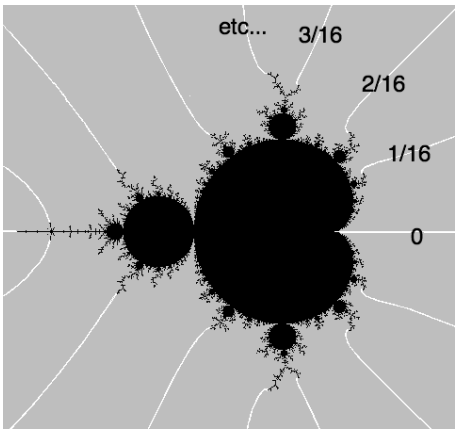

Figure 1.4: Parameter rays on the Mandelbrot set

These assignments yield an intuitive ordering of external rays on the Mandelbrot set, as

the angles of these parameter rays increase as we travel counterclockwise around M. (See Figure 1.4.) A subtle point to note since the boundary of the Mandelbrot set is tree-like in places is that there is not a 1-1 correspondence between values of θ and c for Misiurewicz points. If a parameter point c lies on a branch point of M, multiple parameter rays will land at c. (Any point on $J(f)$ where multiple external rays land is called **multiply accessible**.) This is reflected in the local similarity of $c \in J(f)$ to $c \in M$, so multiple external rays will also land at $c \in J(f)$ as well. Thus, for these c we obtain multiple values of θ such that $f_\theta = f_c$.

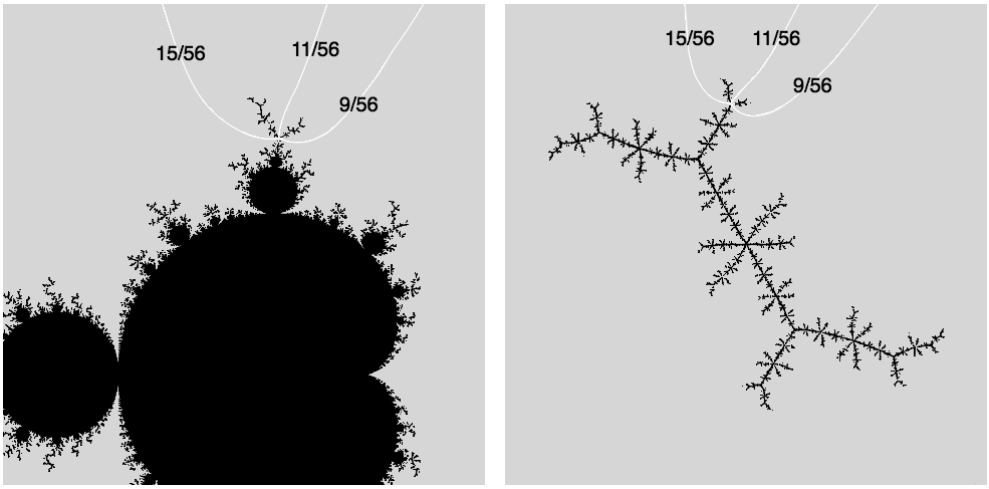

Figure 1.5: We have $f_{9/56} = f_{11/56} = f_{15/56}$ due to parameter rays landing at a branch point in M.

Since the focus of our paper is primarily on matings of preperiodic quadratics, we shall adopt the usage of the notation f_θ in favor of f_c. Further, all notation which has previously made use of the subscript c (i.e., $R_c(t)$ and $\gamma_c(t)$) will reflect this change as well.

1.2.3 Hubbard Trees

While Julia sets are useful invariant structures to know of, it will be beneficial to obtain "simpler" invariant structures for purposes encountered later in the paper. Ideally, such a structure would still be able to record information on postcritical points, and could work in line with the external-angle based parameter system described in the previous section.

Thus, we introduce the following useful tool for discretizing the invariant structures discussed earlier in the paper:

Definition 1.8. *Let $f_\theta : \mathbb{C} \to \mathbb{C}$ be given by $f_\theta(z) = z^2 + c$ for c some Misiurewicz point, and let f_θ have Julia set $J(f_\theta)$ and postcritical set P_{f_θ}. The* **Hubbard tree**, *T_θ, is the minimum spanning tree of P_{f_θ} on the dendrite $J(f_\theta)$.*[7]

While this definition can be extended to polynomials of higher degree (and even to polynomials whose Julia sets are not dendrites), we present the definition in this simplified

form to emphasize our later focus on matings of quadratics that stem from Misiurewicz points.

Bruin and Schleicher give an alternative combinatorial definition of the Hubbard tree which emphasizes several useful properties of the Hubbard tree defined above:

Definition 1.9. *A* **Hubbard tree** *is a tree T equipped with a map $f : T \to T$ and a distinguished point, the critical point c_0, satisfying the following:*

1. *$f : T \to T$ is continuous and surjective.*
2. *Every point in T has at most 2 preimages under f.*
3. *For points in $T \backslash \{c_0\}$, the map f is a local homeomorphism onto its image.*
4. *All endpoints of T are in P_f.*
5. *The critical point is periodic or preperiodic, but not fixed.*
6. *Expansivity: If x and y with $x \neq y$ are branch points or points in P_f, then there is an $n \geq 0$ such that $f^{on}([x, y])$ contains the critical point.* [2]

The definition from Bruin and Schleicher is quite restrictive in that it only yields Hubbard trees whose maps are of degree 2, much like our initial definition. It is simultaneously lenient, however, in that it allows for purely topological Hubbard trees to occur whose maps cannot be neatly embedded in $\mathbb{C}$.

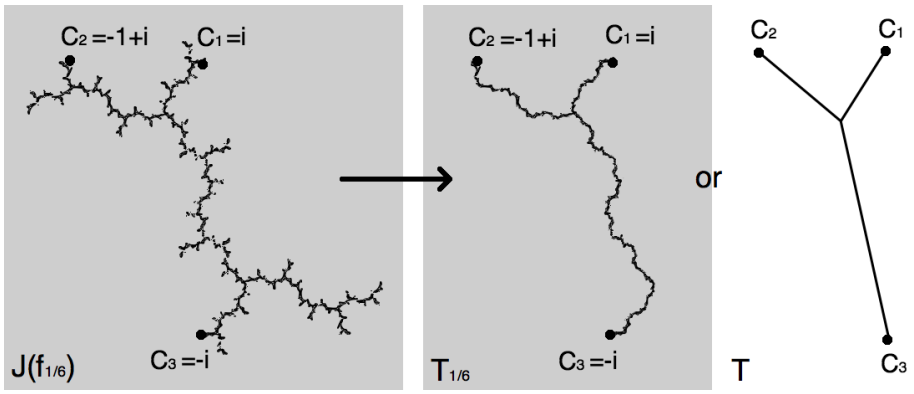

Figure 1.6: Generation of the Hubbard tree for $f_{1/6}$

To see how these two definitions relate, consider the preperiodic quadratic polynomial f_θ and its Hubbard tree T_θ as given in our initial definition:

1. f_θ is a polynomial and thus continuous.
2. Every point has at most two preimages sincef_θ is quadratic.

3. As a quadratic polynomial, f_θ is a local homeomorphism everywhere except at its critical point.

4. As we've defined the Hubbard tree to be the minimum spanning tree of P_{f_θ} on $J(f_\theta)$, the endpoints *must* be in P_{f_θ}.

5. Since c is a Misiurewicz point, f_θ is preperiodic. Thus, c is not fixed.

It is a bit trickier to check the remaining assertions—that f_θ maps T_θ onto itself, and that the expansivity condition is met—but these hold as well. (See [2].) In short, these conditions imply that T_θ is forward invariant under f_θ, and that iterated preimages of T_θ under f_θ approach the Julia set for f_θ. Another useful point for later on is that the closure of each component of $f^{-1}(T_\theta)\backslash\{0\}$ maps bijectively onto T_θ via f_θ—or in other words, the preimage of T_θ looks like two miniature copies of T_θ glued together at the critical point. Further, the nth preimage of T_θ resembles 2^n miniature copies of T_θ glued together at the $(n-1)$th preimages of the critical point.

This insight into the behavior of Hubbard trees under their associated map is not all that we may find in [2]. Bruin and Schleicher also provide several algorithms which detail how we can use θ and the combinatorial structures associated with T_θ to gain information on f_θ—in other words, how we may start with discrete data and build back analytic information! Since we have been very interested in observing how external angle parameters relate to the functions they generate, a natural question to ask here is whether or not we can generate an explicit relationship between parameter angles and Hubbard Trees.

The answer to this question is that we can. To illustrate this connection, we will briefly discuss itineraries and an algorithmic test that will aid in the construction of a Hubbard tree when given a parameter θ.

Definition 1.10. *Let θ be an external angle in $\mathbb{R}/\mathbb{Z}$. We associate the* **itinerary of t with respect to** *θ to any $t \in \mathbb{R}/\mathbb{Z}$, by $v_\theta(t) = v_1v_2v_3...$ with $v_i \in \{\star, 0, 1\}$. Here, the v_i are determined via the following assignments:*

$$v_i = \begin{cases} \star & \text{if } 2^{i-1}\theta = \frac{\theta}{2} \text{ or } \frac{\theta+1}{2} \\ 0 & \text{if } \frac{\theta+1}{2} < 2^{i-1}\theta < \frac{\theta}{2} \\ 1 & \text{if } \frac{\theta}{2} < 2^{i-1}\theta < \frac{\theta+1}{2}, \end{cases}$$

where the inequalities are interpreted with respect to cyclic order on $\mathbb{R}/\mathbb{Z}$. (If it is unambiguous what θ is, we simply call this the **itinerary of** *t.) The* **kneading sequence** *of θ is the itinerary of θ with respect to θ, $v_\theta(\theta)$.* [2]

Intuitively, we are starting with some function, f_θ, and splitting $J(f_\theta)$ into three components. The first component is the set containing the critical point, $\{\star\}$. The two remaining disjoint components are obtained by cutting $J(f_\theta)$ in half at the critical point—along the $R_\theta(\frac{\theta}{2})$ and $R_\theta(\frac{\theta+1}{2})$ rays. The component(s) on the side of this ray-pair which contain(s) $\gamma_\theta(\theta)$ we denote by T_1. (T_1 contains the landing points of rays with external angles between

$\frac{\theta}{2}$ and $\frac{\theta+1}{2}$.) The remaining component(s) we will call T_0. (T_0 contains the landing points of rays with external angles between $\frac{\theta+1}{2}$ and $\frac{\theta}{2}$.)

Now we can assign the itinerary of an external angle t by listing in order which components the forward iterates of $R_\theta(t)$ land in, starting with the initial position for t: $\star$ if the ray in question lands at $\star$, 1 if we land in T_1, and 0 if we land in T_0. (Note: in [2], the authors restrict T_0 and T_1 to be subsets of the Hubbard tree and not necessarily of the Julia set due to their combinatorial approach. We would like to keep open the possibility of mentioning the itinerary of points in $J(f_\theta)\backslash T_\theta$ though, so we have slightly modified the usage of their notation to include these points.)

For a concrete example of developing the itinerary for a point, consider the following example:

Example 1.11. Suppose we wish to determine the itinerary of $t = 1/12$ with respect to $\theta = 1/6$. Essentially, this means that we are seeking the forward itinerary of $\gamma_{1/6}(\frac{1}{12})$ on $J(f_{1/6})$—thus, we must revisit the function of Example 1.7, $f_{1/6}$.

Here, the critical point is $\gamma_{1/6}(\frac{1}{12}) = \gamma_{1/6}(\frac{7}{12}) = \star$. T_1 must contain $\gamma_{1/6}(\frac{1}{6})$, thus we have that T_1 is the component of $J(f_{1/6})\backslash\{\star\}$ on the upper half of Figure 1.7. This leaves T_0 as the remaining component on the bottom half of Figure 1.7.

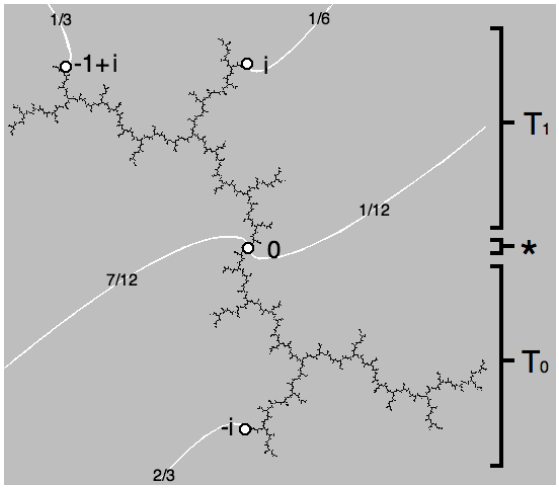

Figure 1.7: $\star$, T_0, and T_1 on $f_{1/6}$

To find $v_{1/6}(\frac{1}{12})$, we now need to note the location of external rays in the forward orbit of $R_{1/6}(\frac{1}{2})$. This is done fairly easily by considering the landing points of these rays. Recall that the forward orbit of $\gamma(\frac{1}{12})$ under $f_{1/6}$ can be determined by applying the angle-doubling map:

$$\gamma(\tfrac{1}{12}) = \gamma(\tfrac{7}{12}) \longrightarrow \gamma(\tfrac{1}{6}) \longrightarrow \gamma(\tfrac{1}{3}) \longrightarrow \gamma(\tfrac{2}{3})$$

We start out in $\{\star\}$, map to a point in T_1, map to a different point in T_1, map to a point in T_0, and then cycle between the last two points. This yields $v_{1/6}(\frac{1}{12}) = \star1\overline{10}$.

If the kneading sequence associated with this function was desired instead, we would have to find the itinerary of 1/6: $v_{1/6}(\frac{1}{6}) = 1\overline{10}$. $\square$

While it is helpful to have prior knowledge of the function to develop an itinerary, as in Example 1.11, it is not wholly necessary. Relying strictly upon the definition of the itinerary, we do not need to know the structure of $J(f_\theta)$ to develop the itinerary for t with respect to θ—we merely need to know what t and θ are. It is thus not terribly difficult to collect combinatorial data on the orbits of the postcritical points of f_θ.

This should come as little surprise: it is usually much easier to start with an analytic object and collect combinatorial data than the other way around. The problem is often found trying to go in the reverse direction—obtaining analytic information from combinatorial objects. So, how may we attempt to gain information on the structure of f_θ, strictly given nothing but its parameter angle θ?

Here, it will be useful to combine information that we know about Hubbard trees with the information that we know about forward orbits of points. Since the Hubbard tree maps onto itself and its associated function is locally a homeomorphism everywhere except at the critical point, we can take information on the itineraries of points and extend this to obtain information on the itineraries of edges. For example, if $\gamma_\theta(t)$ has itinerary 10... and $\gamma_\theta(t')$ has itinerary 11..., we should suspect that the arc on the Julia set between $\gamma_\theta(t)$ and $\gamma_\theta(t')$ starts out in T_1. This is because the itinerary places both points initially in T_1. Further, we should suspect that this arc maps to an arc that starts in T_0 and ends in T_1. This is because f_θ is locally a homeomorphism on T_1, and because the second digit of the itinerary places each image point in a separate subcomponent of $J(f_\theta)$.

With a little ingenuity, it is also possible to see where larger sections of the Hubbard tree map forward, and whether or not they collapse under forward iteration of the function. To clarify what is meant here by "larger sections," we define the following:

Definition 1.12. *A* **triod** *is a connected compact set homeomorphic to a subset of the letter Y. We shall let* $[a, b, c]$*, with* $a, b, c \in J(f)$ *denote the triod which is formed by taking the minimum spanning tree of the points* a, b *and* c *on* $J(f)$*.*

We say that a triod is **degenerate** *if it is homeomorphic to an arc or a point, and* **nondegenerate** *if it is homeomorphic to the letter Y.* [2]

Since we will be frequently referring to triods of postcritical points (as well as where they map), it will be a matter of practicality to label the postcritical points of a given map in sequential order: i.e., $f^{\circ n}(\star) = c_n, n \in \mathbb{N}$. We will let $\star = c_0$, so that $c_0 \mapsto c_1 \mapsto c_2 \mapsto ...$ etc. In the case of periodic points, we will write the smallest n that can used to describe that point.

In later sections, it will be of use to discuss points which are iterated preimages of the critical point of a map. While preimages branch off for quadratic maps (that is, each point which is not a critical value will have two preimages under the map), with additional information we will let c_{-n} denote a point such that $f^{\circ n}(c_{-n}) = c_0$. Once fixing a particular c_{-n}, we will extend the above labeling convention for the forward orbit of c_{-n} so that $c_k \mapsto c_{k+1}$. (Fixing a particular c_{-n} is important, as we obtain two possible preimages for any point—one which prepends 0 and another which prepends 1 to the initial point's itinerary.)

As an example of how this c_n notation may be utilized, on $f_{1/6}$ (as shown in Figure 1.7) we have the following mapping scheme of points on the critical orbit:

$$\gamma(\tfrac{1}{12}) = \gamma(\tfrac{7}{12}) \longrightarrow \gamma(\tfrac{1}{6}) \longrightarrow \gamma(\tfrac{1}{3}) \longrightarrow \gamma(\tfrac{2}{3})$$

, or alternatively,

$$\star = c_0 \longrightarrow c_1 \longrightarrow c_2 \longrightarrow c_3 .$$

Further, we have that on this same example that $[c_1, \star, c_3]$ forms a triod which is degenerate and $[c_1, c_2, c_3]$ forms a triod which is nondegenerate. (We can confirm this by referring back to Figure 1.3.)

Now that we have notation to describe these larger sections of the Hubbard tree, what happens if we try to use the forward image of these points to predict where the triods map?

Examining the $[c_1, c_2, c_3]$ triod, the mapping scheme would seemingly suggest that $f_{1/6}$ sends it to $[c_2, c_3, c_2]$. This cannot be true: $[c_1, c_2, c_3]$ is the whole Hubbard tree and $[c_2, c_3, c_2]$ is but an arc between c_2 and c_3. Something must be wrong here, since the Hubbard tree should map onto itself, and not just onto an arc.

The problem is that we failed to consider that our initial triod included the critical point, which is the only point at which $f_{1/6}$ does not act like a local homeomorphism. If we "chop" an arm of the triod at $\star$, however—thus removing the part of the triod that extends past the critical point—$f_{1/6}$ will act like a homeomorphism on this newer triod. In fact, the nondegenerate triod $[c_1, c_2, \star]$ maps onto the whole Hubbard tree, $[c_2, c_3, c_1]$, as suggested by the mapping scheme.

This observation can be developed into a much more powerful tool which tells us when triods on a Julia set are degenerate, strictly based on the forward orbits of external rays landing at their endpoints and not on any prior knowledge of the structure of the Julia set. This algorithm is developed in [2], and summarized below:

Definition 1.13. *The following algorithm serves as a test for the degeneracy of a given triod $[a, b, c]$ on a Julia set $J(f)$. We check whether a triod is degenerate by iterating it:*

1. *Note the locations of a, b, and c in either $\{\star\}$, T_1, or T_0. (If these are given as landing points of external rays, we need not know the structure of $J(f)$ to proceed.)*

2. *If a, b, and c are in three different locations, the triod is degenerate and the coordinate in $\{\star\}$ is in the middle of a segment pair connecting the other two coordinates.*

3. *If more than one of a, b, or c is in $\{\star\}$, the triod is degenerate. The triod is either homeomorphic to an arc (two points are contained in $\{\star\}$) or a point ($a, b, c \in \{\star\}$).*

4. *If a, b, and c are contained in two locations, T_0 and T_1, "chop" off the odd one out by replacing it with $\star$.*

5. *If either all of a, b, and c are contained in $T_0 \cup \{\star\}$ or all of a, b, and c are contained in $T_1 \cup \{\star\}$, we apply f to a, b, and c to see where this triod maps.*

6. *Repeat this process until we've obtained a periodic cycle of coordinates, or have noted that we have a degenerate cycle. If we have chopped an end of the triod off at least once in each coordinate location of our ordered triple, the triod is nondegenerate. If we have only chopped 2 ends of the triod, we have a degenerate segment pair, with the non-chopped coordinate in the middle.* [2]

Consider the triod $[c_1, c_2, c_3]$ on $J(f_{1/6})$:

Example 1.14. To test a triod for degeneracy, we need to be able to determine the forward orbit of each of the points at the ends of the triod, as well as their locations in T_1, T_0, or $\{\star\}$. Keep in mind that based on external angle considerations, we have determined that $c_1, c_2 \in T_1$ and $c_3 \in T_0$. Further, the angle-doubling map has given us the forward orbits of each of these points as noted in the example above. Using this information, we can test a triod for degeneracy:

$[c_1, c_2, c_3]$ (Located respectively in T_1, T_1, T_0. We must "chop" the third coordinate.)
$[c_1, c_2, \star]$ (Located respectively in $T_1, T_1, \{\star\}$. We may apply $f_{1/6}$.)
$[c_2, c_3, c_1]$ (Located respectively in T_1, T_0, T_1. We must chop at the second coordinate.)
$[c_2, \star, c_1]$ (Located respectively in $T_1, \{\star\}, T_1$. We may apply $f_{1/6}$.)
$[c_3, c_1, c_2]$ (Located respectively in T_0, T_1, T_1. We must chop at the first coordinate.)
$[\star, c_1, c_2]$ (Located respectively in $\{\star\}, T_1, T_1$. We may apply $f_{1/6}$.)

It is possible to continue mapping forward under $f_{1/6}$ and chopping where appropriate, but note that we come back to the very triod that we started with on the last suggested iteration under $f_{1/6}$. We've reached a periodic cycle of triods, and have chopped off an arm of the forward iterates of the triods in each of the three coordinate locations of our ordered triple. By the above algorithm, we can confirm that this (as well as any other triod we have cycled through) is a nondegenerate triod. □

The remarkable thing about this test is that it suggests an iterative construction of the Hubbard tree purely from any parameter angle θ associated with a Misiurewicz point. This will be a combinatorial copy of the Hubbard tree T without embedded coordinates in $\mathbb{C}$, but it will share the essential topoplogical structures of T_θ as detailed earlier in this section.

We can obtain a Hubbard tree by first placing and drawing edges between three initial points—any point from T_0, any point from T_1, and $\star$. These will have a minimum spanning tree resembling an arc with $\star$ in the middle. We use this as a launching point to iteratively place postcritical points of $T_k, k \in \{0, 1\}$, on T by testing whether the to-be-added point is degenerate or nondegenerate with pairs of previously placed points in $T_k \cup \star$: If the new point is degenerate with any collection of pairs, the test yields a location for the postcritical point on a currently existing arc (or on an extension of a currently existing arc) on the already drawn subset of T. If the new point is nondegenerate with all collections of pairs from T_k, it does not lie on any pre-established arcs of T and must connect to some branch point of T. We must then test this branch point to see where the new limb of T is to be inserted on the already-drawn subset of T. [2]

Here, one can utilize the external angles associated with the c_n to determine where the new limb should be placed. (This is to ensure that the limbs about any branch point are oriented in the correct order.) Once we exhaust the collection of postcritical points by placing them in this manner, we have the desired copy of T.

Example 1.15. As a Hubbard tree with only one branch point, $T_{1/6}$ can be approximated in this manner relatively quickly.

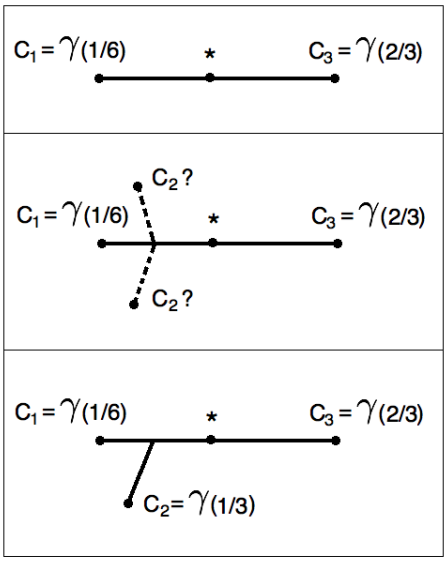

Figure 1.8: Construction of the Hubbard tree associated with $f_{1/6}$

As we can see in Figure 1.8, placing a point from each of T_0, T_1, and $\star$ takes care of all but one postcritical point of $f_{1/6}$. We now need to determine where to place the missing c_2 by testing whether it forms any degenerate triods with pairs of points from $T_1 \cup \star$. There is only one possible pair of points to test with c_2, forming the triod $[\star, c_1, c_2]$. However, since this triod was contained in the periodic sequence of triods from the previous example, we have by that test that this is a nondegenerate triod. This means that c_2 does not lie on any previously drawn arcs of T, and must be connected to T via some branch point in T_1. Which "side" of T should this new limb containing c_2 be drawn on?

If we pay attention to the fact that each postcritical point has an associated external angle, we should be able to use this to determine how to embed our tree: angles increase cyclically as we travel counterclockwise around T. This means that the appropriate placement of c_2 is *below* the already drawn arc, as it yields the appropriate cyclic order $1/6, 1/3, 2/3$. □

Recall that backwards iteration of the Hubbard tree under its associated map approximates the map's Julia set. Since this section demonstrates that only θ is needed to obtain a combinatorial copy of T_θ, it should be clear that the parameter θ carries quite a large amount

of information. We will make heavy usage of the link between θ and T_θ in subsequent chapters to emphasize important structures on f_θ through use of T.

For small $|P_f|$, the above algorithm for generating T may be fairly straightforward to work through by hand. For more complicated quadratics, however, the process becomes much more tedious. A program based upon this algorithm was generated by the author for use in developing Hubbard trees for the motivating examples in this paper. Every Hubbard tree structure asserted has been verified using this program and cross-comparison to [11]. For the interested reader, a record of the code used to generate the program is located in Appendix A.

1.3 Matings of polynomials

Informally, a mating is a map which is obtained by gluing two polynomials together. The vagueness of the operation suggested here naturally raises a few concerns: Can we mate just any pair of polynomials? What polynomial domains do we consider when performing this gluing? Can we perform this operation so that the resulting mating acts nicely on any "boundary" obtained between our initial pair of functions? What sort of quotient space do we obtain as a result of this gluing?

While there are some general restrictions to be addressed, the answer to most of these questions is choice-dependent because there are several types of mating functions. We start by developing a particular compactification of the complex plane needed to form the **formal mating**, and proceed from there: all types of matings are either quotients of or related to quotients of this formal mating map.

Definition 1.16. *Let $\widetilde{\mathbb{C}}$ be the* **compactification of the complex plane** *given by adding the circle at infinity: $\widetilde{\mathbb{C}} = \mathbb{C} \cup \{\infty \cdot e^{2\pi i t} | t \in \mathbb{R}/\mathbb{Z}\}$. Give $\widetilde{\mathbb{C}}$ the natural topology so that it is homeomorphic to $\overline{\mathbb{D}}$. If considering a monic quadratic polynomial on such a space, let $R^*(t)$ denote the usual external ray along with its landing point at ∞.* [10]

Here, two important points are of note. First, we can continuously extend any monic polynomial $f : \mathbb{C} \to \mathbb{C}$ of degree d to a polynomial $\tilde{f} : \widetilde{\mathbb{C}} \to \widetilde{\mathbb{C}}$ by letting $\tilde{f}(\infty \cdot e^{2\pi i t}) = \infty \cdot e^{2\pi i t d}$. Essentially, any such f will act on the circle at infinity much like $z \mapsto z^d$ acts on the unit circle—multiplying the argument of the initial point by d. This extension gives a landing point of sorts at infinity for the external rays of f.

Second, we can form a topological two-sphere $\mathbb{S}^2_{a,b}$ by taking $\mathbb{S}^2_{a,b} = \widetilde{\mathbb{C}}_a \bigsqcup \widetilde{\mathbb{C}}_b / (\infty \cdot e^{2\pi i t}, a) \sim (\infty \cdot e^{-2\pi i t}, b)$. Here, we're essentially gluing the circles at infinity on two copies of $\widetilde{\mathbb{C}}$ together with opposing angle identifications to form our two-sphere. With these two notes, we define our first mating function:

Definition 1.17. *Let $f_a, f_b : \mathbb{C} \to \mathbb{C}$ be two same-degree postcritically finite monic polynomials. We define the* **formal mating** *of f_a and f_b, $f_a \amalg_f f_b$, to be the map $f_a \amalg_f f_b : \mathbb{S}^2_{a,b} \to \mathbb{S}^2_{a,b}$ given by $f_a \amalg_f f_b|_{\widetilde{\mathbb{C}}_a} := \tilde{f}_a$ and $f_a \amalg_f f_b|_{\widetilde{\mathbb{C}}_b} := \tilde{f}_b$.* [10] [16]

To phrase the above definition more intuitively, note that we are gluing the compactified domain spaces of f_a and f_b at their boundaries. Once this space is obtained, the collection of equivalence classes containing identified boundary points now forms the equator of a topological two-sphere. The formal mating is the map given by having f_a and f_b act on their own respective hemispheres of this quotient space. (See Figure 1.9.) While formal matings may be defined for general post-critically finite pairs of monic polynomials, we will emphasize the quadratic case in this paper. Notably, when presented with a pair of functions f_a and f_b, we will take a and b to be parameter angles as discussed in Section 1.2.1.

An immediate question to be raised here is whether the behavior on the equator is "nice". The prescribed manner in which we suggested gluing copies of $\widetilde{\mathbb{C}}$—by identifying $(\infty \cdot e^{2\pi i t}, a)$ to $(\infty \cdot e^{-2\pi i t}, b)$—aligns the "$z \mapsto z^d$" behavior obtained at the boundaries of our respective copies of $\widetilde{\mathbb{C}}$. (Note that this also identifies landing points at infinity of $R_a(t)$ and $R_b(-t)$.) This forces $f_a \amalg_f f_b$ to be a continuous branched covering from $\mathbb{S}^2_{a,b}$ to itself.

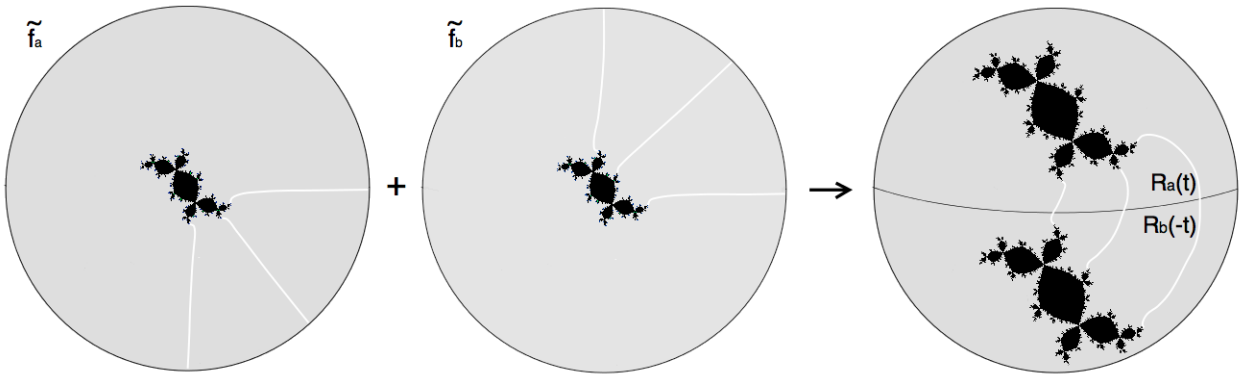

Figure 1.9: $\tilde{f}_a$ and $\tilde{f}_b$ on their own respective copies of $\widetilde{\mathbb{C}}$. To obtain the domain of the formal mating, identifications are made between the respective landing points at infinity of $R_a(t)$ and $R_b(-t)$.

Starting with the formal mating, $f_a \amalg_f f_b$, it is possible to obtain other types of matings as quotient maps, much like the following: The most closely related to $f_a \amalg_f f_b$ of these maps is the degenerate mating:

Definition 1.18. *We define two equivalence relations, $\sim_{top}$ and $\sim_{degen}$, on the space of the formal mating as follows: Each point on the equator corresponds to two external rays which land on the Julia sets of f_a and f_b. Let the point on the equator, pair of rays, and pair of landing points generate an equivalence class $[x]$ under the equivalence relation $\sim_{top}$. Let $[x_1], ..., [x_n]$ be the equivalence classes containing at least 2 postcritical points. Then, let $[y_1], ..., [y_m]$ be the collection of $[x_1], ..., [x_n]$ along with iterated preimages of these equivalence classes containing at least one point on the critical orbit of $f_a \amalg_f f_b$. Set $p \sim_{degen} q$ if $p, q \in [y_i]$ for some i.*

If each of the $[y_i]$ are simply connected, the quotient space is a 2-sphere, and we define a branched covering on $\mathbb{S}^2$ as follows: On the complement of open neighborhoods of the

equivalence classes $[y_i]$ *from* $y = 1, ..., m$*, let* $f_a \amalg_d f_b(z) = f_a \amalg_f f_b(z)$*. On the equivalence classes themselves, let* $f_a \amalg_d f_b([y_i]) = [f_a \amalg_f f_b(y_i)]$ *for* $y = 1, ..., m$*. Finally, set* $f_a \amalg_d f_b$ *to be homeomorphic on the remainder of* $\mathbb{S}^2$*.* $f_a \amalg_d f_b$ *is known as the* **degenerate mating** *of* f_a *and* f_b*.* [10] [12]

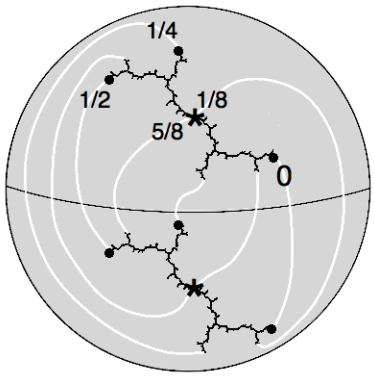

Figure 1.10: Ray equivalence classes of $\sim_{degen}$ for $f_{1/4} \amalg_d f_{1/4}$. Stars denote critical points; filled dots denote postcritical points.

Again, to phrase the above more intuitively, what we are doing is starting with the quotient space $\mathbb{S}^2_{a,b}$ and building an equivalence relation that identifies along external ray-pair groupings, $\sim_{top}$. (Since $\sim_{top}$ is constructed on the quotient space of the formal mating—which we specified starts with postcritically finite quadratics—the filled Julia sets for the associated maps are locally connected, and we can expect these external ray-pairs to land.) Next, we form a secondary quotient space by identifying along a finite collection of equivalence classes generated by $\sim_{top}$. Namely, we build a quotient space by identifying along the ray-pair groupings that contain pairs of points on the critical orbit, and preimages of these groupings which contain at least one postcritical or critical point of $f_a \amalg_f f_b$. The equivalence relation for which only these equivalence classes of $\sim_{top}$ are nontrivial is $\sim_{degen}$.

As an example, consider Figure 1.10, which shows the nontrivial equivalence classes of $\sim_{degen}$ for $f_{1/4} \amalg_d f_{1/4}$: we include the ray-pairs leading from $\gamma(0)$ and $\gamma(\frac{1}{2})$ of the upper tree because they include pairs of postcritical points. We also include preimages of these ray-pairs under the formal mating which contain at least one point on the critical orbit of the formal mating. This accounts for the remaining ray-pair groupings. At this point we've exhausted all possible postcritical points on the map, so there are no more nontrivial equivalence classes for $\sim_{degen}$.

Once we pinch along equivalence classes of $\sim_{degen}$, we alter the implied quotient map slightly to yield a homeomorphism from the two-sphere to itself: The critical orbit suggests a mapping scheme on equivalence classes of $\sim_{degen}$, and we take the degenerate mating to be equivalent to the formal mating off open neighborhoods of the equivalence classes. We patchwork the rest of the map together by setting the degenerate mating to be homeomorphic in the remaining space on the two-sphere. Despite the last portion of $f_a \amalg_f f_b$ being defined arbitrarily, $f_a \amalg_f f_b$ is uniquely determined up to Thurston equivalence. (In other words,

the dynamics of the map do not change based on which homeomorphism we pick in the last part of the definition.)

If no pairs of postcritical points are identified by $\sim_{degen}$, we have that $f_a \amalg_d f_b = f_a \amalg_f f_b$. This happens most frequently when a and b are angles whose denominators are not offset by powers of two (e.g. $f_{1/6}$ and $f_{1/4}$), as well as in some other special cases where the periodic postcritical points of f_a and f_b do not "align" by the t and $-t$ pairing (e.g. $f_{1/14}$ and itself). We also must have in these types of cases that postcritical points are not identified "through" the opposing Julia set. (More on this in Section 2.4.1.)

If we are less restrictive in picking and choosing equivalence classes to identify, we obtain another type of mating map:

Definition 1.19. *Consider the quotient space $K(f_a) \amalg K(f_b)$ formed when each equivalence class of $\sim_{top}$ is respectively identified to a point. (All points not in $K(f_a) \subset \widetilde{\mathbb{C}}_a$ or $K(f_b) \subset \widetilde{\mathbb{C}}_b$ are contained in an equivalence class of $\sim_{top}$ which contains a point of $K(f_a)$ or $K(f_b)$, thus the quotient space collapses all such points.)*

We then define the **topological mating**, *$f_a \amalg_t f_b$, to be the map $f_a \amalg_t f_b : K(f_a) \amalg K(f_b) \to K(f_a) \amalg K(f_b)$ given by $f_a \amalg_t f_b|_{K(f_a)} = f_a$ and $f_a \amalg_t f_b|_{K(f_a)} = f_b$.* [16]

Here, we are collapsing ray-pair groupings (particularly, collections of external ray-pairs with shared landing points) respectively to a point. Unlike the degenerate mating, however, we are not selective in choosing which identified ray-pair groupings to collapse. An alternative way to think about the quotient space formed with $\sim_{top}$ is the following: identify the boundaries of $K(f_a)$ and $K(f_b)$ together under the relation $\gamma_a(t) \sim \gamma_b(-t)$. (We assumed a while ago that f_a and f_b were postcritically finite, which tells us that their filled Julia sets are locally connected and that they have external rays which land, so this is allowed.) The topological mating is the map given by having f_a and f_b act on their own respective filled Julia sets within this quotient space. (See Figure 1.11.)

Again, a potential concern regarding $f_a \amalg_t f_b$ is whether the function is "nice" on the edge we just glued along. Similar to forming the formal mating, the identification $\gamma_a(t) \sim_{top} \gamma_b(-t)$ aligns the "$z \mapsto z^d$" behavior obtained at the boundaries of $K(f_a)$ and $K(f_b)$; thus $f_a \amalg_t f_b$ is continuous.

A point of note for the degenerate mating and the topological mating is that while we've described the construction of the quotient spaces for these maps, we have not yet made any explicit mention of what they actually *look like*. The space associated with the formal mating is a two-sphere, but what about $f_a \amalg_d f_b$ and $f_a \amalg_t f_b$?

It *is* possible that we can glue along the boundaries of $K(f_a)$ and $K(f_b)$ (or just at important points on their boundaries) and obtain a topological two-sphere. (Again, see Figure 1.11.) In the case that a two-sphere is the resulting quotient space of the topological mating, we have the following definition:

Definition 1.20. *If there exists some topological conjugacy from $f_a \amalg_t f_b$ to some rational map F on the Riemann sphere $\hat{\mathbb{C}}$, then we call F the* **geometric mating** *of f_a and f_b and say that f_a and f_b are* **matable**. *We will alternatively use $f_a \amalg_g f_b$ to denote this map.* [16]

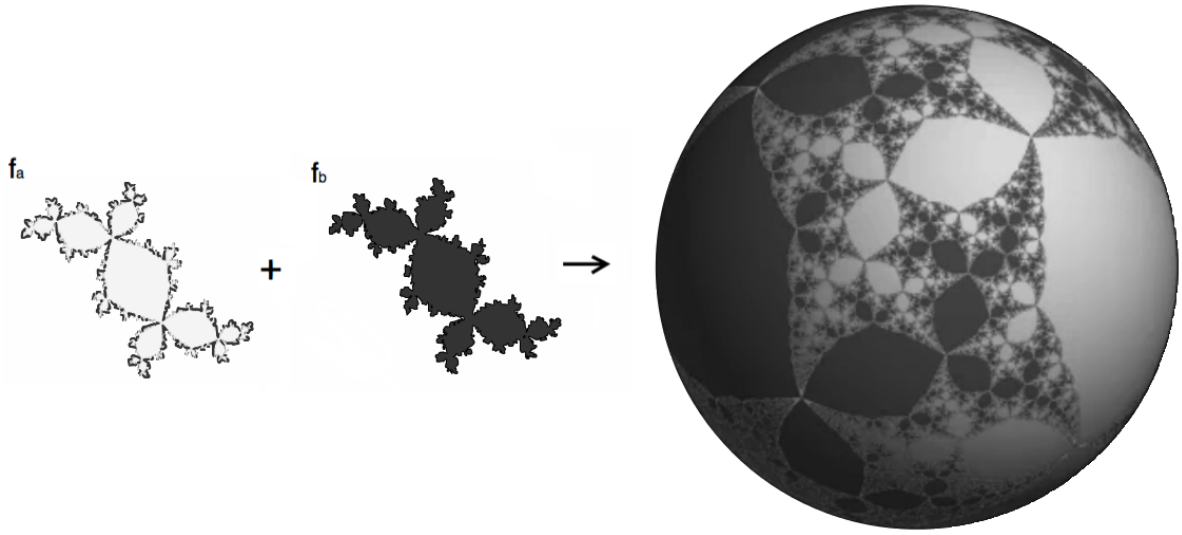

Figure 1.11: The topological mating of $f_a = f_{1/7}$ and $f_b = f_{1/7}$. (Base graphics from [6].)

In other words, not only can some topological matings determine quotient spaces which are two-spheres, such maps also have dynamics which emulate those of rational maps!

It cannot always be guaranteed, however, that the quotient space $K(f_a) \amalg K(f_b)$ (or even the quotient space of the degenerate mating) is a two-sphere. As a somewhat trivial example, consider the following:

Example 1.21. Examine $f_{1/2} \amalg_t f_{1/2}$. The Julia set of $f_{1/2}$ is given by $[-2, 2] \subset \mathbb{R}$, with $\gamma_{1/2}(1/2) = -2$ and $\gamma_{1/2}(0) = 2$. We have that each point in $(-2, 2)$ is biaccessible to external rays, and further, that $\gamma_{1/2}(t) = \gamma_{1/2}(-t)$ for all t. When self-mating $f_{1/2}$, this identifies each point in $J(f_{1/2})$ with its copy on the opposing Julia set. (See the sample ray equivalence classes marked in Figure 1.12.) We end up with $K(f_{1/2}) \amalg K(f_{1/2}) \cong K(f_{1/2})$.

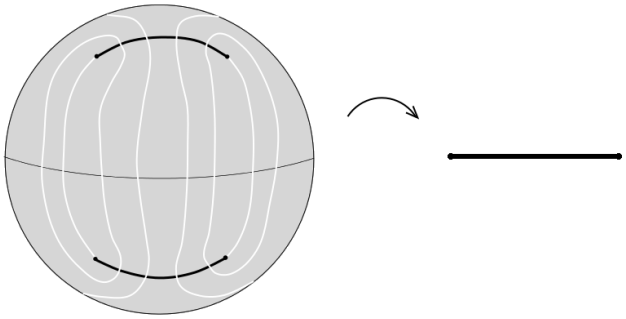

Figure 1.12: The quotient space of $f_{1/2} \amalg_t f_{1/2}$: collapsing equivalence classes of $\sim_{top}$ yields a line segment.

If the quotient space of the topological mating is not the two-sphere, we cannot have a rational map on the two-sphere which is topologically conjugate to our mating map. Thus, the geometric mating of f_a and f_b need not always exist. So when do we know that we can obtain a two-sphere in taking the topological mating? We utilize a result of H.L. Moore's:

Theorem 1.22. *Let $\sim$ be any equivalence relation on the sphere $\mathbb{S}^2$ which is topologically closed. (That is, we assume that the set of all pairs (x, y) with $x \sim y$ forms a closed subset of $\mathbb{S}^2 \times \mathbb{S}^2$.) Assume also that each equivalence class is connected, but is not the entire sphere. Then the quotient space $\mathbb{S}^2/\sim$ is itself homeomorphic to $\mathbb{S}^2$ if and only if no equivalence class separates the sphere into two or more connected components.* [18]

We have that $\sim_{top}$ is a topologically closed equivalence relation whose equivalence classes are connected. (All equivalence classes are formed of external ray-pairs joined at landing points on $K(f_a)$ or $K(f_b)$.) Further, none of these equivalence classes contain all of $\mathbb{S}^2_{a,b}$. (For identification and forward orbit considerations, the external angles of periodic landing points associated within the same ray equivalence class must have the same denominator.) The underlying implication of this theorem for us is then that $\mathbb{S}^2_{a,b}/\sim_{top}$ is a quotient two-sphere if and only if no equivalence class of $\sim_{top}$ contains a Jordan curve on $\mathbb{S}^2_{a,b}$. Intuitively, the problem caused is this: an equivalence class of $\sim_{top}$ containing a Jordan curve will collapse to a point in the quotient space $\mathbb{S}^2_{a,b}/\sim_{top}$. This effectively "pinches off" a section of $\mathbb{S}^2_{a,b}$—so our resulting quotient space cannot be homeomorphic to $\mathbb{S}^2$.

We have already seen a fairly trivial example (Figure 1.12) whose quotient space is not a two-sphere. Another example of a topological mating whose quotient space is not $\mathbb{S}^2$ is shown in Figure 1.13.

Now that we know what type of equivalence classes to avoid when pursuing a quotient two-sphere, a natural question to ask is for what function pairs f_a and f_b can $\sim_{top}$ actually yield a geometric mating. An elegant result in the case of postcritically finite quadratic functions is due to Lei, Rees, and Shishikura:

Theorem 1.23. *For c, c' such that $z \mapsto z^2 + c$ and $z \mapsto z^2 + c'$ are postcritically finite, this function pair admits a geometric mating if and only if c and $\overline{c'}$ are not in the same connected component of $M \backslash \overline{W}$ (where W denotes the main cardioid of M).*

A synonymous phrasing of this theorem is as follows: for Misiurewicz points c and c', $z \mapsto z^2 + c$ and $z \mapsto z^2 + c'$ are matable if and only if c and c' do not lie in complex conjugate limbs of M.[10] [20] [21]

This is an astounding result in that strictly based on parameters alone, we can tell whether the boundaries of two filled Julia sets will glue together to form a quotient two-sphere. This is a *particularly* astounding result when noting the fact that not all filled Julia sets have interiors—it is thus possible to obtain a topological two-sphere by identifying points on two dendrites. (Equivalence classes here can be surprisingly complex, as multiple accessibility of points on these dendrites often allows for several "chains" of external rays to be in the same class. See Figure 1.14.)

For sake of seeking results which can possibly be extended to this rational case and subsequently observed as embedded in $\hat{\mathbb{C}}$, all of the matings investigated subsequently in

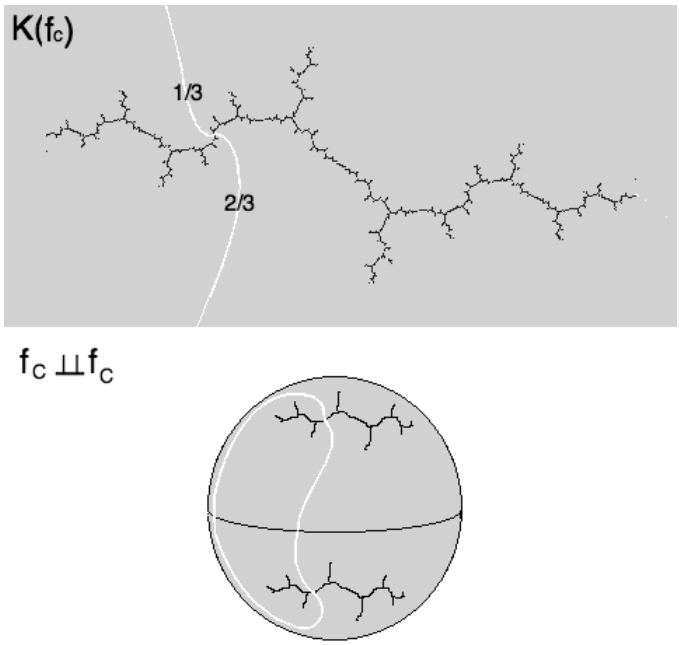

Figure 1.13: A mating possessing a ray equivalence class that forms a Jordan curve. The quotient space of the topological mating cannot be a two-sphere due to collapsing along the depicted equivalence class of rays.

this paper will be constructed from preperiodic quadratic pairs which meet Lei, Rees, and Shishikura's restriction on parameters for c unless otherwise specified.

1.4 Finite Subdivision Rules

If we are to make rigorous the notion of subdivision of tiles, it will be of use to mention the space that formal finite subdivision rules are developed upon: *CW complexes*.

Definition 1.24. *We construct a space inductively via the following procedure:*

1. *Start with a discrete set X^0, whose points we will call* **0-cells**.
2. *Form the* **n-skeleton** X^n *from* X^{n-1} *by attaching open* **n-cells** e^n_α *via maps* $\varphi_\alpha : \mathbb{S}^{n-1} \to X^{n-1}$. *Thus,* X^n *is the quotient space of the disjoint union* $X^{n-1} \bigsqcup_\alpha \overline{e^n_\alpha}$ *of* X^{n-1} *with a collection of closed n-cells* $\overline{e^n_\alpha}$ *under the identifications* $x \sim \varphi_\alpha(x)$ *for* $x \in \partial e^n_\alpha$. *Alternatively, we have* $X^n = X^{n-1} \bigsqcup_\alpha e^n_\alpha$.
3. *Stop the inductive process at some* $n < \infty$, *and set* $X = X^n$.

Any space X constructed in this manner is a **n-dimensional CW complex**. [9]

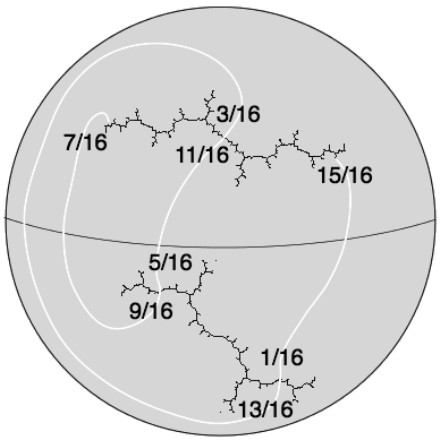

Figure 1.14: The formal mating of $f_{3/8}$ (top) and $f_{1/4}$ (bottom), and a "winding" ray equivalence class. Parameter rays 3/8 and 1/4 do not land in complex conjugate bulbs of M, so $K(f_{3/8}) \amalg K(f_{1/4})$ is actually a two-sphere.

A layman's interpretation of the inductive building process is this: points are 0-cells, open edges are 1-cells, open disks are 2-cells, et cetera—until we have that open n-disks are n-cells. We start with a collection of 0-cells, and attach the boundaries of 1-cells to these 0-cells (without allowing the open 1-cells to "cross" themselves or any other previously placed structure) to form a 1-skeleton. We then attach the boundaries of 2-cells to the 1-skeleton (similarly disallowing "crossing" of previous structures) to form a 2-skeleton. We continue inductively until we form an n-skeleton, i.e., an n-dimensional CW complex.

Graphs are rudimentary examples of 1-dimensional CW complexes: we can picture this inductive construction by starting with the collection of vertices of the graph, and then gluing in open edges to connect the appropriate points. Of utmost importance to us in studying finite subdivision rules will be special 2-dimensional CW complexes which we will refer to as **tilings**. We can think of these as connected planar graphs with tiles attached in the open regions enclosed by the graph's edges and vertices.

In studying how such structures subdivide, it will be useful to formalize what we mean by "subdivision":

Definition 1.25. *We say that Y is a* **subdivision** *of X if $Y = X$ and each closed cell of Y is contained in a closed cell of X.*

For sake of the 2-dimensional CW complexes that we will focus on, this means that our complexes must cover the same space. Further, vertices of Y must be contained somewhere in X, edges of Y must be a subedge of an edge in X or contained in a tile of X, and tiles of Y must be subtiles of tiles of X.

Finite subdivision rules offer a rigorous way to combinatorially characterize how certain tilings can be subdivided:

Definition 1.26. *A* **finite subdivision rule** $\mathcal{R}$ *consists of the following three things:*

1. *A tiling. Formally, this is a finite 2-dimensional CW complex $S_{\mathcal{R}}$, called the subdivision complex, with a fixed cell structure such that $S_{\mathcal{R}}$ is the union of its closed 2-cells. We assume that for each closed 2-cell $\tilde{s}$ of $S_{\mathcal{R}}$ there is a CW structure s on a closed 2-disk such that s has ≥ 3 vertices, the vertices and edges of s are contained in ∂s, and the characteristic map $\psi_s : s \to S_{\mathcal{R}}$ which maps onto $\tilde{s}$ restricts to a homeomorphism on each open cell.*

2. *A subdivided tiling. Formally, this is a finite 2-dimensional CW complex $\mathcal{R}(S_{\mathcal{R}})$ which is a subdivision of the above CW complex $S_{\mathcal{R}}$.*

3. *A continuous cellular map $g_{\mathcal{R}} : \mathcal{R}(S_{\mathcal{R}}) \to S_{\mathcal{R}}$, called the subdivision map, whose restriction to any open cell is a homeomorphism.* [4]

Thus, not only are we restricting to tilings formed by "filling in" connected planar graphs with tiles, these tilings must also have a finite number of vertices, edges, and faces; none of which are monogons or digons. Further, each edge of the tiling must be a boundary edge to some tile. Once we subdivide this tiling, we will need a map that takes open cells of the subdivision tiling homeomorphically to open cells of the original tiling. Only when we have all three components—the initial tiling, the subdivision tiling, and a subdivision map—do we have a complete finite subdivision rule. With all three elements, we obtain a finite combinatorial rule that determines a subdivision of our finite planar tiling. Then, this rule can be applied recursively to yield iterated subdivisions of the original tiling.

Example 1.27. As a fairly simple example, consider the following: on the Riemann sphere, $\widehat{\mathbb{C}}$, mark the real line along with the points $z = 0, \pm 1, \infty$. This gives us a tiling of the sphere by 2 tiles which are topological quadrilaterals—one formed by the upper half plane, one formed by the lower half plane.

If I examine the preimage of this structure under the map $z \mapsto z^2$, I get back both the real and imaginary axes as marked lines, along with the marked points $z = 0, \pm 1, \pm i, \infty$. The preimage of my original tiling—a quadrilateral pillowcase on the two-sphere—has sectioned $\widehat{\mathbb{C}}$ into "orange slices". (See Figure 1.15.) Taking subsequent preimages under $z \mapsto z^2$, we obtain further subdivisions of our initial tilings that yield smaller and smaller "orange slices." □

In the above example, it is fairly simple to visualize the arrangement of tiles, as I've given a familiar analytic map, and concrete 1-skeleton structures in $\widehat{\mathbb{C}}$ for our tiling and subdivided tiling. (In fact, a similar example is reproduced in many introductory complex analysis textbooks.) These analytic and embedded structures, however, are not requirements for a finite subdivision rule. We just need a subdivision complex, its subdivision, and a subdivision map between the two—and as hinted at in the initial definition, these do not need to be analytic. (See Figure 1.16.)

It is entirely possible to obtain much more complicated combinatorial examples with maps of higher degree. Some of these examples, unlike the example above, may not be realizable by a rational map.

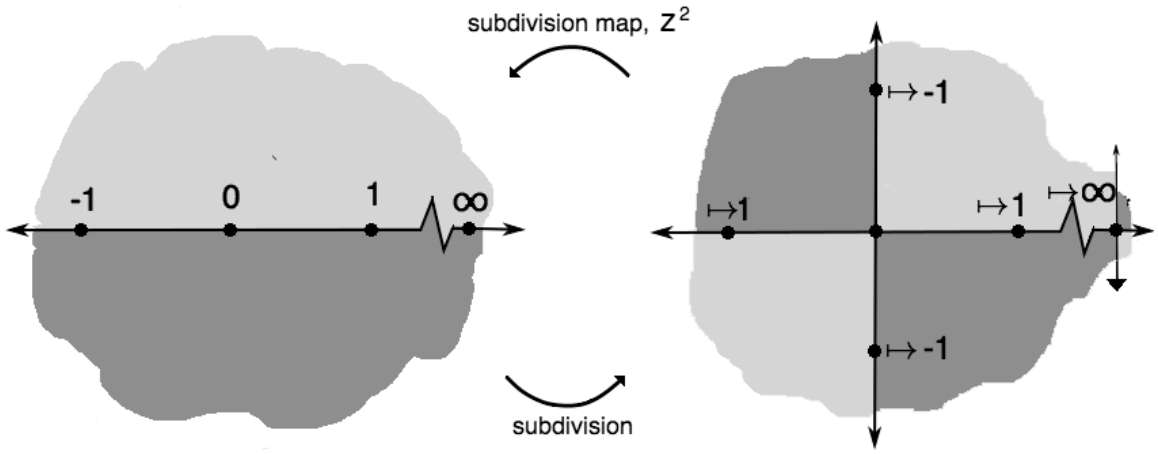

Figure 1.15: Preimages of the map $z \mapsto z^2$ subdivide a tiling of $\widehat{\mathbb{C}}$

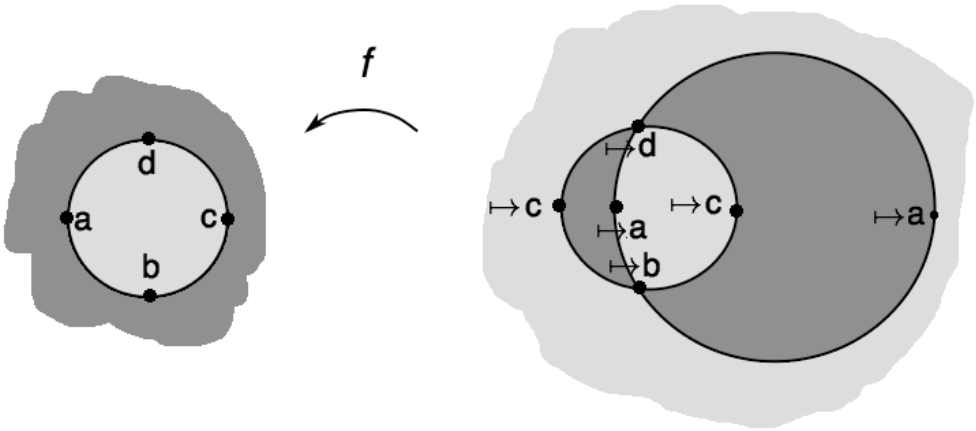

Figure 1.16: Preimages of the map f subdivide a tiling of $\widehat{\mathbb{C}}$. We may take this to be a combinatorial version of our original example.

1.5 Rational maps

With the breadth of background material covered to this point, it may appear that each of the topics discussed so far have barely related—if related at all. Julia sets and external rays were needed in the construction of the mating map, and it can be argued that the emphasis on the combinatorial structure of Hubbard trees plays into the combinatorial emphasis of finite subdivision rules—but how can we link matings and finite subdivision rules?

Here, two results from the literature stand out. First, it is possible to start with a rational map, and then obtain a subdivision rule:

Theorem 1.28. *Suppose that f is a postcritically finite rational map with no periodic critical points. If n is a sufficiently large positive integer, then f^{on} is the subdivision map of a finite subdivision rule."* [1] [5]

Second, it is also possible to start with a rational map, and then obtain a mating of two polynomials:

Theorem 1.29. *Suppose that f is a postcritically finite rational map with no periodic critical points. Then there exists an iterate $f^{\circ n}$ that is obtained as a topological mating of two polynomials P_w, P_b.*[1] [13]

Theorem 1.29 makes heavy utilization of Theorem 1.28 in it's approach: the essence of both is in constructing a finite subdivision rule with 1-skeleton given by a Jordan curve containing the postcritical set of the rational map. Meyer continues along this line of reasoning, however, and in [13] and [15] discusses how edge mappings in the two tile subdivision rule can be used to obtain external angle parameters for two polynomials which mate to form the iterated rational map.

There are also results in the relevant literature on conditions under which finite subdivision rules may yield rational maps (see [3]), and it is trivial from the definition of geometric mating that obtaining rational maps from matings is possible as well. As there are potentially several paths to travel to switch between a subdivision map of a finite subdivision rule, a rational map, and a mating, it is my belief that insight into the links between any pair of these three topics will eventually yield insight into each and on the connections between all three. Thus, although a core emphasis of this paper is to develop insight into the dynamics and structure of matings through the lens of finite subdivision rules, it should be noted that this is a potential stepping stone to the understanding of how rational maps can be composed and decomposed as well.

At this point we have developed the fundamental tools for discussing finite subdivision rules and matings, as well as a brief motivation for investigating connections between the two topics. From here we would like to obtain constructions for developing finite subdivision rules from matings, and determine when these constructions will work. It is thus time to move on to chapter two!

Chapter 2

Constructions

2.1 An introductory construction

Before developing finite subdivision rules on mated maps, we shall start small and apply our prerequisites to tackle a simpler case. How might one develop a finite subdivision rule from a preperiodic polynomial on $\widehat{\mathbb{C}}$?

Recall that we need a tiling which subdivides under a map. If we are given a polynomial, $p : \widehat{\mathbb{C}} \to \widehat{\mathbb{C}}$, that we wish to develop into a finite subdivision rule, it is assumed that we take p to be our subdivision map. This leaves us to find a tiling whose preimage under p yields a subdivision of the initial tiling. Herein lies our interest in Hubbard trees: These forward-invariant trees provide a useful "guess" at base structures to develop subdivision complexes from. Consider the map $f_{1/4}$ as applied to two different structures on $\widehat{\mathbb{C}}$: the Julia set and the Hubbard tree.

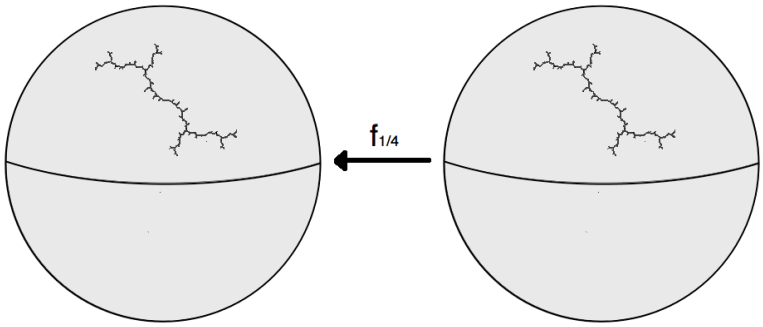

Figure 2.1: The Julia set for $f_{1/4}$ on $\widehat{\mathbb{C}}$

The Julia set $J(f_{1/4})$, as shown in Figure 2.1, is both forward and backward invariant under iterations of the map $f_{1/4}$. The Hubbard tree $T_{1/4}$, as shown in Figure 2.2, is only forward invariant under $f_{1/4}$, and backwards iterations under $f_{1/4}$ approach the Julia set.

We may visualize the complements of these structures in $\widehat{\mathbb{C}}$ as open tiles that we wish to subdivide in our finite subdivision rule. The Julia set does not resemble a 1-skeleton for a

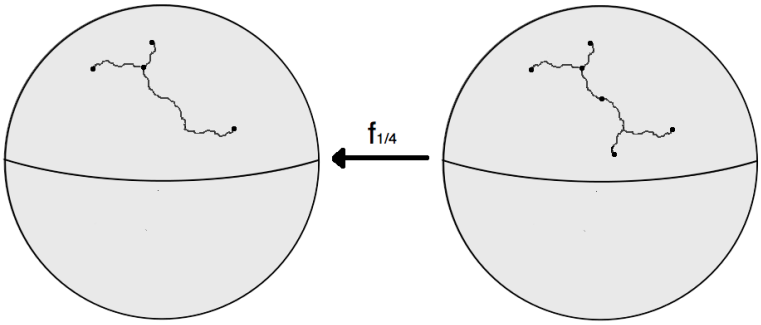

Figure 2.2: The Hubbard tree for $f_{1/4}$ on $\widehat{\mathbb{C}}$

finite subdivision rule, however—it lacks the finite structure which is necessary for our tiling. Thus, as a potential tiling, this option is out. In the case of the Hubbard tree, we have a connected planar graph embedded in $\widehat{\mathbb{C}}$—thus suggesting that we can take $\widehat{\mathbb{C}} \backslash T_{1/4}$ to be an open tile and $T_{1/4}$ to be the 1-skeleton of a subdivision complex. We have two out of three needed components for a subdivision rule and only need a subdivided tiling—but alas, the tiling given by using $T_{1/4}$ as a 1-skeleton does not subdivide under preimages of $f_{1/4}$. As we have merely doubled the number of edges of our original tile rather than subdividing it, we have no subdivision tiling and thus have not constructed a finite subdivision rule for $f_{1/4}$.

Let us examine instead what happens when we consider these sets along with the external ray at 0 out to a marked point at ∞:

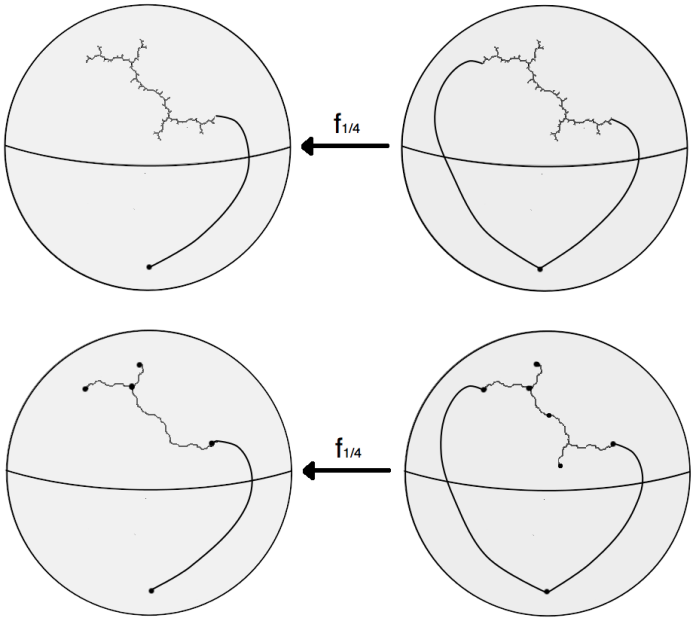

Figure 2.3: The Julia set and Hubbard tree for $f_{1/4}$ along with the external ray of angle 0 on the left; respective preimages on the right.

Taking preimages of both of these structures under $f_{1/4}$ suggests a subdivision of our only tile—but again, only the Hubbard tree variant offers an edge and vertex structure which yields a 1-skeleton that may potentially be used as a subdivision complex. We obtain this complex with very little sacrifice in visualizing the behavior of $f_{1/4}$ on $\widehat{\mathbb{C}}$. Further, allowing this minor sacrifice finally yields a structure which fits the requirements we have sought after: we have a tiling, a subdivision tiling, and a map that sends open cells of the subdivided CW complex to open cells on the original complex. $f_{1/4}$ is thus the subdivision map of a finite subdivision rule.

In retrospect this is a quite natural construction, as we should expect that the 1-skeleton of our tiling contains the postcritical points of our map. (Under subdivisions, our 1-skeletons can be used to observe the local degree behavior of the map, and thus should record where critical and postcritical points are located.) In this example, the insertion of ∞ in forming the Riemann sphere adds a single periodic critical point to the map $f_{1/4}$. By adding an edge to ∞, we include this necessary postcritical point in our 1-skeleton.

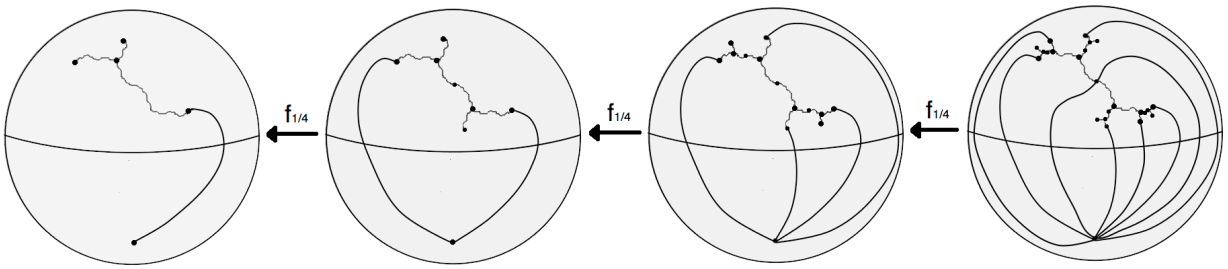

Figure 2.4: Subdivisions of the tiling given by $T_{1/4} \cup R_{1/4}(0)$ under the map $f_{1/4}$

Now that we have the necessary components for a finite subdivision rule, we can take preimages of our 1-skeleton under $f_{1/4}$ to subdivide. Upon taking subsequent subdivisions of this tiling, we can observe as in Figure 2.4 how a series of stripe-like tiles are obtained, bounded by part of the Hubbard tree (or an iterated preimage of the Hubbard tree) and a pair of external rays. We can use such pairings of external rays to denote closed tiles on a particular subdivision by $[R(t_1), R(t_2)]$, where $[R(t_1), R(t_2)] = \bigcup_{t \in [t_1, t_2]} \overline{R(t)}$. Further, we also denote open tiles on a particular subdivision $\mathcal{R}^{on}(S_{\mathcal{R}})$ by $(R(t_1), R(t_2))$, where $(R(t_1), R(t_2)) = [R(t_1), R(t_2)] \backslash X_n$ with X_n being the 1-skeleton of $\mathcal{R}^{on}(S_{\mathcal{R}})$. (See Figure 2.5.)

Since we are dealing with a quadratic map in the example that we've been detailing above, external rays double upon forward iterations of the map. Thus, we can exploit the angle-doubling property along with our interval-like tile structure to easily determine the forward orbit and potential preimages of any given tile under $f_{1/4}$. As all postcritically finite monic quadratic maps share this relationship between external rays and the angle-doubling map, we can generalize this tile behavior. That is, for $t_1, t_2 \in \mathbb{R}/\mathbb{Z}$, we have that:

$$f_\theta([R(t_1), R(t_2)]) = [R(2t_1), R(2t_2)].$$

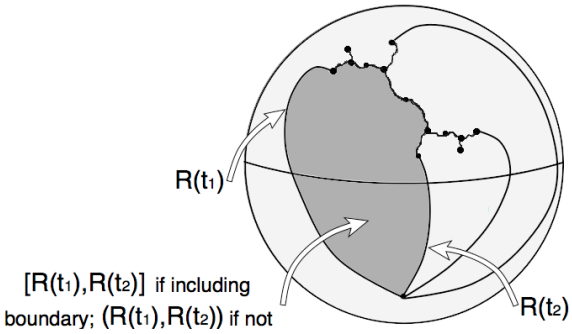

Figure 2.5: Naming scheme for tiles about T_θ

If $0 \notin (t_1, t_2]$, we further have that:

$$(f_\theta)^{-1}([R(t_1), R(t_2)]) = [R(\tfrac{t_1}{2}), R(\tfrac{t_2}{2})] \cup [R(\tfrac{t_1+1}{2}), R(\tfrac{t_2+1}{2})].$$

Finally, if $0 \in (t_1, t_2]$, then:

$$(f_\theta)^{-1}([R(t_1), R(t_2)]) = [R(\tfrac{t_1+1}{2}), R(\tfrac{t_2}{2})] \cup [R(\tfrac{t_1}{2}), R(\tfrac{t_2+1}{2})].$$

Note that we obtain two tiles from each tile preimage—this is because our polynomial is a degree 2 map. The distinction between how tiles split into pairs based on whether they contain the 0 ray stems purely from preserving the cyclic nature of our angle coordinates.

As an example, in the particular finite subdivision rule example we have been developing for $f_{1/4}$, the external ray boundaries of tiles on any nth subdivision are given by dyadic rational numbers: closed tiles look like $[R_{1/4}(\frac{k}{2^n}), R_{1/4}(\frac{k+1}{2^n})], k \in \mathbb{R}/\mathbb{Z}$. Thus, we have that the preimage of the $[R_{1/4}(0), R_{1/4}(\frac{1}{2})]$ tile is $[R_{1/4}(0), R_{1/4}(\frac{1}{4})] \cup [R_{1/4}(\frac{1}{2}), R_{1/4}(\frac{3}{4})]$. This implies that the preimage of the $[R_{1/4}(\frac{1}{2}), R_{1/4}(0)]$ tile is the complementary tile pair $[R_{1/4}(\frac{1}{4}), R_{1/4}(\frac{1}{2})] \cup [R_{1/4}(\frac{3}{4}), R_{1/4}(0)]$.

We must note, however, that we can't pick just any external ray (or rays) to develop a finite subdivision rule. Consider what happens when we use $T_{1/4} \cup R_{1/4}(1/2)$ as our initial 1-skeleton, as in Figure 2.6:

The preimages of $R_{1/4}(1/2)$ are the external rays of angle $1/4$ and $3/4$. The preimage of the suggested CW complex under $f_{1/4}$ here does not yield a subdivision because the open tiles of the "subdivision tiling" do not map to the original tiling. (Notably, $(R_{1/4}(\frac{1}{4}), R_{1/4}(\frac{3}{4}))$ is not contained in $(R_{1/4}(\frac{1}{2}), R_{1/4}(\frac{1}{2}))$.) Another way to view this problem is to note that the 1-skeleton of our chosen CW complex is not forward invariant under $f_{1/4}$. If some edge E is included in our 1-skeleton while $f(E)$ is not, E will be missing in the preimage tiling—as we saw in the previous example. Then, the open tile in the "subdivision" containing E will not map forward to an open tile in the original CW complex.

We can generalize the outcome of the previous example and the above comment by noting the following: if an external ray is included in our initial structure, the forward orbit of that ray under our map must also be included in the structure for there to be a subdivision rule.

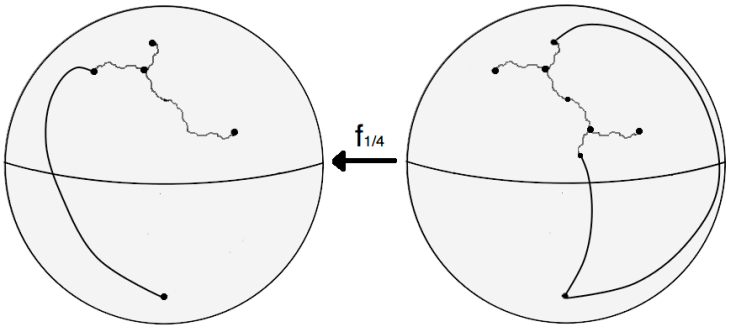

Figure 2.6: The Hubbard tree for $f_{1/4}$ paired with the external ray of angle 1/2 fails to serve as a 1-skeleton for a finite subdivision rule.

We must also impose a similar rule for marked points of our tree structure: any marked point on our 1-skeleton must have all points on its forward orbit be marked points as well.

Further, if we are starting with the Hubbard tree and utilizing external rays, we must ensure that the union of this collection of objects is a connected set before attempting to use it to form a tiling. If it does not form a connected set, we have an annular tile, which is not permissible for a subdivision complex of a finite subdivision rule. (Annular shapes are not n-gons, and thus are not permissible tile shapes.) We can, however, make a modification to the Hubbard tree in order to rectify this problem: start with the minimum spanning tree of the postcritical set *and* landing points of problematic external rays rather than just the minimum spanning tree of the postcritical set. (See Figure 2.7.) If we look at the union of the structures found in the forward orbit of this 1-skeleton, we have a connected set. Further, we meet the condition of having a forward invariant 1-skeleton structure. This new structure now forms a subdivision complex for a finite subdivision rule.

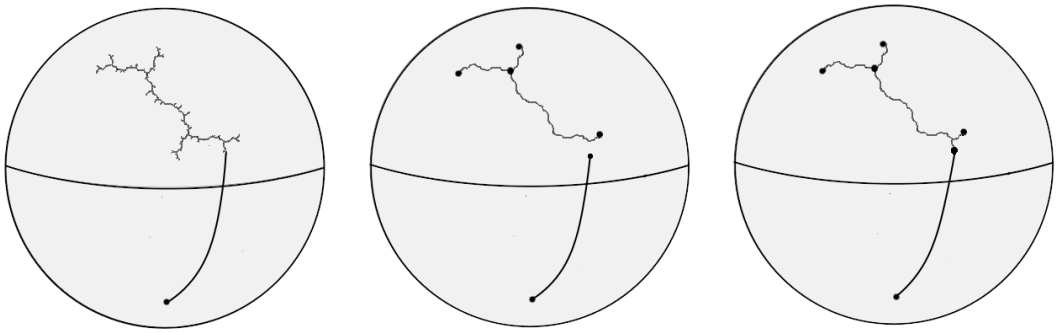

Figure 2.7: If $\gamma_\theta(t) \in J(f_\theta) \backslash T_\theta$, then $R_\theta(t)$ does not land on the Hubbard tree. If none of our chosen rays land on T_θ, we have an annular tile. This can be fixed as shown on the far left by using a modified Hubbard tree.

An important lesson here to carry into subsequent sections is the following: while Hubbard trees are useful building blocks for creating finite subdivision rules, we typically cannot

rely on them alone, or haphazardly glue other components to them in order to develop tilings for finite subdivision rules.

Now that we have seen how a Hubbard tree may be utilized in forming a finite subdivision rule for a polynomial, a natural line of inquiry following Chapter 1 regards how to develop an analogous process for matings. There are a variety of types of matings to start with (formal, degenerate, topological, geometric), and given that matings require a pair of functions, we now have *two* trees to build from. How do we start?

The first step is to consider on which matings a Hubbard-tree based finite subdivision rule construction will be useful. We will show in the following sections that there is much use of this approach in the settings of the formal and degenerate matings. What about the topological and geometric cases? Consider the following example:

Example 2.1. Let θ be some preperiodic angle landing outside of the leftmost bulb of the Mandelbrot set, and examine $f_{1/2} \amalg_t f_\theta$. (Recall that to obtain a geometric mating, the parameter rays for our chosen angles cannot land in complex conjugate bulbs—and that the leftmost bulb is its own complex conjugate.) Before considering any sort of finite subdivision rule structure, we must determine the quotient space for this mating.

Since we've selected our angles to meet the criteria for a geometric mating, the quotient space for the topological mating is topologically equivalent to $\mathbb{S}^2$. Since our quotient space is formed by identifying the boundary of $J(f_{1/2})$ to that of $J(f_\theta)$, and both of the associated functions here are preperiodic, neither of these sets has an interior. We may imagine building S^2 by folding over and gluing $J(f_{1/2})$ to the dendrite $J(f_\theta)$ in a manner prescribed by the equivalence relation $\sim_{top}$ associated with this particular mating.

Here, it should be recalled that $J(f_{1/2}) = T_{1/2} = [-2, 2] \subset \mathbb{R}$. Since we remove no limbs in constructing $T_{1/2}$ from $J(f_{1/2})$, *all* external rays land on $T_{1/2}$ and all of the equivalence classes of $\sim_{top}$ can thus be represented by points in $T_{1/2}$. Thus, if we are to consider building a finite subdivision rule on $\mathbb{S}^2$ for the topological mating $f_{1/2} \amalg_t f_\theta$ by starting with $T_{1/2}$, we are sorely out of luck: $T_{1/2}$ after quotienting by $\sim_{top}$ to obtain the topological mating yields a topological two-sphere. We are then also out of luck for the geometric mating, as it relies on a map which is topologically conjugate to the topological mating. □

While this example suggests that the techniques developed previously in this section are not generalizable to topological or geometric matings, this does not mean that finite subdivision rules have no place in studying these maps. Visualizing how identifications between dendrites builds a topological two-sphere is difficult—thus, it may be beneficial to apply our combinatorial tools to help understand how these quotient spaces are pieced together from pairs of Julia sets.

To tackle this problem in following sections, we will develop several construction schemes for finding finite subdivision rules on formal and degenerate matings. As these schemes are not without problems for certain cases of note, potential obstacles to finding a finite subdivision rule are highlighted along with suggested alternate constructions for reconciling these problems. These obstacles suggest the development of several modified degenerate mating maps, whose constructions will be given later on in this chapter. In these degenerate cases, recursive subdivisions of the combinatorial finite subdivision rule suggest a way to

visualize important point identifications in the topological mating. (This is also detailed later in the chapter.)

As a reminder, all of the matings in the following sections are presumed to be constructed from pairs of functions which are preperiodic monic quadratics, unless otherwise specified. Such quadratics will be labeled f_θ, where θ refers to a parameter ray on M which lands at a Misiurewicz point. We will also assume that these pairs of functions do not correspond to Misiurewicz points in complex conjugate limbs of M, also unless otherwise specified.

To begin, we will build finite subdivision rules starting with the simpler case of our potential mating maps—the formal mating.

2.2 The formal mating

2.2.1 Construction 0

Suppose we are given two preperiodic quadratic polynomials f_a and f_b, and wish to construct a finite subdivision rule on $\mathbb{S}^2$ with subdivision map given by the formal mating $f_a \amalg_f f_b$. As in the previous section, this leaves us to find a tiling whose preimage under $f_a \amalg_f f_b$ yields a subdivision of the initial tiling. If we mimic the approach of the last section by starting with the Julia sets or Hubbard trees related to our subdivision map, note that we now start with two disjoint components: a copy of $J(f_a)$ (or its associated Hubbard tree) on one hemisphere of $\mathbb{S}^2$, and a copy of $J(f_b)$ (or its associated Hubbard tree) on the opposing hemisphere. Preimages of the Julia set pairs are invariant under the formal mating, and preimages of the Hubbard tree pairs iteratively approximate the Julia set pairs under the formal mating. (Recall that the formal mating was defined to have its constituent polynomials acting on their own respective hemispheres—-so we should expect local polynomial behavior off of the equator of $\mathbb{S}^2$.) As an example, we may consider Figure 2.8, which shows these invariant structures for the map $f_{1/4} \amalg_f f_{1/4}$.

If we wish to start with either a single Julia set or single Hubbard tree, or even a single Julia set or Hubbard tree along with a collection of external rays associated with that individual polynomial, we will not obtain a finite subdivision rule with subdivision map given by the formal mating. Here, we run into the same initial problem encountered in developing the finite subdivision rule in the last section: our 1-skeleton does not contain the postcritical set of our map. Further, if we start with the Julia set or Hubbard tree pair (or even one of each), we begin with an annular tile. Such tiles are not permitted in CW complexes that admit a subdivision complex for a finite subdivision rule because they do not possess a 2-disk structure.

To draw upon the lessons learned from the previous example, we could try adding in the external rays $R_a(0)$ and $R_b(0)$ to our Julia set or tree pair to obtain a connected set containing $P_{f_a \amalg_f f_b}$ that will be used to develop a 1-skeleton for a finite subdivision rule. (Note that our external rays must line up at the equator and "connect" our invariant structures to each other somehow; if they do not, our initial tile is still annular.) We see what happens when we apply this construction to $f_{1/4} \amalg_f f_{1/4}$ in Figure 2.9.

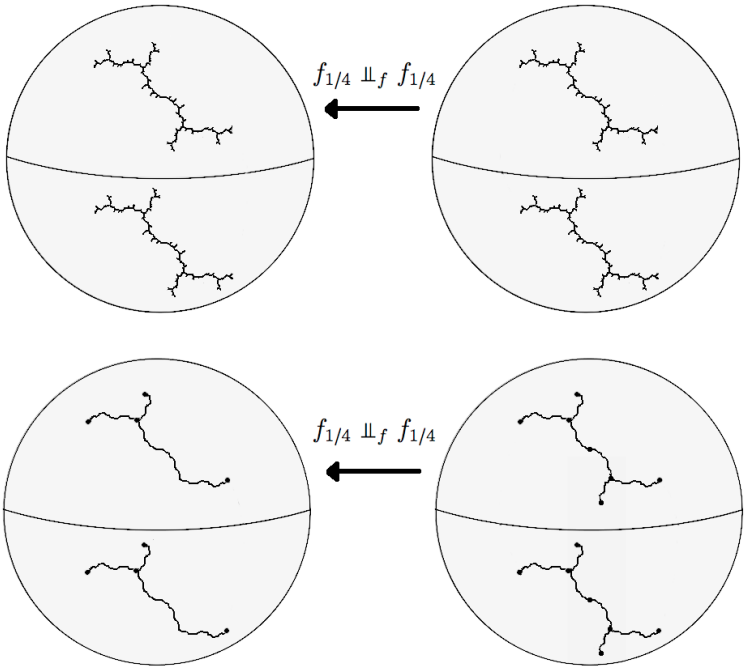

Figure 2.8: Preimages of the Julia set and Hubbard tree pairs on the formal mating $f_{1/4} \amalg_f f_{1/4}$.

As the Hubbard trees reflect the base structure of our map *and* offer an edge and vertex structure suggestive of a 1-skeleton, we opt for using this pairing over the Julia set pairing. Taking the preimage of this structure under the mating $f_{1/4} \amalg_f f_{1/4}$ suggests a subdivision, and restricting to the Hubbard tree and external ray-pairs offers an edge and vertex structure which suggests tilings of $\mathbb{S}^2$. The polynomial structure off the equator and the semiconjugacy relationship near the equator yield that $f_{1/4} \amalg_f f_{1/4}$ acts locally homeomorphically on the two-sphere, as long as we are not on a set including critical points of the map. Since the critical points are included in the 1-skeleton structure we've built, this forces $f_{1/4} \amalg_f f_{1/4}$ to send open cells of the subdivision to open cells of the original tiling. Thus, the tiling, subdivision, and formal mating map in this particular example yield a finite subdivision rule.

We draw further parallels to the previous construction:

1. We can utilize general finite collections of $R_a(t)$ and $R_b(-t)$ ray-pairs in our 1-skeleton (instead of emphasizing the external rays of angle 0), and require that the forward orbit of any ray-pair present in our initial tiling again needs to be present in our initial tiling.

2. If a chosen external ray does not land on its Hubbard tree—i.e., $\gamma(t) \in J(f) \backslash T$—use the minimum spanning tree of the forward orbit of $\gamma(t)$ and the postcritical set instead of the Hubbard tree as the base structure.

3. Marked points on our structure are given by postcritical points, landing points of rays

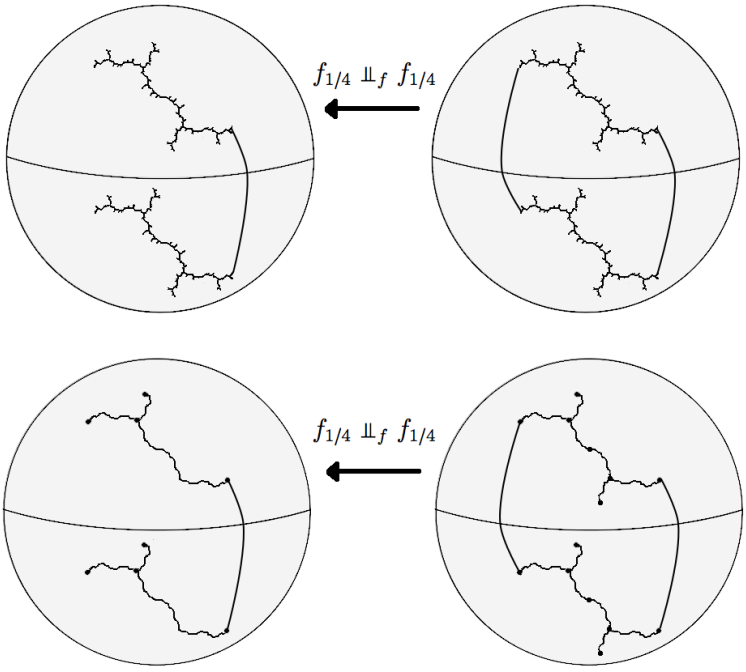

Figure 2.9: Preimages of the Julia set and Hubbard tree pairs along with the 0 rays on $f_{1/4} \amalg_f f_{1/4}$.

off of the equator, branch points, and all of their respective forward images under the mating map.

The above may be formalized with the following definition:

Definition 2.2 (Construction 0)**.** *Given a formal mating $f_a \amalg_f f_b$, select a finite set of external rays on f_a, $\{R_a(t_k)\}_{k=1}^n$, which contains all of the forward images of each of its elements under f_a. Form the disjoint union of the minimum spanning tree of $P_{f_a} \cup \{\gamma_a(t_k)\}_{k=1}^n$ on $J(f_a)$, the minimum spanning tree of $P_{f_b} \cup \{\gamma_b(-t_k)\}_{k=1}^n$ on $J(f_b)$, the collection of rays $\{R_a(t_k)\}_{k=1}^n$, and the collection of rays $\{R_b(-t_k)\}_{k=1}^n$ along with their landing points at infinity. Give this set a graph structure on the quotient space of the formal mating by marking $\{\gamma_a(t_k)\}_{k=1}^n \cup \{\gamma_b(-t_k)\}_{k=1}^n\}$ and all postcritical points and all branch points as vertices. The associated 2-dimensional CW complex will yield our subdivision complex, $S_{\mathcal{R}}$.*

We then take the preimage of this structure under $f_a \amalg_f f_b$, noting preimages of marked points where appropriate. This "subdivided" tiling will be denoted $\mathcal{R}(S_{\mathcal{R}})$. Then, $f_a \amalg_f f_b : \mathcal{R}(S_{\mathcal{R}}) \to S_{\mathcal{R}}$ serves as a subdivision map and $\mathcal{R}$ yields a finite subdivision rule of **Construction 0**.

As an example, consider $f_{1/4} \amalg_f f_{1/4}$:

Example 2.3. We perform Construction 0 on the formal mating $f_{1/4} \amalg_f f_{1/4}$ using the external rays $R_{1/4}(0)$ and $R_{1/4}(\frac{1}{2})$. These identify at the equator, respectively, with the

1/2 and 0 rays of the opposing tree—so we must include these external rays as well. We determine a graph structure on the two-sphere by taking these ray-pairs along with both copies of the Hubbard trees for $f_{1/4}$ and marking postcritical points and branch points as vertices. The associated 2-dimensional CW complex is our subdivision complex.

Preimages of this tiling under $f_{1/4} \amalg_f f_{1/4}$ yield subdivisions of our initial tiling, as in Figure 2.10. □

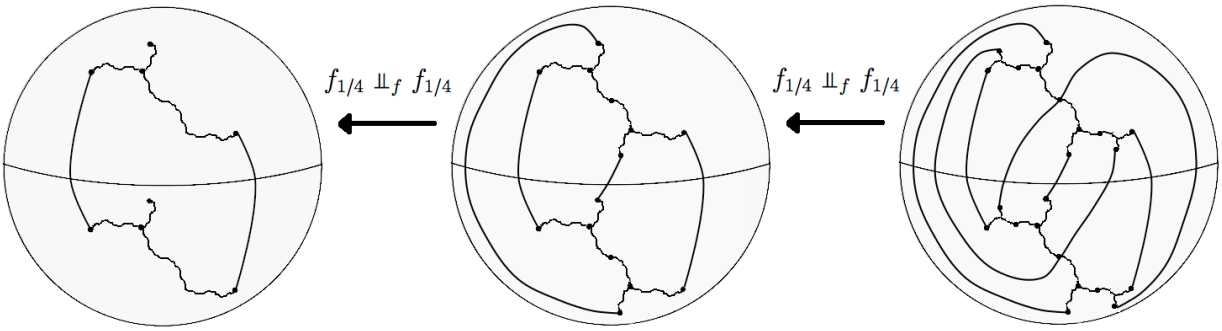

Figure 2.10: Subdivisions of a Construction 0 finite subdivision rule on $f_{1/4} \amalg_f f_{1/4}$. The initial external rays selected for our 1-skeleton are the 0 and $\frac{1}{2}$ rays.

Upon taking successive subdivisions of the tiling, we obtain a series of stripe-like tiles, bounded in part by two external ray-pairs—much like our introductory quadratic polynomial construction. Now that we have a method of constructing finite subdivision rules in the setting of the formal mating, we will adopt a tile naming convention similar to before where we utilize collections of external rays to represent tiles. In this case (and for all subsequent constructions), let $[R_a(t_1), R_a(t_2)]$ denote any closed tile of $\mathcal{R}^{on}(S_{\mathcal{R}})$ with the associated external ray-pair as a boundary and let $(R_a(t_1), R_a(t_2))$ denote any open tile of $\mathcal{R}^{on}(S_{\mathcal{R}})$ with the associated external ray-pair as a boundary. More formally, given a formal mating $f_a \amalg_f f_b$, we have that:

$$[R_a(t_1), R_a(t_2)] = \bigcup_{t \in [t_1, t_2]} \overline{R_a(t)} \cup \bigcup_{t \in [-t_2, -t_1]} \overline{R_b(t)}, \text{ and further,}$$

$$(R_a(t_1), R_a(t_2)) = [R_a(t_1), R_a(t_2)] \backslash X_n, \text{ where } X_n \text{ is the 1-skeleton of } \mathcal{R}^{on}(S_{\mathcal{R}}).$$

As a naming convention we will use the first constituent polynomial referenced in the mating function as a reference polynomial to name tiles from, as noted by the subscripted a notation in our intervals of external rays.

2.3 The degenerate mating

2.3.1 Construction 1: The basic construction

Recall that a major step in forming the degenerate mating is forming the quotient space of $f_a \amalg_d f_b$ by identifying equivalence classes of $\sim_{degen}$ to a point. The only nontrivial equivalence classes of the equivalence relation $\sim_{degen}$ are those composed of external ray chains which contain 2 or more points from the postcritical and critical sets of the formal mating. Preimages of such ray chains that contain at least one point from the postcritical and critical sets are also equivalence classes of $\sim_{degen}$. As the degenerate mating is obtained from the formal mating, it is a natural supposition that we could attempt to form a finite subdivision rule by extending previous methods from the formal mating. The cases in which we are able to do this directly, however, are limited.

A very simple case where we may perform such an extension is when the formal mating is equivalent to the degenerate mating. This occurs when $\sim_{degen}$ is the equality equivalence relation—i.e., each of its equivalence classes contains a single point. We obtain such an equivalence relation when the points in the postcritical and critical set of the formal mating are not identified to any other postcritical or critical points under $\sim_{top}$. (i.e., none of these points lies on a shared chain of ray-pairs collapsed by $\sim_{top}$.) If the formal and degenerate matings are equal, Construction 0 as detailed in the previous section also works for the degenerate case because we start with the same map.

Suppose that postcritical or critical identifications of some sort *were* obtained via $\sim_{degen}$, and that our degenerate mating was not trivially constructed, though. What happens when we start with a permissible tiling for a formal mating and try to use this as a base model for the non-equivalent degenerate mating?

The answer here depends on the two polynomials in our mating, as well as on our choice of external ray-pairs for developing the tiling for our finite subdivision rule. Since any equivalence class of $\sim_{degen}$ collapses to a point in the degenerate mating, this may collapse edges of a Construction 0 tiling for a formal mating if any of the ray chains included in the 1-skeleton are in equivalence classes of $\sim_{degen}$. This effectively takes the two Hubbard tree structures of the constituent polynomials in our mating and glues them directly to each other at a point or at multiple points. (See Figure 2.11.)

Another possible consequence is that ray chains might be left unchanged by moving to the degenerate mating—if a ray-pair is not part of an equivalence class of $\sim_{degen}$, such edges in our Construction 0 tiling will be left alone. A final consequence is that we might obtain new identifications between Hubbard trees which were not previously accounted for in the tiling built using Construction 0. If the forward orbit of our collection of ray-pairs does not contain the collection of rays that form equivalence classes of $\sim_{degen}$, the remaining equivalence classes will still necessarily be identified to their respective representative points. This could again result in the two Hubbard tree structures being glued directly to each other at a point or at multiple points. (See Figure 2.12 for an example which demonstrates both of these potential outcomes.)

Some of these "quotiented tilings" yield permissible tilings for finite subdivision rules

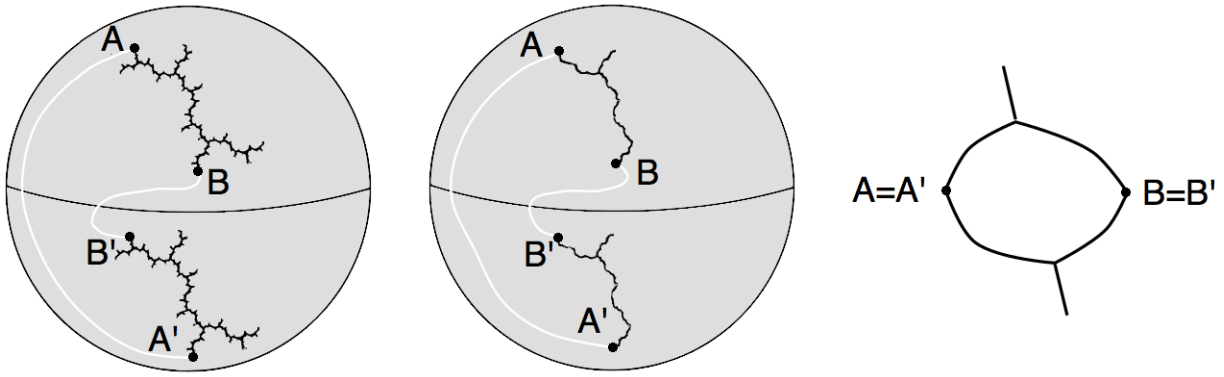

Figure 2.11: External ray-pairs landing at periodic postcritical points of $f_{1/6} \amalg_f f_{1/6}$, and a similar construction restricted to Hubbard trees. The rays shown here collapse under $\sim_{degen}$.

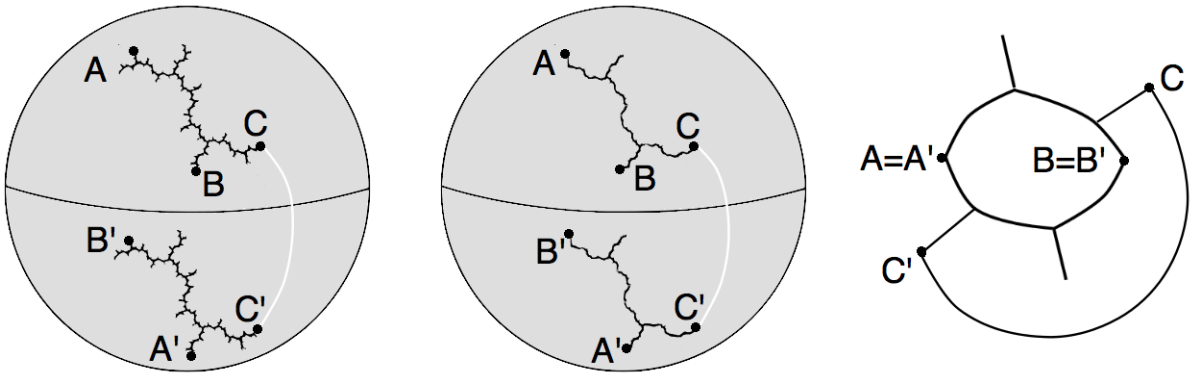

Figure 2.12: The zero external ray-pair on $f_{1/6} \amalg_f f_{1/6}$, and a similar construction restricted to Hubbard trees. This ray-pair does *not* collapse under $\sim_{degen}$; further, we are still forced to collapse identified postcritical points even though this construction did not initially make note of them here.

along with the degenerate mating map—with such cases being documented in this section. Others spawn major problems in developing a finite subdivision rule—such as having our "subdivision map" take an edge of the subdivision tiling (i.e., the preimage tiling) to a single point. (We will discuss these as a motivating case for other constructions as well.) We simply cannot expect the quotient of a tiling to always yield a permissible tiling for a finite subdivision rule in the general case.

With the above revelations, one might notice that we were actually fairly indiscriminate in selecting which external ray-pairs to use for Construction 0 in the first place. As long as the forward orbit of all included external ray-pairs and arms to them from $J(f)$ were included in the construction along with the necessary marked points, we obtained a valid 1-skeleton for a finite subdivision rule. While formally allowable, being this indiscriminate will neither aid in finding working subdivision rules for the degenerate case, nor will it help us use these rules to develop intuition regarding the structure and dynamics of the topological mating.

Consequently, we will focus on tilings which emphasize postcritical and critical identifications unless it is unavoidable to do otherwise. We begin by detailing Construction 1: that is, a suggested method for using the aforementioned "quotiented tiling" as a subdivision complex for a finite subdivision rule. This will be shortly followed by a theorem detailing the cases in which Construction 1 should be expected to generate an admissible rule.

Definition 2.4 (Construction 1)**.** *Given a degenerate mating $f_a \amalg_d f_b$, start with the disjoint union of the pair of Hubbard trees associated with f_a and f_b. If 2 or more points in any equivalence class of $\sim_{degen}$ are present on these trees, collapse the equivalence classes and identify the points as prescribed for the degenerate mating. Give the resulting collection of points a graph structure on the quotient space of the degenerate mating by marking all postcritical points and branched points as vertices. (If need be, we mark additional periodic or preperiodic points on either of the Hubbard trees—along with the points on their forward orbits—to avoid tiles which form digons.) The associated 2-dimensional CW complex will yield our subdivision complex, $S_{\mathcal{R}}$.*

We then take the preimage of this structure under $f_a \amalg_d f_b$, noting preimages of marked points where appropriate. This "subdivided" tiling will be denoted $\mathcal{R}(S_{\mathcal{R}})$.

If $\mathcal{R}(S_{\mathcal{R}})$ is a subdivision of $S_{\mathcal{R}}$ and if the degenerate mating $f_a \amalg_d f_b : \mathcal{R}(S_{\mathcal{R}}) \to S_{\mathcal{R}}$ is a subdivision map (i.e. if it is a continuous cellular map taking open cells of $\mathcal{R}(S_{\mathcal{R}})$ to open cells of $S_{\mathcal{R}}$), then $\mathcal{R}$ yields a finite subdivision rule of **Construction 1**.

The central idea behind this approach is that regardless of whether we intend to identify them or not, groupings of postcritical points and critical points which collapse under the degenerate mating *will* need to be identified on our Hubbard trees if we wish to use the degenerate mating as a subdivision map. (This is due to the fact that these points are identified in the quotient space that the degenerate mating is defined on.) Some identifications which are made between the Julia sets of our polynomials, on the other hand, might not show up in the one-skeleton built in Construction 1—but it turns out that this is necessary for us to develop a finite subdivision rule. Recall that the Hubbard tree iteratively approximates the Julia set under preimages—it is this building back of limbs (whose endpoints are subsequently identified under the degenerate mating) which yields the subdivision of our tiling when we take a preimage under the degenerate mating. We formalize how these notions fit in with Construction 1 with the following theorem:

Theorem 2.5. *Let $\{y_1, ..., y_n\} \subset T_a \bigsqcup T_b, n > 1$, with $y_i \sim_{degen} y_j$ for $i, j \in \{1, ..., n\}$ be an identified point grouping. If $x_1, ..., x_m \in (f_a \amalg_f f_b)^{-1}(\{y_1, ..., y_n\})$ such that $x_i \sim_{top} x_j$ for all $i, j \in \{1, ..., m\}$, we say that the preimage point grouping $\{x_1, ..., x_m\}$ meets condition $(*)$ if and only if $\{x_1, ..., x_m\}/\sim_{degen}$ is a single point.*

Then, Construction 1 admits a finite subdivision rule with subdivision map $f_a \amalg_d f_b$ if and only if $\sim_{degen}$ identifies some point of T_a with some point of T_b and all identified point groupings on $T_a \bigsqcup T_b$ have **only** *preimage point groupings meeting condition $(*)$.*

Essentially, what Theorem 2.5 calls for is a check on the preimages of points identified under $\sim_{degen}$. Each identified point grouping yields two preimage point groupings under the

formal mating (counted up to multiplicity). These preimage groupings identify respectively under $\sim_{top}$. If a preimage point grouping is already identified under $\sim_{degen}$, we avoid the nasty case of possibly having an unidentified ray-pair grouping map to a vertex under the degenerate mating. If all identified points have preimage groupings meeting these conditions, we obtain a finite subdivision rule under Construction 1. Further, if we have a finite subdivision rule under Construction 1, we are required to meet these constraints to avoid having open edges of $\mathcal{R}(S_{\mathcal{R}})$ map to vertices on $S_{\mathcal{R}}$.

Proof. ($\Leftarrow$) : Let $f_a \amalg_d f_b \neq f_a \amalg_f f_b$ and all $x, y \in J(f_a) \bigsqcup J(f_b)$ with $x \sim_{degen} y$ have **only** preimage pairs meeting condition ($*$). Further, let $S_{\mathcal{R}}$ and $\mathcal{R}(S_{\mathcal{R}})$ be constructed for the mating $f_a \amalg_d f_b$ as suggested in Construction 1. In seeking to show that Construction 1 yields a finite subdivision rule, we must show that the following requirements are met:

1. The 1-skeleton of $S_{\mathcal{R}}$ is a connected, forward invariant, finite, planar graph containing all postcritical points as vertices.

2. The complement of this graph on the two sphere has components (i.e. tiles) that are not monogons or digons as dictated by the edges and vertices on the boundaries of respective tiles.

3. The map $f_a \amalg_d f_b$ takes open cells of $\mathcal{R}(S_{\mathcal{R}})$ to open cells of $S_{\mathcal{R}}$.

Requirement 1 is fairly simple: since $\sim_{degen}$ identifies some point of T_a with some point of T_b, we must have that the 1-skeleton which is developed in Construction 1 is connected. Since our base structures T_a and T_b are forward invariant, finite, planar graphs containing postcritical points as vertices on their respective initial spaces, the degenerate mating construction implies that the identified $S_{\mathcal{R}}$ structure of Construction 1 will also be a forward invariant, finite, and planar graph containing all postcritical points on its space under $f_a \amalg_d f_b$.

Requirement 2 is also fairly simple, as it comes trivially with the definition given for Construction 1: we've been given provisions to insert vertices in our construction of $S_{\mathcal{R}}$ to avoid the situation where any tiles are monogons or digons. Since these vertices were inserted along with their forward images, we do not interfere with the above forward invariant requirement on the 1-skeleton of our subdivision complex. Since these vertices are assumed to be periodic or preperiodic, they also do not interfere with the above requirement that our 1-skeleton is a finite graph.

Requirement 3 comes with a bit more work. Since only a finite number of ray-pairs are members of equivalence classes of $\sim_{degen}$, we need to be careful about ensuring that the open 1-cells of $\mathcal{R}(S_{\mathcal{R}})$ map to open 1-cells of $S_{\mathcal{R}}$: these equivalence classes collapse into points on the quotient space of $f_a \amalg_d f_b$. Thus, if there is a case where a non-collapsed edge of $\mathcal{R}(S_{\mathcal{R}})$ maps to a collapsed edge (i.e. vertex) of $S_{\mathcal{R}}$ under the degenerate mating, we have an open 1-cell mapping onto a closed 0-cell. This would mean that the degenerate mating does not serve as a subdivision map and we will not have a finite subdivision rule. Thus, we must check where each of the edges developed in $\mathcal{R}(S_{\mathcal{R}})$ map under $f_a \amalg_d f_b$.

Edges on $\mathcal{R}(S_{\mathcal{R}})$ may come from one of three possible locations: either they are subedges of one of our initial Hubbard trees, preimages of sub edges of one of our initial Hubbard trees, or potentially, we may obtain edges as preimages of identified postcritical points on $S_{\mathcal{R}}$ as noted above.

In the first two cases, note that critical points will be marked points of $\mathcal{R}(S_{\mathcal{R}})$. (They are preimages of the first postcritical points that they map to under the mating.) Since $f_a \amalg_d f_b$ is defined to be equivalent to $f_a \amalg_f f_b$ off an open neighborhood about identified equivalence classes (and the formal mating is homeomorphic off of the critical points) and equivalent to a homeomorphism in the remaining space off of the identified equivalence classes, we have that $f_a \amalg_d f_b$ is a homeomorphism in all places that could potentially contain an open edge of $\mathcal{R}(S_{\mathcal{R}})$. This forces these Hubbard tree-based open 1-cells to map to open 1-cells of $S_{\mathcal{R}}$.

In the event that we must examine preimages of identified postcritical points on $S_{\mathcal{R}}$, we must check whether these preimages yield edges or vertices of $\mathcal{R}(S_{\mathcal{R}})$. If these preimages are all vertices and never edges, we will have already shown that the only possible open 1-cells of $\mathcal{R}(S_{\mathcal{R}})$ map to open 1-cells.

It is here that we rely on the fact that all preimages of identified postcritical or critical point pairs here have been assumed to meet condition $(*)$. This condition implies that any point identified under the degenerate mating only has preimages which look like collections of points from $J(f_a) \bigsqcup J(f_b)$ that have been identified under $\sim_{degen}$. Thus, since preimages of vertices of $S_{\mathcal{R}}$ can only be vertices of $\mathcal{R}(S_{\mathcal{R}})$, we cannot have open 1-cells mapping to points.

We finally check that open 2-cells of $\mathcal{R}(S_{\mathcal{R}})$ map to open 2-cells of $S_{\mathcal{R}}$. Since $S_{\mathcal{R}}$ contains the postcritical set, and the degenerate mating is a branched covering map of the two-sphere to itself, we must take open tiles to open tiles.

Since the map $f_a \amalg_d f_b$ takes open cells of $\mathcal{R}(S_{\mathcal{R}})$ to open cells of $S_{\mathcal{R}}$, it serves as a subdivision map, and $(S_{\mathcal{R}}, R(S_{\mathcal{R}}), f_a \amalg_d f_b)$ as given by Construction 1 is a finite subdivision rule.

$(\Rightarrow)$: We proceed by contradiction. Suppose that Construction 1 yields a finite subdivision rule for the degenerate mating $f_a \amalg_d f_b$ and either:

Case 1: $\sim_{degen}$ does not identify any point of T_a with any point of T_b, or

Case 2: there exists some identified point grouping $\{x_1, ..., x_n\}$ on $T_a \bigsqcup T_b$ with some preimage grouping $\{x_1', ..., x_n'\}$ failing to meet condition $(*)$.

In Case 1, note that the 1-skeleton formed by $T_a \bigsqcup T_b / \sim_{degen}$ is not a connected set. We have an annular tile in $S_{\mathcal{R}}$, which is contrary to the notion that $S_{\mathcal{R}}$ is the subdivision complex of a finite subdivision rule.

In Case 2, the failure to meet condition $(*)$ on all identified point groupings implies the following: there exists some collection of vertices $\{y_1, ..., y_n\}$ identified under $\sim_{degen}$ with a preimage point grouping $\{x_1, ..., x_m\}$ that is identified under $\sim_{top}$ but not under $\sim_{degen}$. This means that there is some collection of ray-pairs on the formal mating containing $\{x_1, ..., x_m\}$ that identifies to a point in the topological mating. Since this collection does not identify under $\sim_{degen}$, however, we have that this collection of ray-pairs forms a nontrivial tree on the quotient space of the degenerate mating. This tree maps forward to a separate tree

containing $\{y_1, ..., y_n\}$ under the formal mating—but since this image tree and $\{y_1, ..., y_n\}$ identify under $\sim_{degen}$, this implies that the tree containing $\{x_1, ..., x_m\}$ maps to a point under the degenerate mating. Since the tree containing $\{x_1, ..., x_m\}$ was nontrivial, we have that the degenerate mating takes a collection of edges to a point. This is contrary to the notion that the degenerate mating is a subdivision map for a finite subdivision rule, since we have open 1-cells being sent to closed 0-cells under the map.

In consideration of both of these cases, we must have that if Construction 1 yields a finite subdivision rule for the degenerate mating, then the degenerate mating is not equivalent to the formal mating and all identified point groupings on $T_a \sqcup T_b$ have only preimage point groupings meeting condition $(*)$. □

As a side note, it *might* be possible that the hypothesis of the above theorem could be rephrased to ask for $f_a \amalg_d f_b$ to be a nontrivial mating rather than specifically requiring that $\sim_{degen}$ identifies a point of T_a to T_b. Why? If all nontrivial degenerate matings involve identifications between opposing trees, we could obtain a connected 1-skeleton by simply requesting a nontrivial mating rather than requesting that the Hubbard trees are identified together. If it is possible to preclude the case where the postcritical points of f_a identify to a multiply accessible point of $J(f_b) \backslash T_b$ (or vice versa), we could make this substitution of hypotheses and the conclusion of Theorem 2.5 would still hold—but the author has only anecdotal evidence towards this conjecture.

To highlight a case where Construction 1 yields a finite subdivision rule, consider the mating $f_{1/6} \amalg_d f_{1/6}$:

Example 2.6. Given the mating $f_{1/6} \amalg_d f_{1/6}$, Construction 1 prescribes that we start with the disjoint union of Hubbard trees of the two constituent polynomials in the mating, $f_{1/6}$ and $f_{1/6}$. Rather obviously, the Hubbard tree structures for both of the polynomials here comes out the same, and the Hubbard tree is presented on the left of Figure 2.13.

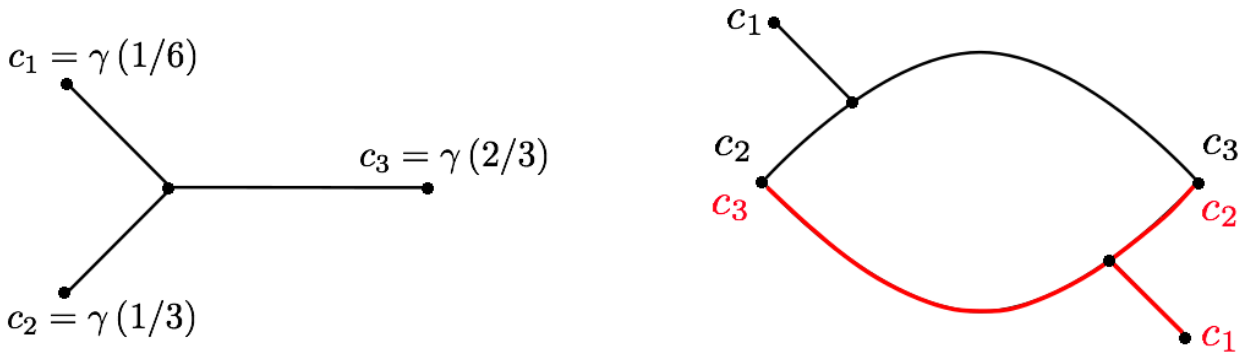

Figure 2.13: The Hubbard tree for $f_{1/6}$, and the Construction 1 subdivision complex, $S_{\mathcal{R}}$, for $f_{1/6} \amalg_d f_{1/6}$

Construction 1 next calls for us to collapse the equivalence classes of $\sim$ *degen*. While all postcritical points of our function pair are contained in nontrivial equivalence classes of $\sim_{degen}$,

the only equivalence classes that collapse points on our Hubbard trees are those associated with the periodic postcritical points. Both identifications as noted on the right of Figure 2.13 make use of the $\frac{1}{3}$–to–$\frac{2}{3}$ angle identification of external rays landing at these points. This identified Hubbard tree pair, along with marked branch points and postcritical points, forms the 1-skeleton $S_{\mathcal{R}}$. (Here the astute reader may have noticed that the Construction 1 subdivision complex for $f_{1/6} \amalg_d f_{1/6}$ has a 1-skeleton that was first hinted at in Figure 2.11.)

We now need to take a preimage of this subdivision complex under the degenerate mating to obtain the subdivided complex $\mathcal{R}(S_{\mathcal{R}})$. Since we developed the construction with emphasis on the topological rather than embedded 1-skeleton structure, it may not be obvious to the reader how we may determine what the resulting 1-skeleton looks like. The Hubbard tree structure is very helpful here: recall that the first preimage of a Hubbard tree yields two miniature copies of the tree which map homeomorphically onto the original, joined at the critical point. This suggests "missing limbs" which when filled in will subdivide the tiles of $S_{\mathcal{R}}$. Noting where each of the marked points maps forward shows where to embed these trees, since the initial 1-skeleton tells us which vertices (and thus which preimages) must be identified. This yields the 1-skeleton of the subdivided complex, $\mathcal{R}(S_{\mathcal{R}})$, as shown in Figure 2.14.

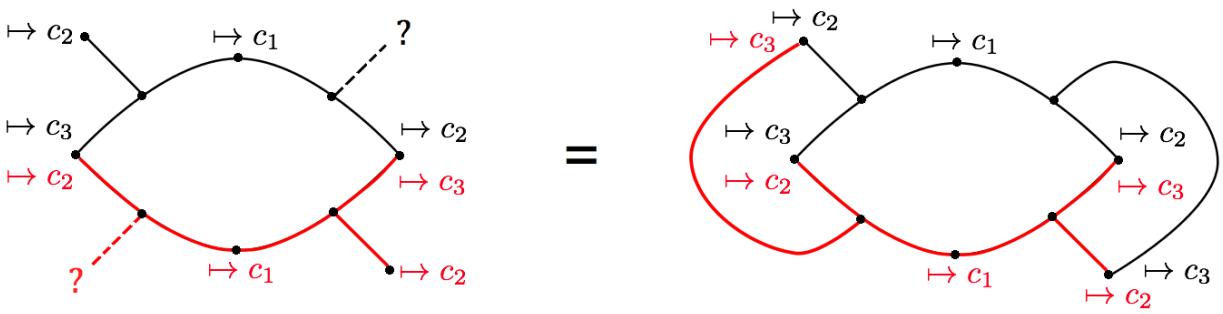

Figure 2.14: Determining the Construction 1 subdivided complex, $\mathcal{R}(S_{\mathcal{R}})$

Note that per Figure 2.14, the endpoints of these missing limbs *are* collapsed as prescribed in Construction 1: here we have that preimages of the initially identified vertices of $S_{\mathcal{R}}$ contain postcritical points, and $\sim_{degen}$ admits nontrivial equivalence classes for such points. □

An important thing to note in the above example is that we can obtain up to the first two subdivisions utilizing the given degenerate mating map, but subsequent subdivisions do not subdivide in the manner suggested by the original tiles. This is because after two subdivisions we exhaust all of the equivalence classes which collapse to form the quotient space for the degenerate mating. This means there are now whole edges in the "subdivisions" after the second recursion that map to points, meaning that the degenerate mating is not actually an allowable subdivision map for these later iterations. This was precisely the problem that we were trying to avoid in developing a setting for when Construction 1 admits a finite subdivision rule.

While it may seem that we have a lost cause in using these examples to study the topological mating, that is not true: keep in mind that finite subdivision rules do not require embedded structures or maps to yield a rule—combinatorially defined rules are perfectly fine. In this case, we may use our Hubbard tree structure and degenerate mating map to pave the way for developing a purely combinatorial finite subdivision rule on the first iteration. (This is, in part, why the figures and examples after developing Construction 1 have somewhat de-emphasized the mating map as being embedded on the two-sphere.) After we find a workable rule, we can then take the purely combinatorial structures inherent in the construction to determine future subdivisions. While this is not the degenerate mating per se (the subsequent subdivisions would suggest an infinite number of point identifications by $\sim_{degen}$ as we keep on subdividing; and we can only have a finite number of identifications per the definition of the degenerate mating map), the initial combinatorial rule is determined by the degenerate mating structure. It tells us upon subsequent subdivisions what key identifications are made in the topological mating—any time the opposing Hubbard tree structures meet, we have a point identification which was made in developing the topological mating.

Now that we are armed with motivation for applying our basic construction to mating maps, it would be wise to find other examples to study and apply our methods to. Theorem 2.5 certainly gives a criterion for when a particular quadratic pair yields a Construction 1 finite subdivision rule, but it does not give much insight into how we could seek out function pairs that work. So, when is there potential for Construction 1 to yield a valid finite subdivision rule?

To answer this question, condition $(*)$ of Theorem 2.5 suggests that we think about when nontrivial degenerate mating maps identify points in their quotient spaces. We have one of two potential manners in which the points of a disjoint union of Hubbard trees can collapse under $\sim_{degen}$. As all nontrivial degenerate matings involve postcritical identification somewhere, we may have critical orbit to critical orbit identifications only, or alternatively we have critical-orbit to non–critical-orbit identifications somewhere on the 1-skeleton of $S_{\mathcal{R}}$.

In the first case, we can look at parameter rays to suggest functions: the denominators need to be offset by some power of 2. Further, the external angles of periodic postcritical points on one function must be "conjugate" to the external angles of periodic postcritical points for the opposing function. In Example 2.6, the points in the critical orbit on both our Hubbard trees follow the mapping scheme:

$$\gamma(\tfrac{1}{12}) = \gamma(\tfrac{7}{12}) \longrightarrow \gamma(\tfrac{1}{6}) \longrightarrow \gamma(\tfrac{1}{3}) \longrightarrow \gamma(\tfrac{2}{3})$$

Since there is a 1/3 and 2/3 parameter on one tree and an opposing $-1/3 \cong 2/3$ and $-2/3 \cong 1/3$ on the other tree, we are guaranteed postcritical identifications. Whether this map will actually meet the criteria posed in Theorem 2.5 is not purely guaranteed by noting identifications on this mapping scheme—but noting parameters and forward orbits of the critical point of our function pairs does give us at least a starting ground for functions to test.

In the alternate case of function pairs that could potentially yield Construction 1 finite subdivision rules, we have postcritical to non-postcritical identifications somewhere on the

1-skeleton of $S_{\mathcal{R}}$. These are a bit harder to single out based on function parameters, since postcritical points of one tree may identify through multiply accessible points on the opposing tree. These multiply accessible points are not necessarily on any critical orbit. To demonstrate, consider the following example:

Example 2.7. Compare the critical orbits of the polynomials $f_{1/6}$ and $f_{85/252}$:

$$\gamma(\tfrac{1}{12}) = \gamma(\tfrac{7}{12}) \longrightarrow \gamma(\tfrac{1}{6}) \longrightarrow \gamma(\tfrac{1}{3}) \longrightarrow \gamma(\tfrac{2}{3})$$

$$\gamma(\tfrac{85}{504}) = \gamma(\tfrac{337}{504}) \longrightarrow \gamma(\tfrac{85}{252}) \longrightarrow \gamma(\tfrac{85}{126}) \longrightarrow \gamma(\tfrac{22}{63}) \longrightarrow \gamma(\tfrac{44}{63}) \longrightarrow \gamma(\tfrac{25}{63}) \longrightarrow \gamma(\tfrac{50}{63}) \longrightarrow \gamma(\tfrac{37}{63}) \longrightarrow \gamma(\tfrac{11}{63})$$

The angles at landing points here do not suggest any identifications between postcritical points. If we are particularly worried about having missed postcritical identifications somehow, it can be verified that this is *not* due to having a non-unique parameter labeling of functions (recall this characteristic of Figure 1.5) and further, that the postcritical points of $f_{85/252}$ do not identify to any points on the body of the Hubbard tree $T_{1/6}$.

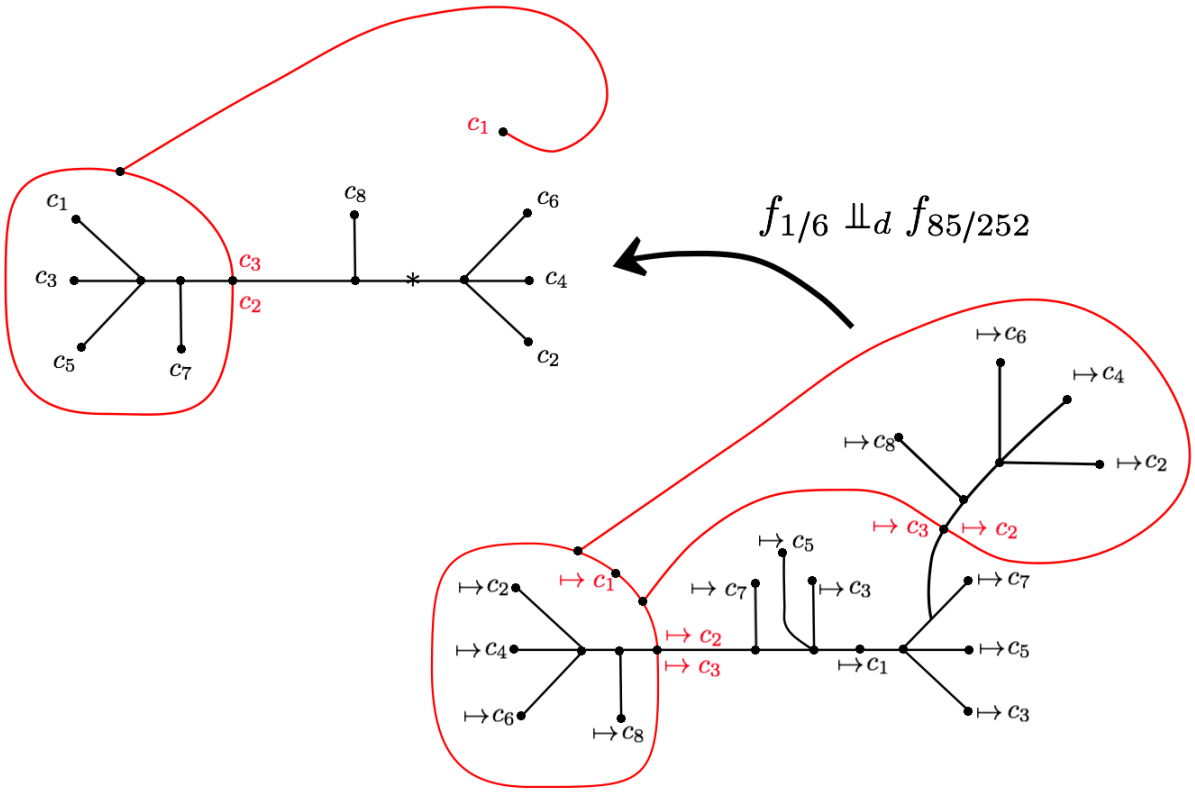

Figure 2.15: The subdivision associated with $f_{1/6} \amalg_d f_{85/252} : \mathcal{R}(S_{\mathcal{R}}) \to S_{\mathcal{R}}$. The Hubbard tree for $f_{1/6}$ is in black; the tree for $f_{85/252}$ is in red.

With that said, the periodic postcritical points of $f_{1/6}$ *do* identify to a multiply accessible point on $T_{85/252}$—namely, the fixed point $\gamma_{85/252}\left(\frac{1}{3}\right) = \gamma_{85/252}\left(\frac{2}{3}\right)$. Thus, we identify two postcritical points of $f_{1/6}$ to each other, but we do it through the *opposing* tree, as shown in Figure 2.15. The 1-skeletons shown in this figure are the subdivision complex $S_{\mathcal{R}}$ and the subdivided complex $\mathcal{R}(S_{\mathcal{R}})$ given by Construction 1 for the degenerate mating map $f_{1/6} \amalg_d f_{85/252}$. □

Now that we have developed an idea of what types of function pairs we may attempt to perform Construction 1 on, the astute reader may observe that the necessary criteria rule out an overwhelming number of maps. This is problematic, as a goal in developing the construction was to create a tool for studying the construction and dynamics of the topological mating. We will need to find other tools to tackle this issue—but first we must develop an understanding of the hurdles in construction that we face in order to prompt ways to work around them.

2.3.2 Problems and motivation for alternate constructions

We've hinted at a few examples in the previous section which will force major problems to occur in using the degenerate mating as the subdivision map of a finite subdivision rule involving Hubbard trees. More generally, when can we expect that these problems occur? Using the postcritical identification scheme as in the last section has typically led to the following 3 "Goldilocks" outcomes experimentally: just the right number of identifications, too few identifications, or too many identifications. An explanation of these outcomes and the types of function pairings most likely to lead to them are briefly summarized as follows:

1. Case 1: The identification between Hubbard trees works out so that preimages yield subdivisions for which the degenerate mating is a subdivision map. This yields a finite subdivision rule as the number of identifications is "just right." This occurs in some (but not all) cases where θ_1 and θ_2 parameters are offset by some power of 2, and some of the external angles of the periodic postcritical points on the respective trees are conjugate (as in Example 2.6). This also occurs in some (but not all) cases where postcritical points of one polynomial identify through a multiply accessible point on the body of the opposing Julia set (as in Example 2.7). If either of these is the case, we may recursively subdivide as much as we desire to in order to iteratively model how identifications between Julia set pairs will work. This identification scheme is detailed by the above **Construction 1**.

2. Case 2: The degenerate mating is equivalent to the formal mating. In such a case, $\sim_{degen}$ is the equality equivalence relation, which does not identify any collection of points on our starting Hubbard tree pair. This failure to connect the 1-skeleton of the CW complex in forming $S_{\mathcal{R}}$ using Construction 1 leaves us with an annular tile. Thus, the number of identifications is "too few"—annular tiles are not permissible in subdivision complexes for finite subdivision rules.

This is easy to fix if we modify our degenerate mating map and/or select appropriate limbs to append to the Hubbard trees prior to determining identifications. Essentially, if we wish to develop a finite subdivision rule which glues together points on the Julia sets of our two functions and avoids external rays to the equator of $\mathbb{S}^2$, we should develop an analogue of the formal mating construction method for the degenerate case. This will be **Construction 2**.

3. Case 3: A number of equivalence classes of points not noted by $\sim_{degen}$ (possibly infinitely many) are "forced" under preimages. This occurs in some (but not all) cases where θ_1 and θ_2 parameters are offset by some power of 2, and the external angles of the periodic postcritical points on the respective trees are conjugate. This also has potential to occur in some (but not all) cases where postcritical identifications are made through a multiply accessible point on one of the Hubbard trees. These settings are in most respects identical to Case 1 where Construction 1 yields a working finite subdivision rule—but subtle differences prevent the degenerate mating from acting as a subdivision map due to these extra identifications. (Details which distinguish these examples from those in which Construction 1 works will be provided later.) Here we do not obtain a finite subdivision rule under Construction 1 because the number of identifications is "too many."

   Some cases as described above can be reconciled by modifying the degenerate mating map. (If reconciling things in this manner is a possibility, this will be **Construction 3**.) Other cases can be reconciled by using only one of the Hubbard tree structures in developing a tiling for the finite subdivision rule. (If reconciling things in this manner will be a possibility, this will be **[De]construction 4**.)

A final potential construction method relating to Hubbard trees will be given for matings that yield subdivision rules utilizing some base structure developed with Construction 1, 2, or 3. This will be **Construction 5**. Construction 5 yields a purely combinatorial finite subdivision rule which does not preserve the embedded structures that we emphasize here. The means of construction for this rule are quite different than those for Constructions 1-4, and if the construction can be successfully applied, the resulting finite subdivision rule relates to the current work of Daniel Meyer. (See [13],[14], and [15].) The author is not yet aware of the circumstances under which this construction is forced to succeed or fail, and hence will provide anecdotal examples with emphasis on relation to the current literature.

2.4 The modified degenerate mating

2.4.1 Construction 2: Too few identifications

Recall that for cases where there are no postcritical identifications in $\sim_{degen}$, $\sim_{degen}$ yields the equality equivalence relation, and we have that the degenerate mating is equivalent to the formal mating. While we have thus far glossed over examples of function pairs that allow

this to occur and only mentioned them in passing, now it will actually be useful to question why and when this happens. So, why no identifications?

To help develop an answer, we will examine the following examples: $f_{1/4} \amalg_d f_{1/6}$, and $f_{1/4} \amalg_d f_{13/14}$:

Example 2.8. Consider the critical orbit of $f_{1/4}$:

$$\gamma_{1/4}(\tfrac{1}{8}) = \gamma(\tfrac{5}{8}) \longrightarrow \gamma_{1/4}(\tfrac{1}{4}) \longrightarrow \gamma_{1/4}(\tfrac{1}{2}) \longrightarrow \gamma_{1/4}(0)$$

Now, consider the critical orbit of $f_{1/6}$:

$$\gamma_{1/6}(\tfrac{1}{12}) = \gamma(\tfrac{7}{12}) \longrightarrow \gamma_{1/6}(\tfrac{1}{6}) \longrightarrow \gamma_{1/6}(\tfrac{1}{3}) \longrightarrow \gamma_{1/6}(\tfrac{2}{3})$$

None of the arguments of the postcritical points of $f_{1/4}$ and $f_{1/6}$ imply that there should be direct identifications between $T_{1/4}(t)$ and $T_{1/6}(-t)$. Our only possible hope is to have postcritical to non-postcritical identifications that involve multiply accessible points, forcing a chain of identified external ray-pairs—but it turns out that there are no such chains for $f_{1/4} \amalg_d f_{1/6}$. (See Figure 2.16.) Here, $f_{1/4} \amalg_d f_{1/6} = f_{1/4} \amalg_f f_{1/6}$. Since no identifications can be made as suggested in Construction 1, we have an annular "tiling". This means that here we cannot have a finite subdivision rule under Construction 1. □

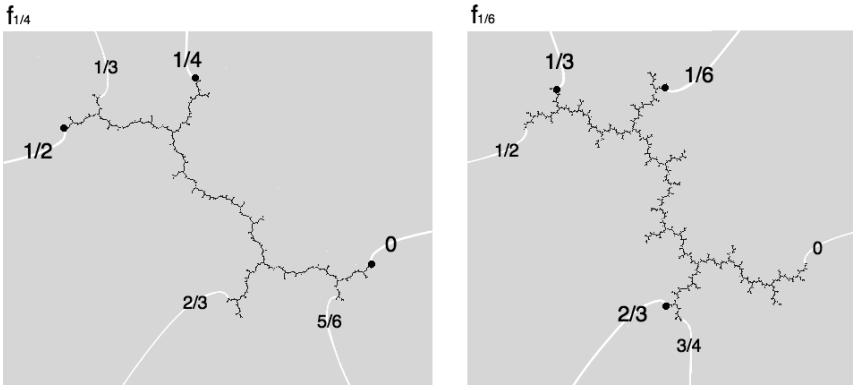

Figure 2.16: External angles to postcritical points on $f_{1/4}$ and $f_{1/6}$, along with where these would identify on the opposing tree.

If we expect a pair of postcritical points to have any hope of being identified in the degenerate mating, the external rays that land at them need to have the same denominator. If postcritical points identify due to being at the ends of an external ray-pair (i.e., their external angles are t and $-t$) this should be clear. I explicitly avoid stating that this is the only allowable case, however, because it simply is not true: if a postcritical point identifies to a biaccessible point or branch point of the opposing Julia set, the external rays leading "out the other side" have a chance at leading to another postcritical point. Since external rays landing at multiply accessible points must have the same denominator, we have that identified postcritical points must have the same denominator.

As hinted at in the last section, it is not difficult to rig our function parameters to guarantee identifications with a little consideration of the angle-doubling map. (Whether these identifications will yield a finite subdivision rule or not is not immediately guaranteed, however). Avoiding immediate identifications—as in Figure 2.16—is similarly easy to rig through consideration of parameters, but it does not guarantee that postcritical points will not be identified under the degenerate mating:

Example 2.9. Consider again the critical orbit of $f_{1/4}$:

$$\gamma_{1/4}(\tfrac{1}{8}) = \gamma(\tfrac{5}{8}) \longrightarrow \gamma_{1/4}(\tfrac{1}{4}) \longrightarrow \gamma_{1/4}(\tfrac{1}{2}) \longrightarrow \gamma_{1/4}(0)$$

And now, consider the critical orbit of $f_{13/14}$:

$$\gamma_{13/14}(\tfrac{13}{28}) = \gamma(\tfrac{27}{28}) \longrightarrow \gamma_{13/14}(\tfrac{13}{14}) \longrightarrow \gamma_{13/14}(\tfrac{6}{7}) \longrightarrow \gamma_{13/14}(\tfrac{5}{7}) \longrightarrow \gamma_{13/14}(\tfrac{3}{7})$$

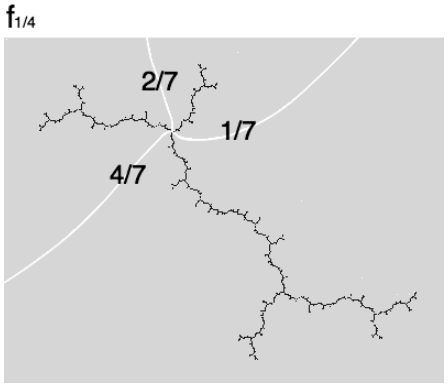

Figure 2.17: External angles at the branch point of $f_{1/4}$.

It's pretty easy to check that we shouldn't expect any immediate postcritical identifications, but consider Figure 2.17: this shows that the periodic postcritical points of $f_{13/14}$ identify at a branch point in $J(f_{1/4})$. This identification of postcritical points of $f_{13/14}$ is not readily apparent from the function parameters, as it occurs through a multiply accessible branch point on the body of the opposing Julia set. □

The previous two examples suggest the following condition to imply that $f_a \amalg_d f_b = f_a \amalg_f f_b$: The periodic postcritical points of f_a do not immediately identify to the periodic postcritical points of f_b, *and* there are no postcritical identifications through multiply accessible points. If this is the case, we can apply Construction 0 to obtain a finite subdivision rule which utilizes $f_a \amalg_d f_b$ as a subdivision map. Alternatively, if we wish to emphasize point identifications (perhaps to get an idea of how the boundaries of $K(f_a)$ and $K(f_b)$ piece together in the topological mating), it is in this specific setting that we wish to develop Construction 2. We now present the required definitions for developing Construction 2 and a theorem asserting the conditions under which it will yield an admissible finite subdivision rule.

Definition 2.10. *Given a pair of preperiodic monic quadratic functions, f_a and f_b, define an equivalence relation $\sim_{con2}$ on the space of the formal mating as follows: select a nonempty finite forward invariant set of periodic and/or preperiodic points on $J(f_a)$, $\{z_1, ..., z_n\}$, and let $[z_1], ..., [z_n]$ be the respective equivalence classes under $\sim_{top}$ of this collection of points. Set $x \sim_{con2} y$ if $x \sim_{top} y$ and $f_a \amalg_f f_b(x), f_a \amalg_f f_b(y) \in [z_i]$ for some i.*

Define a branched covering $f_a \amalg_2 f_b$ as follows: On the complement of open neighborhoods of the nontrivial equivalence classes of $\sim_{con2}$, set $f_a \amalg_2 f_b = f_a \amalg_f f_b$. On the equivalence classes themselves, let $f_a \amalg_2 f_b([z_i]) = [f_a \amalg_f f_b(z_i)]$. Finally, let $f_a \amalg_2 f_b$ be homeomorphic on the remainder of $\mathbb{S}^2$. We will call $f_a \amalg_2 f_b$ the **modified degenerate mating for Construction 2**.

Definition 2.11 (Construction 2)**.** *Given a pair of functions, f_a and f_b, and a collection of points $\{z_1, ..., z_n\} \subset J(f_a)$ as above, let $\{z_1^*, ..., z_m^*\}$ be the collection of points on $J(f_b)$ with $z_i \sim_{top} z_j^*$ for some i, j. Form the disjoint union of the minimum spanning tree of $P_{f_a} \cup \{z_1, ..., z_n\}$ on $J(f_a)$ and the minimum spanning tree of $P_{f_b} \cup \{z_1^*, ..., z_m^*\}$ on $J(f_b)$ and collapse the equivalence classes of $\sim_{con2}$ as prescribed by the modified degenerate mating for Construction 2. Give this set a graph structure on the quotient space of the degenerate mating for Construction 2 by marking all postcritical points, branched points, and points where our trees identify to themselves or each other under $\sim_{con2}$ as vertices. (If need be, we mark additional periodic or preperiodic points on either of the Hubbard trees—along with the points on their forward orbits—to avoid tiles which form digons.) The associated 2-dimensional CW complex will yield our subdivision complex, $S_{\mathcal{R}}$.*

We can then take the preimage of this structure under $f_a \amalg_2 f_b$, noting preimages of marked points where appropriate. This "subdivided" tiling will be denoted $\mathcal{R}(S_{\mathcal{R}})$.

If $\mathcal{R}(S_{\mathcal{R}})$ is a subdivision of $S_{\mathcal{R}}$ and if the modified degenerate mating of construction 2 serves as a subdivision map then $\mathcal{R}$ yields a finite subdivision rule of **Construction 2**.

(Note: We may think of this yielding the same 1-skeleton structures for $S_{\mathcal{R}}$ and $\mathcal{R}(S_{\mathcal{R}})$ as in Construction 0, except with ray-pair groupings in $S_{\mathcal{R}}$ and $\mathcal{R}(S_{\mathcal{R}})$ collapsed under $\sim_{top}$.)

Although not explicitly mentioned in the definition of Construction 2 or its associated modified degenerate mating, recall that an aim of this construction is to determine a finite subdivision rule to model mating maps in which the formal and degenerate cases are equivalent. (It *is* possible to obtain Construction 2 related rules where this is not the case, however.) To find a mating that serves as an intermediate case between the formal and topological constructions, it is then necessary to create a new map. With some discretion, we can pick and choose which identifications to highlight in this new map. As mentioned in the note, this is highly analogous to the formal mating construction described at the beginning of the chapter: instead of needing the forward orbit of all external rays present though, we need the forward orbit of all point identifications present in our 1-skeleton, since here external rays are collapsed. As far as forming a 1-skeleton for a finite subdivision rule utilizing this map, we must not only ensure that we have the appropriate identifications between Hubbard tree structures, we must also ensure that we have made enough identifications to give the preimage 1-skeleton appropriate identifications. Thus, in selecting identifications to

be made, we must require that the first preimages of our selection of identified points are *also* identified. So, in what setting must Construction 2 yield a finite subdivision rule?

Theorem 2.12. *Let $f_a \amalg_2 f_b$, and let $\{y_1, ..., y_n\} \subset J(f_a) \bigsqcup J(f_b)$ with $y_i \sim_{con2} y_j$ for $i, j \in \{1, ..., n\}$ be an identified point grouping. If $x_1, ..., x_m \in (f_a \amalg_f f_b)^{-1}(\{y_1, ..., y_n\})$ such that $x_i \sim_{top} x_j$ for all $i, j \in \{1, ..., m\}$, we say that the preimage point grouping $\{x_1, ..., x_m\}$ meets condition (**) if and only if either*

1. *all of the x_i collapse under $\sim_{con2}$ to a single marked vertex of $S_{\mathcal{R}}$, or*
2. *at most one of the x_i is contained in $S_{\mathcal{R}}$.*

Construction 2 admits a finite subdivision rule with subdivision map $f_a \amalg_2 f_b$ if and only if all identified point groupings on $J(f_a) \bigsqcup J(f_b)$ have **only** *preimage point groupings meeting condition (**).*

Much like the proof of Theorem 2.5, the proof hinges on showing that no identified vertex in $S_{\mathcal{R}}$ has a preimage which is an edge of the 1-skeleton of $\mathcal{R}(S_{\mathcal{R}})$. Since our chosen collection of identified points forces preimage identifications to be included in $\sim_{con2}$, we must check that these forced identifications behave "nicely" when setting up the 1-skeletons for $S_{\mathcal{R}}$ and $\mathcal{R}(S_{\mathcal{R}})$ for our finite subdivision rule.

Proof. ($\Leftarrow$): We again must check the following conditions:

1. The 1-skeleton of $S_{\mathcal{R}}$ is a connected, forward invariant, finite, planar graph containing all postcritical points as vertices.
2. Tiles on $S_{\mathcal{R}}$ are not monogons or digons.
3. The map $f_a \amalg_2 f_b$ takes open cells of $\mathcal{R}(S_{\mathcal{R}})$ to open cells of $S_{\mathcal{R}}$.

Conditions 1 and 2 follow from similar arguments as given in Theorem 2.5 , since the development of the Construction 2 type mating follows a similar structure to that of the degenerate mating. The main point of the proof that necessitates a different argument is showing that all open 1-cells of $\mathcal{R}(S_{\mathcal{R}})$ map to open 1-cells of $S_{\mathcal{R}}$, which depends on the equivalence relation $\sim_{con2}$ and the identifications made in constructing the 1-skeletons of $S_{\mathcal{R}}$ and $\mathcal{R}(S_{\mathcal{R}})$. Much like the proof of Theorem 2.5, however, this is given upon showing that the preimages of all identified points which were collapsed to form the 1-skeleton of $S_{\mathcal{R}}$ are all vertices (and not edges!) of $\mathcal{R}(S_{\mathcal{R}})$.

Let $\{z_1, ..., z_k\}$ be an appropriate collection of points per the definition of the Construction 2 type mating associated with the equivalence relation $\sim_{con2}$. Suppose we have a collection of points $\{y_1, ..., y_n\} \subset J(f_a) \bigsqcup J(f_b)$ identified under $\sim_{con2}$ to a single marked vertex in the 1-skeleton of $S_{\mathcal{R}}$, per the method of Construction 2. Further, suppose that $\{x_1, ..., x_m\} \subset (f_a \amalg_f f_b)^{-1}(\{y_1, ..., y_n\})$ with $\{x_1, ..., x_m\}$ equivalent under $\sim_{top}$. Per the definition of $\sim_{con2}$, since our preimage point grouping identifies under $\sim_{top}$ and maps forward to the same equivalence

class, $[y_1]$, in $\sim_{con2}$, we have that $\{x_1, ..., x_m\}/\sim_{con2}$ is a single point. Thus, any preimage point grouping in $\mathcal{R}(S_\mathcal{R})$ which identifies under $\sim_{top}$ collapses along with the associated external rays contained in its equivalence class to a single vertex. Thus preimages of vertices of $S_\mathcal{R}$ must be vertices (and not edges) of $\mathcal{R}(S_\mathcal{R})$.

($\Rightarrow$): We proceed by contradiction. Suppose that Construction 2 yields a finite subdivision rule for the Construction 2 type mating $f_a \amalg_2 f_b$ and that there exists some identified point grouping $\{y_1, ..., y_n\}$ on $J(f_a) \bigsqcup J(f_b)$ with a preimage point grouping $\{x_1, ..., x_m\}$ that fails to meet condition $(**)$. That is, $\{x_1, ..., x_m\}$ does not collapse to a marked vertex of $S_\mathcal{R}$, and two or more of the x_i are contained in the 1-skeleton $S_\mathcal{R}$.

Since, as above, preimages of vertices of $S_\mathcal{R}$ must be vertices of $\mathcal{R}(S_\mathcal{R})$, we have that the collection of points $\{x_1, ..., x_m\}$ *does* collapse—just not to a vertex of our initial subdivision complex. However, since at least two of the x_i are contained in the 1-skeleton $S_\mathcal{R}$ and we know they identify, this implies that they collapse to a marked point of $S_\mathcal{R}$, per criteria for establishing vertices of this subdivision complex under Construction 2. Thus, we establish a contradiction.

Therefore, we must have that if Construction 2 admits a finite subdivision rule, then all preimage point groupings of marked vertices of $S_\mathcal{R}$ meet condition $(**)$. □

We suggested earlier in this section that $f_{1/4} \amalg_d f_{1/6}$ was a trivial degenerate mating—i.e., this degenerate mating is equivalent to the formal mating of $f_{1/4}$ and $f_{1/6}$. Since trivial degenerate matings are the target setting of Construction 2, let's test out this construction:

Example 2.13. Let $f_a = f_{1/4}$ and $f_b = f_{1/6}$. To determine a finite subdivision rule based on the mating, we must select a nonempty, finite, and forward invariant set of periodic and/or preperiodic points on $J(f_a)$. To keep things simple, let's stick with $\{\gamma_{1/4}(0)\}$. We have only two equivalence classes of $\sim_{top}$ that map onto $[\gamma_{1/4}(0)]$ via the formal mating—$[\gamma_{1/4}(0)]$ itself and $[\gamma_{1/4}(\frac{1}{2})]$. We will set these two equivalence classes of points as the only nontrivial equivalence classes of $\sim_{con2}$ on the two-sphere.

In determining $S_\mathcal{R}$, we must first note the points on $J(f_{1/6})$ that will identify with $\gamma_{1/4}(0)$. We have that only $\gamma_{1/6}(0)$ shares an equivalence class with this point. We can now develop the 1-skeleton of $S_\mathcal{R}$ by forming the disjoint union of the minimum spanning tree of $P_{f_{1/4}} \cup \{\gamma_{1/4}(0)\}$ and the minimum spanning tree of $P_{f_{1/6}} \cup \{\gamma_{1/6}(0)\}$. Since $\gamma_{1/4}(0) \in P_{f_{1/4}}$, the minimum spanning tree of $P_{f_{1/4}} \cup \{\gamma_{1/4}(0)\}$ is the same as the minimum spanning tree of $P_{f_{1/4}}$—which is really just the Hubbard tree $T_{1/4}$. (We can observe in the left and center of Figure 2.18 what the disjoint unions of Hubbard trees and "extended" Hubbard trees look like here.) Once we have this union of trees, we collapse equivalence classes under $\sim_{con2}$. This involves gluing both of our trees together by the landing points of the zero external rays, as in Figure 2.18. (Since the only point that identifies with $\gamma_{1/4}(\frac{1}{2})$ is not on the extended Hubbard tree for $f_{1/6}$, we do not note any identifications there.) At this point, we develop a graph structure by marking vertices which are postcritical, branch points, and points of our trees identified under $\sim_{con2}$. The 2-dimensional CW complex associated with this graph on the 2-sphere is $S_\mathcal{R}$.

To finish up the construction, we must take the preimage of this map under the mating $f_{1/4} \amalg_2 f_{1/6}$ to develop $\mathcal{R}(S_\mathcal{R})$. This is shown in Figure 2.19. □

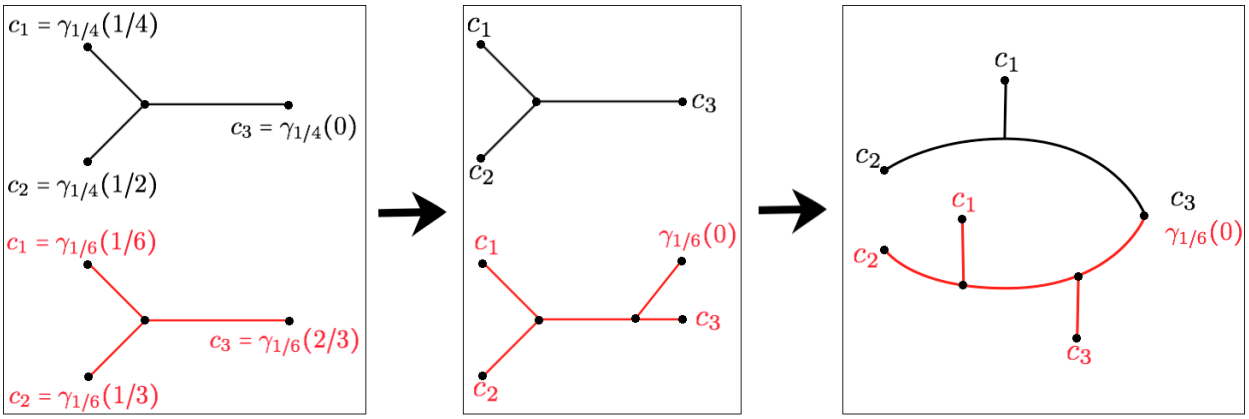

Figure 2.18: Here, we let $f_a = f_{1/4}$ and $f_b = f_{1/6}$, with $T_{1/4}$ shown in black and $T_{1/6}$ shown in red. We determine $S_{\mathcal{R}}$ by identifying the landing points of the 0 rays.

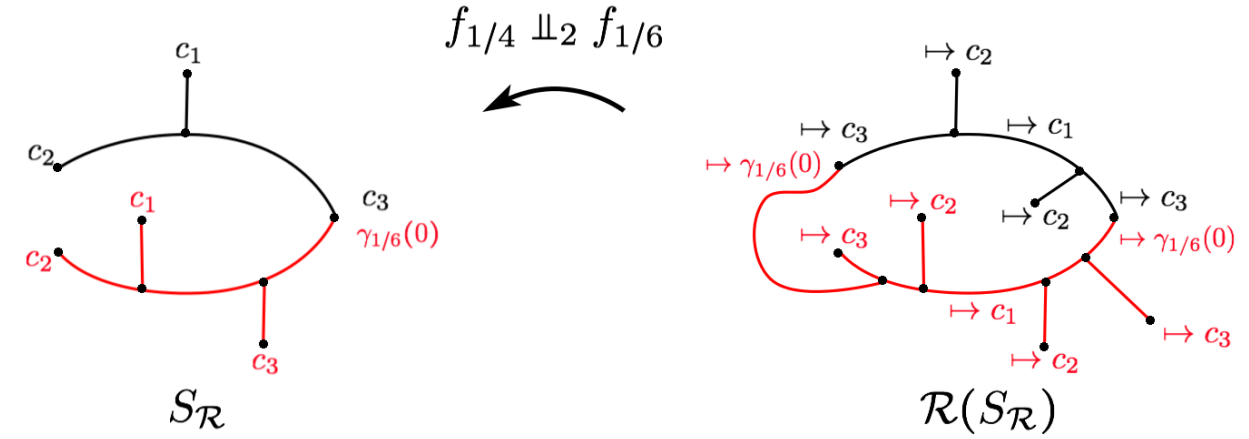

Figure 2.19: A construction 2 type subdivision rule for the mating of $f_{1/4}$ and $f_{1/6}$.

A final note on this construction is that it may actually be applied in cases outside of its intended scope—i.e., for nontrivial degenerate matings. In fact, we may think of the rule given by Construction 1 as a special case of Construction 2 in the event that the degenerate mating directly yields a subdivision rule. (We simply choose the points on $J(f_a)$ which are collapsed and become marked vertices in the 1-skeleton for Construction 1 as our initial collection of vertices in determining $\sim_{con2}$.) In the case that we wish to perform Construction 2 on a function pair that forms a nontrivial degenerate mating, we must be very careful about selecting postcritical points as vertices for developing $\sim_{con2}$, however. While the trivial case lets us choose fairly freely which collection of points to use to form $\sim_{con2}$ (at least as long as it is forward invariant and finite), the tree-to-tree identifications which are "forced" by the degenerate mating might disallow certain selections of points. Consider the following example:

Example 2.14. Recall the Hubbard tree structure of $f_{1/4}$ from Figure 2.18. Given this

information, we may piece together the Construction 2 finite subdivision rule for $f_{1/4} \amalg_{con2} f_{1/4}$ as shown in Figure 2.20 by choosing $\{\gamma_{1/4}(0), \gamma_{1/4}(\frac{1}{2})\}$ as our collection of points in determining $\sim_{con2}$.

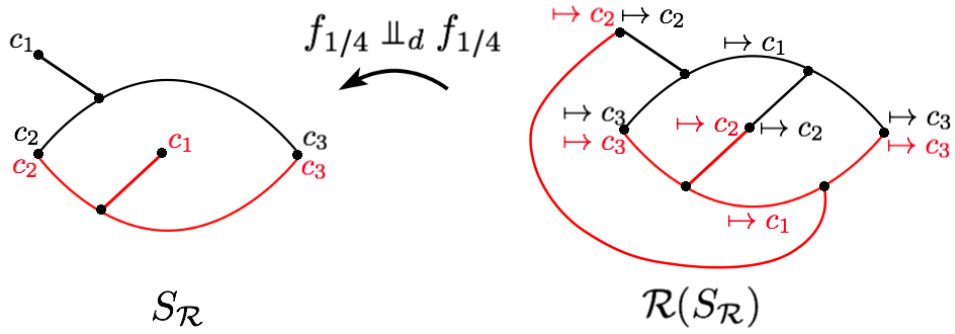

Figure 2.20: A Construction 2 subdivision rule for the self-mating of $f_{1/4}$ which is equivalent to the Construction 1 rule on $f_{1/4} \amalg_d f_{1/4}$

Note, however, what happens in Figure 2.21 if we were to try instead to use the set $\{\gamma_{1/4}(0)\}$ as our collection of points in determining$\sim_{con2}$:

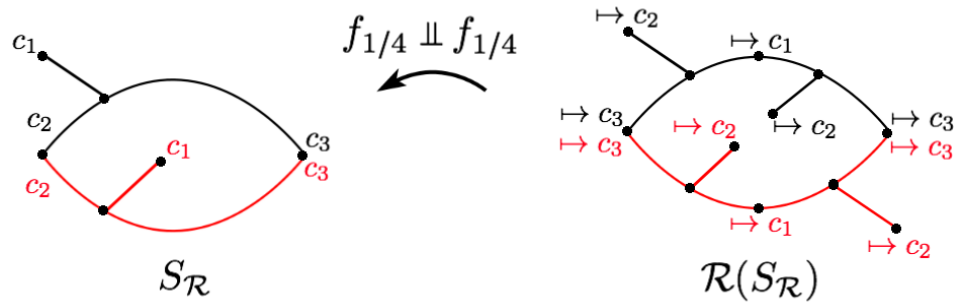

Figure 2.21: Construction 2 can fail to yield a subdivision rule when a nontrivial degenerate mating is involved.

Since preimages of the identified points given in our initial collection become identified under $\sim_{con2}$, the subdivision complex $S_{\mathcal{R}}$ contains vertices that were formed after collapsing the zero external ray-pair *and* the 1/2 external ray-pair. The identifications stop after this first preimage though—so while our initial attempt at a subdivision rule worked, this one fails since it does not identify the necessary preimages of the landing points of the 1/2 rays. (Note that this does indeed fail as a finite subdivision rule: our initial subdivision complex contained two hexagons; the subdivided complex contains two decagons. We do not have that open 2-cells of $\mathcal{R}(S_{\mathcal{R}})$ map homeomorphically to open 2-cells of $S_{\mathcal{R}}$.) □

Since identifications on nontrivial degenerate matings require a bit more rigidity than in Construction 2, we will typically limit the usage of this construction to function pairs whose degenerate mating is equivalent to the formal mating.

2.4.2 Construction 3: Tile pinching and too many identifications

Recall that taking iterated preimages of a Hubbard tree under the map which generates it approximates the Julia set for that polynomial. (Or, in our heavily discretized conception of the Hubbard tree, iterated preimages build back a topological structure which models the Julia set of the polynomial.) We rebuild these structures through preimages by replacing the "missing limbs" which were removed from the Julia set in order to form the Hubbard tree. In Constructions 1 and 2, these missing limbs provide the edges that subdivide tiles of our initial subdivision complexes. To revisit a previous example which yielded a finite subdivision rule under Construction 1, consider Figure 2.20 from the last section, which models a Construction 1/Construction 2 finite subdivision rule based on $f_{1/4} \amalg_d f_{1/4}$. In starting with pairs of identified Hubbard trees for this example, we get that the first preimage under the degenerate mating inserts these missing limbs and simultaneously subdivides both of the initial tiles in our subdivision complex $S_{\mathcal{R}}$. We have that this occurs in a manner that also makes note of the identifications that are made under the degenerate mating. A crucial point to observe here is that the tile subdivision we see upon taking preimages under $f_{1/4} \amalg_d f_{1/4}$ is the result of replacing these missing limbs on our one-skeleton structure: The nth preimage of a quadratic Hubbard tree yields 2^n miniature copies of the Hubbard tree, affixed to each other at the critical point and preimages of the critical point of the associated map. We can use this as a guide to observe where arms are "missing", and can use angle identification considerations to determine where to embed these arms.

As suggested earlier, however, this process can easily go astray. What sort of nontrivial degenerate mating must we have to force Construction 1 to fail? Using Theorem 2.5 to guide our intuition, we should seek a function pairing for our mating with some preimage of identified points not noted by the degenerate mating. Consider the following example:

Example 2.15. We examine Construction 1 as applied to the degenerate mating $f_{1/4} \amalg_d f_{7/8}$. Before beginning our construction, note that the critical orbits of the constituent polynomials in this mating are given by the following:

$$\gamma_{1/4}(\tfrac{1}{8}) = \gamma(\tfrac{5}{8}) \longrightarrow \gamma_{1/4}(\tfrac{1}{4}) \longrightarrow \gamma_{1/4}(\tfrac{1}{2}) \longrightarrow \gamma_{1/4}(0) \circlearrowright$$

$$\gamma_{7/8}(\tfrac{7}{16}) = \gamma_{7/8}(\tfrac{15}{16}) \longrightarrow \gamma_{7/8}(\tfrac{7}{8}) \longrightarrow \gamma_{7/8}(\tfrac{3}{4}) \longrightarrow \gamma_{7/8}(\tfrac{1}{2}) \longrightarrow \gamma_{7/8}(0) \circlearrowright$$

In this case, we have several more t and $-t$ angle identifications under $\sim_{top}$ than we've noted in any example thus far. Noting that $\gamma_{1/4}(1/16), \gamma_{1/4}(9/16) \in T_{1/4}$, we even have identifications of the critical point of $f_{7/8}$ to points not contained on the critical orbit of $f_{1/4}$. Since the only nontrivial equivalence classes of $\sim_{top}$ contained in $\sim_{degen}$ are those that contain a point on the critical orbit of $f_{1/4} \amalg_f f_{7/8}$ and map forward to an equivalence class containing two postcritical points, we have the following identifications of points under $\sim_{degen}$:

$[\gamma_{1/4}(\frac{1}{16})] = [\gamma_{1/4}(\frac{9}{16})] = [\gamma_{7/8}(\frac{7}{16})] = [\gamma_{7/8}(\frac{15}{16})]$
$[\gamma_{1/4}(\frac{1}{8})] = [\gamma(\frac{5}{8})] = [\gamma_{7/8}(\frac{7}{8})]$
$[\gamma_{1/4}(\frac{1}{4})] = [\gamma_{7/8}(\frac{3}{4})]$
$[\gamma_{1/4}(\frac{1}{2})] = [\gamma_{7/8}(\frac{1}{2})]$

$[\gamma_{1/4}(0)] = [\gamma_{7/8}(0)]$

Since we've exhausted all of the points on the critical orbit of $f_{1/4} \amalg_f f_{7/8}$, these are the *only* nontrivial equivalence classes of $\sim_{degen}$. (Also note that the author has emphasized this collection of points because they are the only points of $T_{1/4} \sqcup T_{7/8}$ which are contained in a nontrivial equivalence class of $\sim_{degen}$.)

Now that we have an idea of the structure of $\sim_{degen}$, we may make an attempt at Construction 1 for this mating. We begin with the disjoint union of Hubbard trees of $f_{1/4} \amalg_d f_{7/8}$ (see the left side of Figure 2.22) and then collapse along $\sim_{degen}$ (see the right side of Figure 2.22). To give this a graph structure, we mark all points which are on the critical orbit (this will include all locations where one tree has been glued to another) as well as all points that are branch points of this structure. Since this graph initially gives us a digon (note the tile to the immediate left of the $c_3 \in T_{1/4}$ and $c_4 \in T_{7/8}$ identification in Figure 2.22), we must fix this by marking an additional periodic or preperiodic point so that this tile ends up being a triangle. We choose a point on $T_{7/8}$ which is the preimage of the branched point of $T_{7/8}$. Per the instructions of Construction 1, taking the associated 2-dimensional CW complex with this graph yields $S_{\mathcal{R}}$.

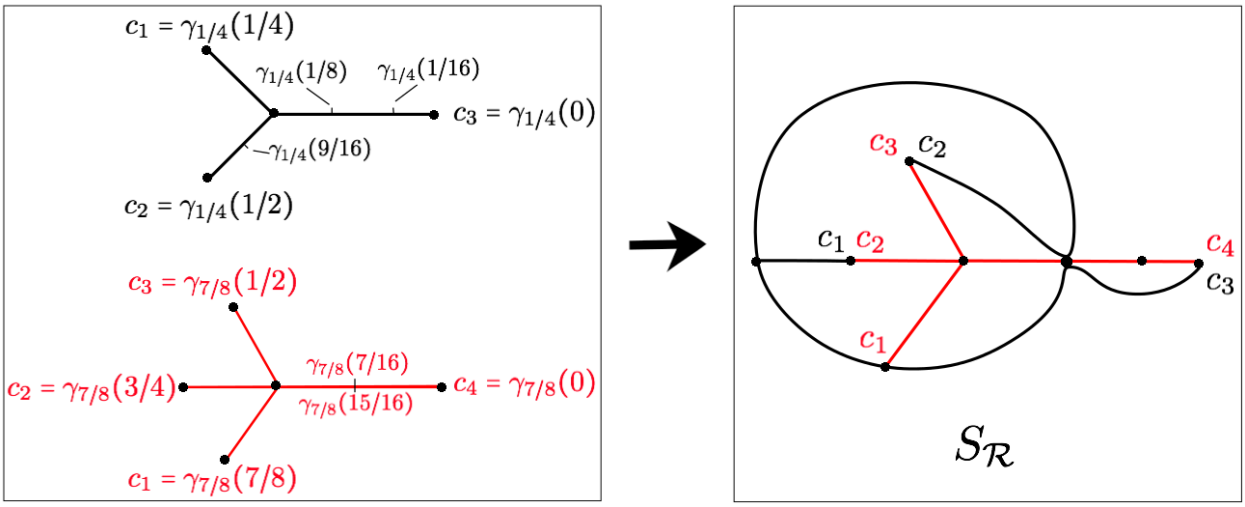

Figure 2.22: $S_{\mathcal{R}}$ for $f_{1/4} \amalg_d f_{7/8}$, as determined by Construction 1. $T_{1/4}$ is shown in black and $T_{7/8}$ in red.

Now we can construct $\mathcal{R}(S_{\mathcal{R}})$ by taking the preimage of $S_{\mathcal{R}}$ under the map $f_{1/4} \amalg_d f_{7/8}$, as in Figure 2.23. We have two hints for how to proceed. First, the preimage of a given Hubbard tree under the mating will appear to yield two miniature copies of that Hubbard tree, affixed to each other at the critical point. (This suggests that we need to embed an arm towards the preimage of the c_2 arm on the black tree, as well as arms toward preimages of points of c_2 and c_3 on the red tree in the figure.) Second, since $S_{\mathcal{R}}$ already contains all possible identifications of points in nontrivial equivalence classes of $\sim_{degen}$, we must embed our missing arms so that they do not intersect other edges or vertices of the graph. (Only the

endpoints of such closed edges may intersect our initial 1-skeleton at the branch point from which the edge extends.) Marking preimages of all marked points gives this new 1-skeleton a graph structure whose associated 2-dimensional CW complex we will denote $\mathcal{R}(S_{\mathcal{R}})$.

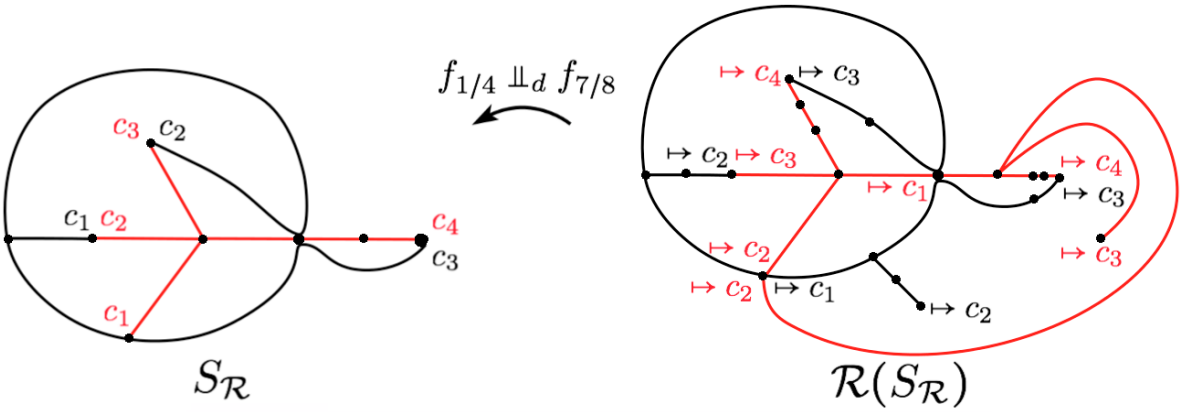

Figure 2.23: A Construction 1 development of $\mathcal{R}(S_{\mathcal{R}})$ for $f_{1/4} \amalg_d f_{7/8}$.

There is a very serious problem in asserting that $\mathcal{R}$ as developed here is a finite subdivision rule. First, note that we are missing some very necessary identifications in $\mathcal{R}(S_{\mathcal{R}})$—for one of the more obvious ones, $S_{\mathcal{R}}$ suggests that there should be an identification between pairs of points that map to $c_2 \in T_{1/4}$ and $c_3 \in T_{7/8}$. The arms we embedded in determining the 1-skeleton of $\mathcal{R}(S_{\mathcal{R}})$ do not meet at the suggested juncture, thus there are preimages of marked points of $S_{\mathcal{R}}$ which do not collapse under $\sim_{degen}$. We do not meet the criteria for Theorem 2.5, and fail to have a finite subdivision rule. The reason for this, as noted in the proof of Theorem 2.5, is that the failure to include preimages of identified points of $S_{\mathcal{R}}$ in nontrivial equivalence classes of $\sim_{degen}$ forces 1-cells of $\mathcal{R}(S_{\mathcal{R}})$ to map to 0-cells of $S_{\mathcal{R}}$. Subdivision maps cannot send open edges to vertices, so we do not obtain a finite subdivision rule. We see in Figure 2.24 all such edges of $\mathcal{R}(S_{\mathcal{R}})$ (marked in dashed blue lines) that map to points of $S_{\mathcal{R}}$. Each distinct dashed blue edge denotes an external ray-pair grouping that collapses under $\sim_{top}$, but not $\sim_{degen}$.

An alternative way to think of the same problem is to note what this does to open tiles in $\mathcal{R}(S_{\mathcal{R}})$: any open tile containing a subsection of a dashed blue edge maps to a chain of open tiles attached by points. These points are where the forward image of the dashed lines collapse. Thus, open 2-cells of $\mathcal{R}(S_{\mathcal{R}})$ do not all map under $f_{1/4} \amalg_d f_{7/8}$ to open cells of $S_{\mathcal{R}}$. This means, again, that the degenerate mating cannot be a subdivision map. We will call this phenomenon **tile pinching**, and observe that it is fairly easy to look for in suggested subdivided complexes $\mathcal{R}(S_{\mathcal{R}})$: if a mated quadratic pair produces a working finite subdivision rule, $\mathcal{R}(S_{\mathcal{R}})$ has twice the number of tiles as $S_{\mathcal{R}}$, since the mating is a degree 2 map. While the initially suggested subdivision complex for $f_{1/4} \amalg_d f_{7/8}$ has six tiles (don't forget to count the "outside" tile!), the suggested $\mathcal{R}(S_{\mathcal{R}})$ only has seven tiles instead of the expected twelve. This is a huge red flag which indicates that we are missing some identifications that are forced by a subdivision map. □

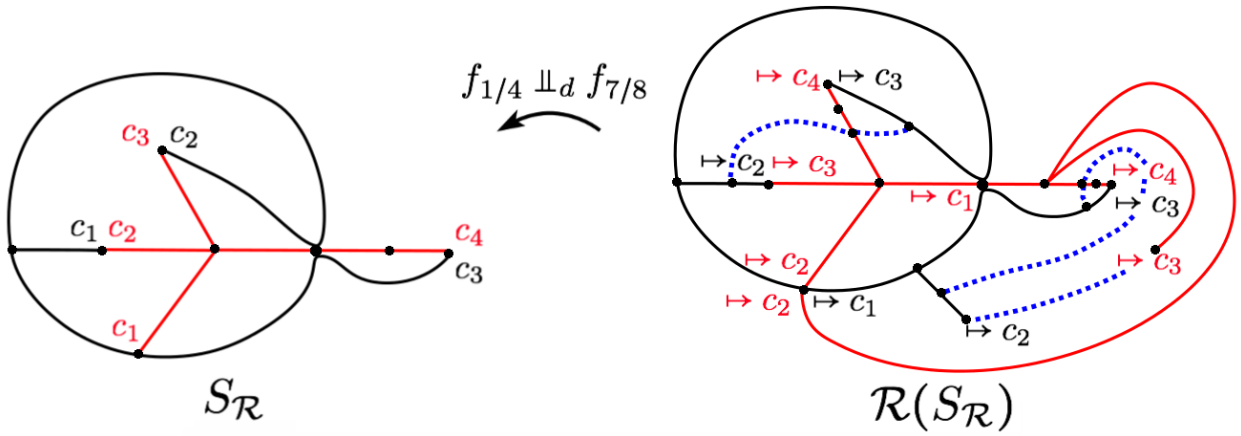

Figure 2.24: Construction 1 fails to form a finite subdivision rule for $f_{1/4} \amalg_d f_{7/8}$—the mating map sends the blue dashed open 1-cells to points.

Here we've demonstrated concretely that degenerate matings with tree–to–tree identifications do not always serve as subdivision maps for attempted Construction 1 type finite subdivision rules. If open 1-cells of the subdivision do not map homeomorphically onto open cells of the original tiling, the degenerate mating cannot serve as a subdivision map for an finite subdivision rule.

This problem in expected mapping properties of open 1-cells hints that there may be "missing" identifications on the 1-skeleton of the suggested subdivision complex of Construction 1, failing the ability to meet condition $(*)$ as given in Theorem 2.5. What is meant by this is that there are locations on the bodies of the two opposing Hubbard trees that *should* have been identified beforehand, but were not: if the problematic edges that map to points were collapsed, we would no longer have a problem with open 1-cells not mapping to open 1-cells via the mating map. We can observe similar problematic behavior when we purposely omit known identifications of the degenerate mating in developing our initial tiling, as in Figure 2.25.

Here, we note the underlying problem: the equivalence relation $\sim_{degen}$ is very rigid about which preimages of identified postcritical points are permitted to be contained together in nontrivial equivalence classes—in some cases we just barely cover enough ground for Construction 1 to admit a useful structure for $S_{\mathcal{R}}$. In other cases, we ignore tree-to-tree identifications that are quite necessary for $S_{\mathcal{R}}$ to have any hope of being practical.

With this idea in mind, how can we formally define a map and relevant construction to form finite subdivision rules with such problematic function pairs? Further, under what conditions can we prove that the construction yields admissible finite subdivision rules?

Definition 2.16. *Let f_a and f_b be a pair of preperiodic monic quadratic functions and let x and y be points in the quotient space of the formal mating. We say that $x \sim_{con3} y$ if and only if x and y meet the following conditions:*

1. $x \sim_{top} y$

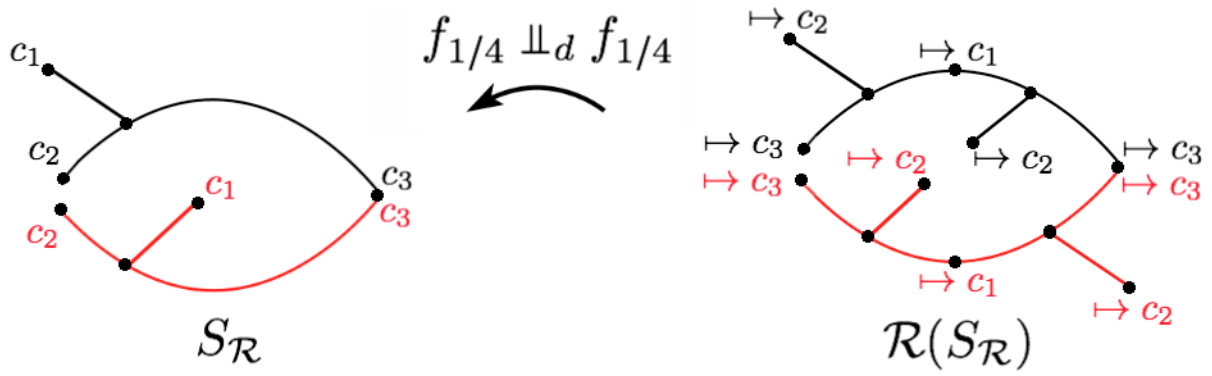

Figure 2.25: We form a map $f_{1/4} \amalg f_{1/4}$ and perform a 1-skeleton construction based on making the zero ray-pair the only nontrivial equivalence class of the associated mating. Omitting previously noted identifications from what would yield a successful Construction 1 rule gives a failed finite subdivision rule.

2. *There exists some $n \in \mathbb{N}$ such that $(f_a \amalg_f f_b)^{on}(x) \sim_{degen} (f_a \amalg_f f_b)^{on}(y)$. (In other words, x and y are contained in an equivalence class of $\sim_{top}$ that eventually maps under the formal mating to some equivalence class containing at least 2 postcritical points of $f_a \amalg_f f_b$.)*

3. *The equivalence class $[x]$ under $\sim_{top}$ either contains two or more points of $T_a \bigsqcup T_b$, or maps via the formal mating $f_a \amalg_f f_b$ to an equivalence class of $\sim_{top}$ containing two or more points of $T_a \bigsqcup T_b$.*

Define a branched covering $f_a \amalg_3 f_b$ as follows: On the complement of open neighborhoods of the nontrivial equivalence classes of $\sim_{con3}$, set $f_a \amalg_3 f_b = f_a \amalg_f f_b$. On the equivalence classes themselves, let $f_a \amalg_3 f_b([x]) = [f_a \amalg_f f_b(x)]$. Finally, set $f_a \amalg_3 f_b$ to be homeomorphic on the remainder of $\mathbb{S}^2$. We will call $f_a \amalg_3 f_b$ the **modified degenerate mating for Construction 3**.

What this modified map does is modeled very strongly after the degenerate mating. Whereas the degenerate mating stops identifying equivalence classes once our preimages exhaust the critical orbit of $f_a \amalg_f f_b$, this new map has potential to keep going and to collapse more equivalence classes if necessary. (We only stop identifying points one iteration after the last Hubbard tree–to–Hubbard tree identification is made.) If there are preimages of points identified under $\sim_{degen}$ that suggest identifications of points on Hubbard trees, $\sim_{con3}$ prescribes for the two trees to be identified where necessary—even if the associated equivalence class contains no points on the critical orbit. The underlying idea in forming $\sim_{con3}$ is to force the preimage of all tree-to-tree identifications to be either pre-existing identifications or tree-to-missing-limb identifications. Once we have the equivalence relation $\sim_{con3}$ settled, the definition of the associated map is formulated similarly to that of the degenerate mating.

So, how might we use this map to determine finite subdivision rules?

Definition 2.17 (Construction 3)**.** *Given a pair of functions, f_a and f_b, start with the disjoint union of the associated pair of Hubbard trees, T_a and T_b. If 2 or more points in any equivalence class of $\sim_{con3}$ are present on these trees, collapse the equivalence classes and identify the points as prescribed for this mating. Give the resulting collection of points a graph structure on the quotient space of the degenerate mating by marking all postcritical points and branched points as vertices. (If need be, mark additional periodic or preperiodic points on either of the Hubbard trees—along with the points on their forward orbits—to avoid tiles which form digons.) The associated 2-dimensional CW complex will yield our subdivision complex, $S_{\mathcal{R}}$.*

We then take the preimage of this structure under $f_a \amalg_3 f_b$, noting preimages of marked points where appropriate. This "subdivided" tiling will be denoted $\mathcal{R}(S_{\mathcal{R}})$.

If $\mathcal{R}(S_{\mathcal{R}})$ is a subdivision of $S_{\mathcal{R}}$ and if the modified degenerate mating of construction 3 serves as a subdivision map, then $\mathcal{R}$ yields a finite subdivision rule of **Construction 3**.

The strong relationship between $\sim_{degen}$ and $\sim_{con3}$ make this construction read much like Construction 1: We start with a pair of Hubbard trees and identify them as prescribed by the mating function that we are using. We may take a preimage to obtain the subdivided tiling, and hopefully the mating will yield a subdivision map to complete our trio of required elements for a finite subdivision rule $\mathcal{R}$. In what cases, however, should we expect that this actually occurs?

Theorem 2.18. *Construction 3 admits a finite subdivision rule with subdivision map $f_a \amalg_3 f_b$ if and only if the number of nontrivial (i.e. not a single point) equivalence classes of $\sim_{con3}$ is nonzero and finite, and if $\sim_{con3}$ identifies some point of T_a to some point of T_b.*

Much as in Construction 2, we are very much at the mercy of our preimages of identified points in determining whether or not our construction will yield a finite subdivision rule: We specify in defining $\sim_{con3}$ that we can form equivalence classes based on preimages as far back as is necessary to take care of all tree-to-tree identifications forced by $\sim_{degen}$. Once we enact this condition however, the map then determines which equivalence classes are forced. There is not necessarily a bound on the number of iterations that will reconcile all identifications—although there is evidence that the number of identifications is parameter-based. In some cases we may be able to take a finite number of steps back to reconcile needed identifications, in other cases there are an infinite number of needed identifications—preventing the existence of a *finite* subdivision rule. (Parameter-based families meeting each of these cases are discussed later on in Chapter 3).

With that said, most of our work in proving the above theorem is fairly similar to the previous cases aside from worrying about this finiteness condition:

Proof. ($\Leftarrow$): We again must check the following conditions:

1. The 1-skeleton of $S_{\mathcal{R}}$ is a connected, forward invariant, finite, planar graph containing all postcritical points as vertices.

2. Tiles on $S_{\mathcal{R}}$ are not monogons or digons.

3. The map $f_a \amalg_3 f_b$ takes open cells of $\mathcal{R}(S_\mathcal{R})$ to open cells of $S_\mathcal{R}$.

Much like Theorem 2.12, Conditions 1 and 2 predominantly follow from similar arguments as given for Theorem 2.5. The only important difference in the case of Construction 3 is that $\sim_{con3}$ is not explicitly defined to have a finite number of nontrivial equivalence classes like $\sim_{degen}$ (associated with Construction 1) or $\sim_{con2}$. Thus, we cannot guarantee for general $\sim_{con3}$ that collapsing trees under $\sim_{con3}$ and marking identified points as vertices will yield a finite graph structure that can be used as a 1-skeleton for $S_\mathcal{R}$—so the general case potentially fails condition 1. Here, however, the hypothesis that we have only a finite number of nontrivial equivalence classes in $\sim_{con3}$ fixes this problem, and we are able to meet the first condition.

Condition 3 follows from a similar argument as given for Theorem 2.12. The argument made in the previous proof relies entirely on the fact that $\sim_{con2}$ is defined to identify the preimage point groupings (as appropriate) for all points that will be marked as vertices of $S_\mathcal{R}$. Since $\sim_{con3}$ does the same, we have that Condition 3 holds as well.

($\Rightarrow$): This argument is also based on noting that preimages of marked points of $S_\mathcal{R}$ are identified under the asserted subdivision map. Thus, it is similar to that given for Theorem 2.12 as well. □

It should be noted that if an example works under Construction 1, Construction 3 will yield an identical combinatorial finite subdivision rule, thanks to the construction of $\sim_{con3}$. With that said, the author has found difficulty in determining nontrivial examples for this case. The failed example detailed as motivation for our construction is a member of a family of matings examined in Subsection 3.2.3 that fails to have subdivision rules by either Construction 1 or Construction 3.

Since we still must find a finite subdivision rule for the pesky unresolved mating of Example 2.15, we move on to examine how such a case has a chance of being resolved.

2.4.3 Construction 4: A "Deconstruction"

As we've seen in the last section, tree-to-tree identifications that show up in preimages of subdivision complexes have a great propensity for causing constructions to fail due to tile pinching. Since we've started out most of our constructions with a pair of Hubbard trees, a natural question to ask is the following: is it possible to throw out one of the trees in order to better our chances of avoiding tile pinching?

In some cases, the answer may be yes. The following problem must be considered in disregarding one of the constituent invariant structures to form a rule, though: If we lose a Hubbard tree, do we lose any postcritical points? Recall from Section 2.1 that a 1-skeleton for a finite subdivision rule must contain the postcritical points of the associated subdivision map. Since we are hoping to build a construction around the mating, this (along with Section 2.1) implies that we cannot randomly remove portions of our invariant structures without giving some consideration to keeping the postcritical set in the 1-skeleton we build.

If we consider the previous trouble-causing function pair of Example 2.15, we may note that in some pairings, there is potential to keep all of the postcritical points on one tree

while deleting the edge structures from the opposing tree on our 1-skeleton. In the pairing of $f_{1/4}$ and $f_{7/8}$, all of the postcritical points of $f_{1/4}$ are identified to postcritical points of $f_{7/8}$. Thus, if we delete $T_{1/4}$, the remaining $T_{7/8}$ still contains all of the identified postcritical points of $f_{1/4} \amalg_d f_{7/8}$.

Before we attempt to form a rule with this example, let's take a look at a formalization of this construction. We will later follow this with a theorem asserting when an admissible finite subdivision should be expected to exist.

Definition 2.19. *Let f_a and f_b be some pair of preperiodic monic quadratic functions with the critical point of f_a identifying via $\sim_{top}$ to some postcritical point of T_b.*

If $T_b/\sim_{degen} \cong T_b$, let $S_{\mathcal{R}}$ be the subdivision complex with 1-skeleton T_b and $\mathcal{R}(S_{\mathcal{R}})$ be the CW complex with 1-skeleton $(f_a \amalg_d f_b)^{-1}(T_b)$.

If $\mathcal{R}(S_{\mathcal{R}})$ is a subdivision of $S_{\mathcal{R}}$ and if the degenerate mating $f_a \amalg_d f_b$ serves as a subdivision map, then $\mathcal{R}$ yields a finite subdivision rule of Construction 4.

Theorem 2.20. *If only two points of $(f_a \amalg_d f_b)^{-1}(T_b)$ are contained in the same equivalence class of $\sim_{degen}$, then $\mathcal{R}$ is a finite subdivision rule.*

In essence, the ideal setting for Construction 4 is the case where one Hubbard tree contains all of the identified postcritical points, and that tree forms a one tile finite subdivision rule under the degenerate mating. (In other words, the complement of the tree on the two-sphere is a tile that is subdivided by the mating map.) For this to happen, a "missing limb" of the Hubbard tree must appear in the preimage, and then be identified to the 1-skeleton $S_{\mathcal{R}}$ at each of its endpoints to subdivide the initial tile.

It is unknown to the author whether the two-point condition given in Theorem 2.20 is a necessary condition for a finite subdivision rule in the setting of Construction 4, but we will show that it is indeed a sufficient one:

Proof. Let $f_a \amalg_d f_b$ be a degenerate mating, and let $S_{\mathcal{R}}$ and $\mathcal{R}(S_{\mathcal{R}})$ be as defined for Construction 4. To show that $\mathcal{R}$ is a finite subdivision rule, we again must check the following conditions:

1. The 1-skeleton of $S_{\mathcal{R}}$ is a connected, forward invariant, finite, planar graph containing all postcritical points as vertices.

2. Tiles on $S_{\mathcal{R}}$ are not monogons or digons.

3. The map$f_a \amalg_d f_b$ takes open cells of $\mathcal{R}(S_{\mathcal{R}})$ to open cells of $S_{\mathcal{R}}$.

To show condition 1, note that $S_{\mathcal{R}} = T_b$, and that the Hubbard tree is a connected, forward invariant, finite, planar structure. T_b contains all of the postcritical points of the mating due to f_b, since the Hubbard tree is defined as the minimal spanning tree of the postcritical points on a polynomial's Julia set. Further, since one of the postcritical points of f_b identifies to the critical point of f_a under $\sim_{top}$, this implies that the forward orbit of these points will also be identified under $\sim_{top}$ due to the angle-doubling semiconjugacy. Thus,

all of the postcritical points of f_a collapse to identify with postcritical points of T_b and we have that our 1-skeleton contains all of the postcritical points as vertices.

To show condition two, note that since our 1-skeleton is a tree, our only possible open tile is given by the complement of that tree in the two-sphere. We cannot obtain a monogon when our 1-skeleton is a tree. To show that we cannot obtain a digon, we proceed by contradiction.

If the only tile of $S_{\mathcal{R}}$ is a digon, we must have a single edge forming the Hubbard tree T_b. This would suggest only two postcritical points in our map.

Recall that our focus has been restricted to the setting of preperiodic monic polynomials for this paper. Because f_b is monic, the critical point must be 0. If we have only two postcritical points, for the map to be preperiodic, we must have the following mapping scheme for f_b:

$$0 \longrightarrow c_1 \longrightarrow c_2 \circlearrowright$$

If $f_b = z^2 + C$, this says that $c_1 = C$, and $c_2 = C^2 + C = c_3 = (C^2 + C)^2 + C$. Solving for C in this equation yields only 0 and -2 as options. We cannot have that $f_b = z^2$, since $z \mapsto z^2$ is not preperiodic. Thus, $f_b = z^2 - 2 = f_{1/2}$.

Recall that per the setting of Construction 4, one of the postcritical points of f_b must identify to a critical point of a. Since the postcritical points of $f_{1/2}$ are $\gamma_{1/2}(1/2)$ and $\gamma_{1/2}(0)$, we must have that f_a has a critical point $\gamma_a(1/2)$ or $\gamma_a(0)$. Using the angle-doubling semi-conjugacy to track the forward orbit of the critical point of f_a, we have that either the critical point is periodic in the case of $\gamma_a(0)$ (which is not permitted since we've restricted to the postcritically finite setting), or that the critical point maps forward to a periodic postcritical point in the case of $\gamma_a(1/2)$. The latter option gives the following mapping scheme for f_a:

$$0' \longrightarrow c_1' \circlearrowright$$

If such is the case and $f_a = z^2 + C'$, this implies that $c_1' = C' = c_2' = (C')^2 + C'$. Solving this equation for C' forces f_a to be periodic, which is again not permitted in the setting of this paper.

Since the only cases that allow digon-shaped tiles to exist involve periodic quadratic functions, we must have that there are no monogons or digons in the tiling.

Finally, to show condition 3 we will need to check that open edges map to open edges (since our 1-skeleton is based on a Hubbard tree and its preimage, this is a given), and further that open tiles map to open tiles. At this point, we require use of the hypothesis for our theorem. We will prove that the nontrivial equivalence class of $\sim_{top}$ referenced must be the equivalence class which contains the critical point of f_a.

As mentioned above, since a postcritical point of f_b identifies with the critical point of f_a, this implies that the forward orbits of these points also collapse pairwise under $\sim_{top}$. Let c_0 and c_1 denote the critical point and critical value of f_a, respectively. Further, let d_0 and d_1 denote the postcritical point of f_b specified in Construction 4 and its image, so that $c_0 \sim_{top} d_0$, and $c_1 \sim_{top} d_1$.

Examine the preimages of c_1 and d_1. Since c_0 is critical, c_1 only has one preimage. Since

d_1 is a postcritical point of a polynomial, it may either have two preimages (one a postcritical point, and one a non postcritical point), or 1 preimage (a critical point). If d_0 *was* critical and identified with c_0, this would suggest that f_a and f_b were complex-conjugate polynomials—which again, is outside of the scope of this section. Thus, d_1 has two preimages—one of which is d_0, and the other which we will denote d_0'.

Since preimages of identified points form identified preimage pairs (and critical points are counted up to multiplicity), we have that $d_0 \sim_{top} c_0$ and $d_0' \sim_{top} c_0$, or $d_0 \sim_{top} d_0'$.

Since only two points in the preimage of T_b are contained in the same equivalence class of $\sim_{top}$, d_0 and d_0' must be these two points. Since $T_b/\sim_{degen} \cong T_b$, d_0' was not a point initially in T_b and must be at the end of a missing limb for this Hubbard tree. Since one endpoint of this limb must be a branch point and the other identifies to d_0, this limb provides a subdivision of our initial tile into two tiles. Do these open tiles map to the complement of T_b in the two-sphere?

The answer is yes, since the degenerate mating is a branched covering map of the two-sphere: T_b is a simply connected closed set containing the postcritical points of the mating, so its complementary tile has a preimage whose components each map onto the original tile. Thus, the open 2-cells of $\mathcal{R}(S_\mathcal{R})$ map to the open 2-cell of $S_\mathcal{R}$.

Since we meet each of the 3 conditions, $\mathcal{R}$ is thus a finite subdivision rule. □

We close this section by applying the construction to our motivating example:

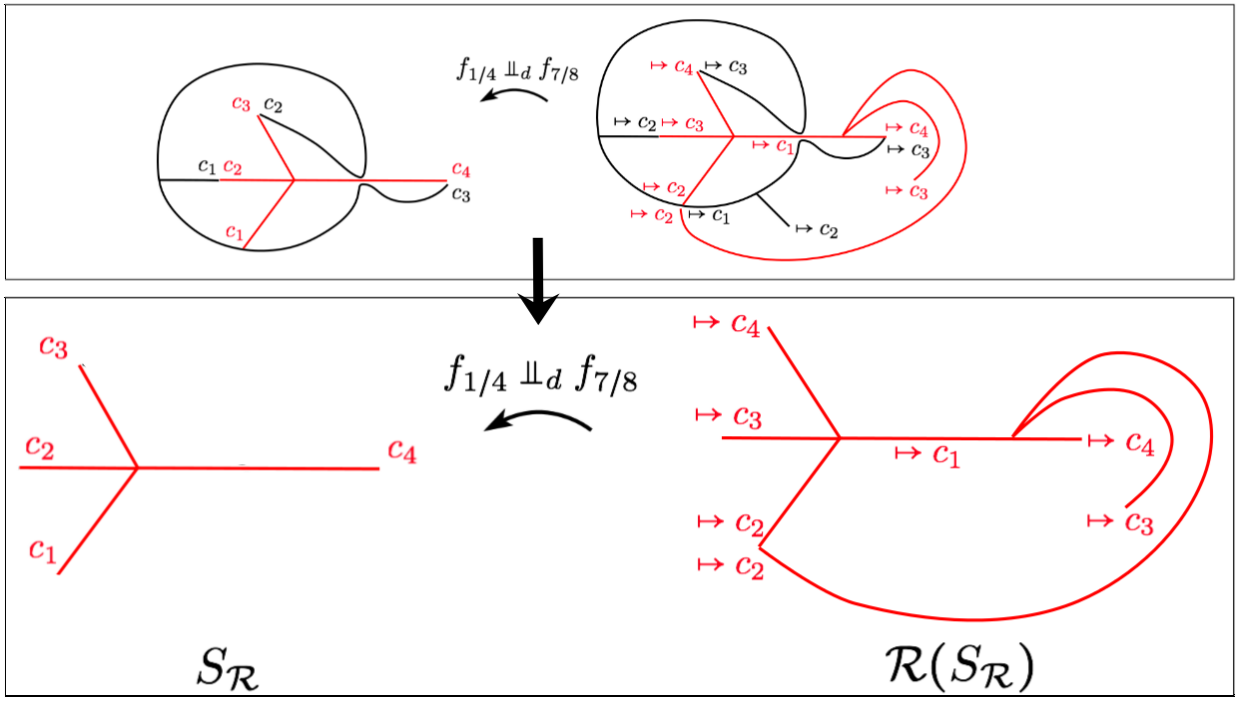

Figure 2.26: Construction 4 applied to $f_{1/4} \amalg_d f_{7/8}$. Notice how the initial Hubbard tree of $f_{7/8}$ does not identify to itself under the degenerate mating, and how only two points of its preimage identify in order to form the subdivided tiling $\mathcal{R}(S_\mathcal{R})$.

Chapter 3

Further Results

3.1 An Introduction: Milnor's Example

The constructions developed in the previous chapter are, as a whole, not entirely unrelated. While various functions may fail to provide a subdivision rule under one or more methods, it is possible to obtain finite subdivision rules for some maps under all of these constructions (or at the very least, subtly modified variants of the constructions.) To point out relationships between these maps, as well as a few notions about when they work or fail, we shall examine in depth the self-mating of $f_{1/4}$.

The function pair of $f_{1/4}$ with itself has been a go-to source for examples throughout much of this paper: see Figure 1.10 noting equivalence classes of the degenerate mating, Section 2.2 for the motivating formal mating used throughout the entire section, Example 2.14 for a finite subdivision rule that can be generated by Constructions 1-3, and Section 3.2 for a parameter-based family of degenerate matings in which $f_{1/4} \amalg_d f_{1/4}$ is a special case. This paper is not alone in its inquiry into the workings of this function pair, as subtleties of the self-mating of $f_{1/4}$ have been discussed by both Milnor and Meyer in great detail. (See [16] and [13].)

We will briefly recap the established claims regarding this mating within the context of this paper, and from there extend and connect our results to those regarding this mating in the literature.

3.1.1 Previous constructions

It will be of use to briefly recap the main points of the constructions we have encountered so far:

In Construction 0, we utilize the formal mating as a subdivision map, and have 1-skeleton of our subdivision complex given by a pair of Hubbard trees and a collection of forward invariant external ray-pairs. (We also include edges to connect landing points of external rays to the Hubbard tree if necessary in this 1-skeleton.) This works for general collections of rays.

In Construction 1, we utilize the degenerate mating as a subdivision map, and have 1-skeleton of our subdivision complex given by a pair of Hubbard trees collapsed under $\sim_{degen}$ This works when preimages of marked points collapse to points under $\sim_{degen}$.

In Construction 2, we utilize a method which can be thought of as similar to Construction 1, but in the case that all of the external ray-pairs involved have been collapsed. This works for general collections of rays if the only tree-to-tree identifications made in $\mathcal{R}(S_{\mathcal{R}})$ are those that have already been established in $S_{\mathcal{R}}$.

In Construction 3, we utilize a method which can be thought of as similar to Construction 1, but in the case that any "forced" identifications are rectified in both $S_{\mathcal{R}}$ and $\mathcal{R}(S_{\mathcal{R}})$. This works if the number of "forced" identifications for a function pair are finite.

In Construction 4, we utilize a method which can be thought of as similar to Construction 1, but in the case that critical points are serial in the mapping scheme for the mating and we can "throw out" one of the Hubbard trees. This works when $S_{\mathcal{R}}$ is an unidentified Hubbard tree whose preimage under the map only contains two points which are in the same equivalence class of $\sim_{top}$.

As a general rule for all of these constructions, we require only a finite number of identifications made in developing $S_{\mathcal{R}}$, and we are required to avoid tree-to-tree identifications forced by the subdivision map that do not appear in the quotient space of the mating. The definitions of the constructions above imply that Constructions 1 and 3 are a special case of Construction 2. (These sub-cases occur when we choose a collection of initial ray-pairs that corresponds with the necessary nontrivial equivalence classes for $\sim_{degen}$ or $\sim_{con3}$.) Further, the rule given for Construction 1, if it exists, is a special case of Construction 3. (In Construction 3, we simply add nontrivial equivalence classes to $\sim_{degen}$ to form $\sim_{con3}$ if necessary. If no additional equivalence classes are necessary, we may as well just start with the degenerate mating as our subdivision map, since the 1-skeletons in these constructions are obtained in the same manner.)

As noted throughout 2.2, $f_{1/4} \amalg_f f_{1/4}$ serves as the subdivision map for several possible finite subdivision rules under Construction 0. As discussed in 2.14, we have a 1-skeleton for a Construction 1 finite subdivision rule which utilizes $f_{1/4} \amalg_d f_{1/4}$ as a subdivision map. Thus, we have that there exists a Construction 1, 2, and 3 finite subdivision rule for the self-mating of $f_{1/4}$.

What about Construction 4? We do not *quite* fit into the framework for this method here, since no postcritical point of $f_{1/4} \amalg_d f_{1/4}$ identifies to a critical point. We should, however, recall that the construction relies on the identification of a tree to itself via a pair of points that map through the critical point of the opposing function in the mating. Examining a few preimages back on the Construction 1 rule for $f_{1/4} \amalg_d f_{1/4}$, we obtain Figure 3.1. Note that on the second preimage, we have identifications through the critical points of both trees.

If we use the intuition given by Construction 4 rather than the formal method itself, this suggests that we can form a one-tile subdivision complex by using the preimage of one of the trees under the degenerate mating as $S_{\mathcal{R}}$, its preimage as $\mathcal{R}(S_{\mathcal{R}})$, and the degenerate mating as the subdivision map. (See Figure 3.2.) Thus, even though Construction 4 does not formally apply, we can obtain a finite subdivision rule here.

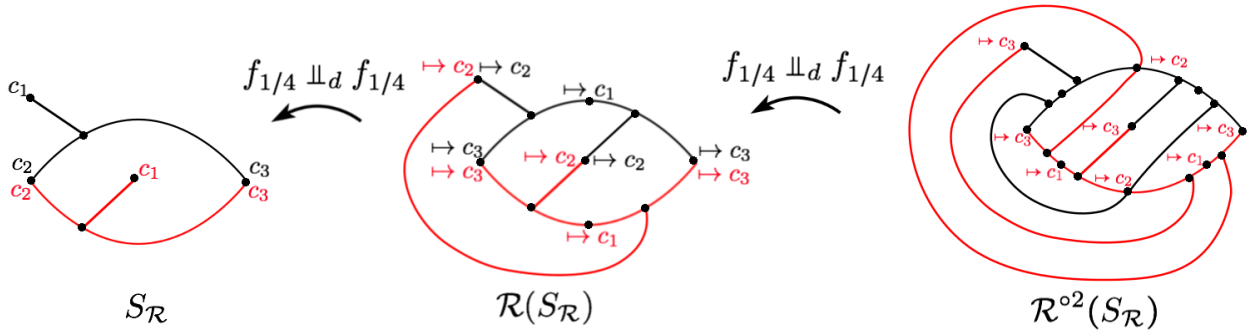

Figure 3.1: Subsequent subdivisions of the Construction 1 rule for $f_{1/4} \amalg_d f_{1/4}$. (Note that the $\mapsto$ symbol on $\mathcal{R}^{\circ 2}(S_{\mathcal{R}})$ denotes where the point in question maps to on $S_{\mathcal{R}}$ under $(f_{1/4} \amalg_d f_{1/4})^{\circ 2}$.)

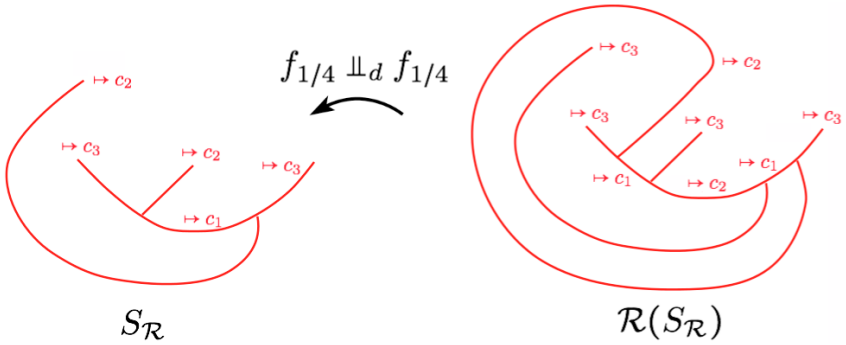

Figure 3.2: A one-tile subdivision rule for $f_{1/4} \amalg_d f_{1/4}$ modeled after Construction 4

3.1.2 Construction 5: connections to deconstructing the mating

Recall that in Section 1.5 we briefly discussed the relationship between rational maps, finite subdivision rules, and matings. It was noted that in key theorems linking the three topics at one juncture that a two-tile subdivision rule with 1-skeleton a Jordan curve containing the postcritical set was an important tool in traveling from rational maps to finite subdivision rules, and ultimately to matings. None of our finite subdivision rules resemble such a curve as in Meyer's work in [13], [14], or [15]. Is there any way that we can link these constructions?

While an authoritative link has not yet been established between the two-tile finite subdivision rules in these papers and the constructions detailed in this document, the following example highlights at least a minor link between the two.

Example 3.1. Consider the Construction 1 finite subdivision rule for $f_{1/4} \amalg_d f_{1/4}$. While $S_{\mathcal{R}}$ in this case is rather obviously not a CW complex with 1-skeleton a Jordan curve, consider what would happen if we tried to impose a Jordan curve-like structure on it in the following manner:

Imagine that the 1-skeleton of $S_{\mathcal{R}}$ is a sidewalk with a series of posts each located at the marked postcritical vertices. Now, suppose that we are walking along this sidewalk carrying

a rope. Our goal is to drag the rope along, hook the rope near a post, drag the rope along, hook the rope near a different post, et cetera—without ever crossing the rope—until we have hooked all of the posts and reached the point at which we started walking with the rope. Once this point is reached, the ends of the rope are to be tied together. Assuming we stay on the sidewalk to complete this task, this scenario models a Construction 1 based Jordan curve containing the postcritical set of $f_{1/4} \amalg_d f_{1/4}$.

If not already obvious, there is a major flaw in assuming that we obtain a Jordan curve in staying "on the sidewalk" to form our curve: the edge of our 1-skeleton has 0 width, while the average sidewalk does not. Such a curve on our actual 1-skeleton is *not* a Jordan curve since it is forced to intersect itself. However, if we let the curve lie within an epsilon window of our 1-skeleton in the space in which it is embedded (i.e., suppose we allow walking in the grass with our rope as long as we don't stray too far from the sidewalk), then we may have a chance at a Jordan curve. We refer to the left of Figure 3.3 for a potential curve constructed in such a manner.

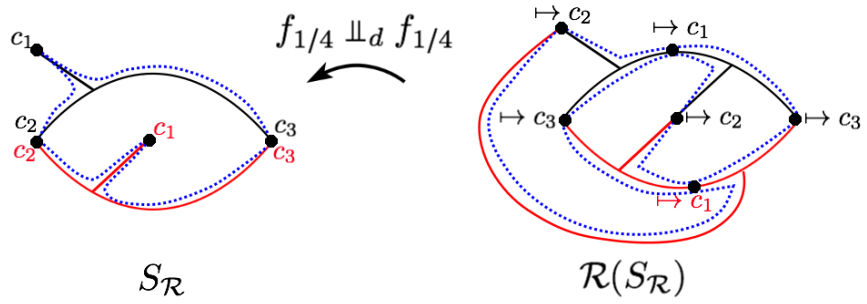

Figure 3.3: The blue dashed line denotes Construction 5 on $f_{1/4} \amalg_d f_{1/4}$.

Now, suppose we take the preimage of this curve under the mating map. We shall call the initial curve with marked postcritical points, the preimage curve with marked points, and the degenerate mating map together a **Construction 5** type rule. Per the right side of Figure 3.3 we have a preimage curve, which–if we hooked posts and not *near* posts in the above scenario–crosses at the critical points on the 1-skeleton. If instead we hooked our rope near our posts, we may think of this as a way to model the preimage as another Jordan curve.

The reason that we do not emphasize Construction 5 to yield a finite subdivision rule in the above case is that in the embedded setting that we have been focusing on, it clearly is not—our structure does not appear forward invariant here like the Hubbard tree structures do.

If we note that our postcritical points lie on the Jordan curve in the same cyclic order we *may* make an argument for the curve being invariant in a combinatorial sense, however. (That is, in traveling a counterclockwise loop along the blue curve, we pass through c_3, c_1, and c_2 of the black tree before passing through c_1 on the red tree in both cases.) If we let the cyclic order of vertices bounding a tile denote where that tile should homeomorphically

map, we even have the open cells of the "subdivision" map to open cells of the original tiling!

It is precisely this type of curve that Meyer discusses in [13], [14], and [15]—however, in these papers he starts with some iterate of a rational map in hopes of obtaining a mating. Upon marking a black/white (i.e. inside/outside) tile structure on the above complexes and/or noting edge mapping properties of this rule, he is able to ascertain external angle information for postcritical points and decompose the map in order to record the constituent polynomials of the mating.

3.2 Related families of matings

The previous section details how we may apply our methods to examine single examples in detail. The emphasis on parameters in their relation to the structure of our initial Hubbard trees and preimages of key points however, strongly suggests that we should spend some time examining how parameters relate to each other and not just how they relate to individual maps. In the following sections, we present parameter-related families of quadradic pairs and show how parameter relationships imply similar properties on the resulting matings.

3.2.1 On a family under Construction 1

Theorem 3.2. *Matings of the form* $f_{1/2^m} \amalg_d f_{1/2^n}, (m, n > 1, m, n \in \mathbb{N})$ *admit a finite subdivision rule under constructions 1, 2, and 3.*

It should be noted that if a Construction 1 finite subdivision rule exists, then it immediately follows that a Construction 2 and 3 rule exist, and further that they yield the same combinatorial rule as Construction 1. We shall thus focus on the Construction 1 finite subdivision rule case from here.

We shall examine the Hubbard trees of the family of maps $\{f_{1/2^n} : n > 2\}$ in detail to prove this claim. We rely heavily upon the algorithms of Bruin and Schleicher detailed in Section 1.2.3 to obtain the itinerary of the critical value and use this itinerary to create a topological Hubbard tree. We subsequently use knowledge of the external angles at points on the itinerary to develop an embedding of this Hubbard tree, and then describe the finite subdivision rules obtained by applying Construction 1 to pairs of maps from this family.

Proof. To develop an itinerary for a map, recall that we need to follow the forward orbit of the critical value c_1 through the regions T_1, T_0, and $\star$ on the Hubbard tree. Here $c_0 = \star$ denotes the critical point, T_1 and T_0 denote the connected components of the Hubbard tree with the critical point removed—T_1 denoting the component that contains c_1. For any $f_{1/2^n}$, the angles of external rays at the critical point (thus of the point in $\star$) are given by $\frac{1}{2^{n+1}}$ and $\frac{2^n+1}{2^{n+1}}$. Since the angle at c_1 is $\frac{1}{2^n}$, this forces T_1 to contain the landing points of external angles contained in $\left(\frac{1}{2^{n+1}}, \frac{2^n+1}{2^{n+1}}\right)$. T_0 contains the landing points of all other external angles.

The angle-doubling semiconjugacy yields $c_1 = \gamma(1/2^n), ..., c_i = \gamma(1/2^{n-i+1}), ..., c_n = \gamma(1/2)$. These are all contained in T_1.

The angle-doubling semiconjugacy also yields that $c_{n+1} = \gamma(0)$, which is a periodic point located in T_0.

This yields the itinerary $\underbrace{1...1}_{\text{n times}}\ \overline{0}$ for the map $f_{1/2^n}$.

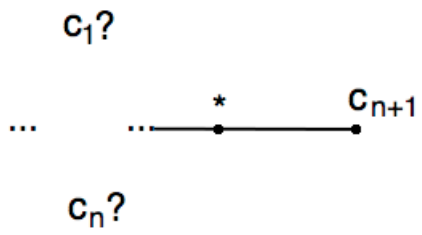

Figure 3.4: First, we determine the itinerary and relative locations of postcritical points in T_1 and T_0.

We can use the test for degenerate/nondegenerate triods to determine the relative location of each of the postcritical points on the Hubbard Tree. Starting with any three distinct $i < j < k$ in $\{1, ..., n\}$, we can observe the forward orbit of the $[c_i, c_j, c_k]$ triod and its truncations to determine whether the triod is degenerate or not. Moving from line to subsequent line represents forward iterations under $f_{1/2^n}$, except where a truncation has been noted:

$[c_i, c_j, c_k]$ (Located respectively in T_1, T_1, T_1.)

...

$[c_{i+n-k+1}, c_{j+n-k+1}, c_{n+1}]$ (Located respectively in T_1, T_1, T_0. We must chop at the third coordinate.)

$[c_{i+n-k+1}, c_{j+n-k+1}, \star]$

...

$[c_{i+n-j+1}, c_{n+1}, c_{k-j}]$ (Located respectively in T_1, T_0, T_1. We must chop at the second coordinate.)

$[c_{i+n-j+1}, \star, c_{k-j}]$

...

$[c_{n+1}, c_{j-i}, c_{k-i}]$, (Located respectively in T_0, T_1, T_1. We must chop at the first coordinate.)

$[\star, c_{j-i}, c_{k-i}]$

...

$[c_i, c_j, c_k]$ (This was our original triod.)

As our sequence of forward iterates has become periodic and we've noted a truncation at each of the three ends of the triod, this triplet (which represents any three postcritical points in T_1) is nondegenerate. With that said, we can actually take *any* triplet of postcritical points of $f_{1/2^n}$ to yield a nondegenerate triod, as the remaining critical point c_{n+1} is featured in lines of the test above which occur pre-truncation. Since all triods with distinct postcritical endpoints are nondegenerate, all elements of the postcritical set are endpoints of the Hubbard tree for $f_{1/2^n}$.

We can elaborate on the structure of the Hubbard tree further by showing it has a star-like shape: there is a single branch point of this Hubbard tree, located at the T_1 fixed point.

To prove this, we show that each triod which contains two postcritical points and this fixed point is degenerate, and that such "triods" present as a two-edged path between the postcritical points linked by the middle vertex p. Let $i < j$ be contained in $\{1, ..., n\}$, and p denote the T_1 fixed point:

$[c_i, c_j, p]$ (Located respectively in T_1, T_1, T_1)
...
$[c_{i+n-j+1}, c_{n+1}, p]$ (Located respectively in T_1, T_0, T_1. We must chop at the second coordinate.)
$[c_{i+n-j+1}, \star, p]$
...
$[c_{n+1}, c_{j-i}, p]$ (Located respectively in T_0, T_1, T_1. We must chop at the second coordinate.)
$[\star, c_{j-i}, p]$
...
$[c_i, c_j, p]$ (This was our original triod.)

Since the sequence of forward iterates has become periodic and has never been truncated in the third column, this triod is degenerate. We may imagine the three marked points as lying on the Hubbard tree in such a way that we can form a path from c_i to p to c_j. Similar to above, as c_{n+1} is featured in our sequence of triods, we can take this to hold for all pairs of postcritical points and not just pairs of the first n postcritical points of $f_{1/2^n}$. (As a note for future reference, since we never utilized that our map was periodic—i.e., we always chopped a vertex off once it mapped to T_0—this star-like tree shape will hold for any kneading sequence that looks like a string of 1's followed by a 0, regardless of the period or preperiod of the sequence.)

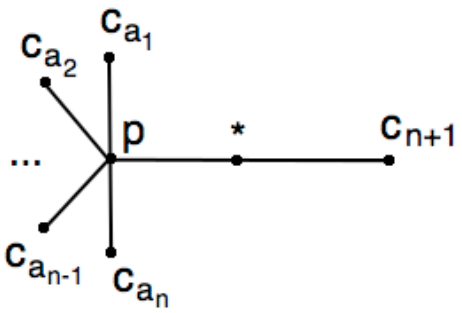

Figure 3.5: Next, we determine an unembedded Hubbard tree for $f_{1/2^n}$. The tree resembles a star.

At this point, we have a topological Hubbard tree for $f_{1/2^n}$. While the unembedded tree for itinerary $\underbrace{1...1}_{\text{n times}}\,\overline{0}$ has $\phi(n+1)$ possible choices for embedding (where ϕ represents the Euler ϕ function), recall that we have external angle information for $\star$ as well as each of the

postcritical points in addition to the itinerary. The ordering of these angles forces a cyclic order for the postcritical points as shown in Figure 3.6.

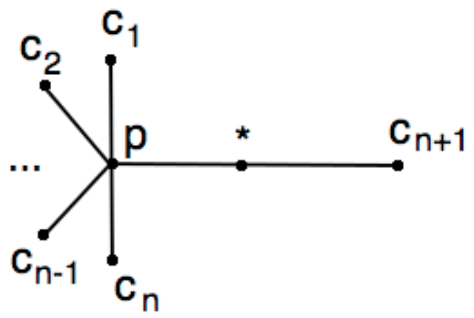

Figure 3.6: The embedded Hubbard tree for $f_{1/2^n}$.

Now that we have an idea of the general structure of the Hubbard trees for the family $\{f_{1/2^n} : n > 2\}$, we can examine what happens when we use Construction 1 to form a mating between pairs of these functions.

When forming identifications between postcritical points, recall that we only identify angles θ and $-\theta$ on opposing trees. Since functions from our family have postcritical points with external angles of the form $1/2^n$, this means that the only possible identifications to be made are at the postcritical points where the external angles are $1/2$ or 0. This yields a two-tile one-skeleton.

The preimages of the 0–to–0 identification are the original identifications in our one-skeleton. The preimages of the $\frac{1}{2}$–to–$\frac{1}{2}$ identification are the pair of $\frac{1}{4}$–to–$\frac{3}{4}$ and $\frac{3}{4}$–to–$\frac{1}{4}$ identifications between the two trees. Since the $\frac{3}{4}$ "limbs" are not present in either of the initial Hubbard trees in our mating, the addition of these edges yields a subdivision of our initial one-skeleton. □

It should be noted that the simplest case of the mating family above—$m = n = 2$, or $f_{1/4} \amalg_d f_{1/4}$—is the example of interest in Section 3.1 and Figure 2.20.

3.2.2 On a family under Construction 3

Conjecture 3.3. *Matings of the form* $f_{\frac{1}{4(2^n-1)}} \amalg_d f_{-\frac{1}{8(2^n-1)}}, n \geq 2$, *admit a finite subdivision rule under Constructions 3, but fail to admit a finite subdivision rule under Construction 1.*

It should be noted that Bruin and Schleicher's degenerate triod test is *heavily* utilized in the following proof to determine whether certain preimage points are on the Hubbard tree for a given polynomial. Much of this mechanical work has been relegated to Appendix B and condensed in Figure 3.9 to clarify the underlying argument.

Proof. We shall begin by examining the Hubbard trees of the family of maps $f_{\frac{1}{4(2^n-1)}}$ and $f_{-\frac{1}{8(2^n-1)}}$, starting with $f_{\frac{1}{4(2^n-1)}}$.

To develop an itinerary, we much follow the forward orbit of the critical value c_1 through the regions T_1, T_0, and $\star$ on the Hubbard tree of $f_{\frac{1}{4(2^n-1)}}$. If a landing point has external angles t with $\frac{1}{8(2^n-1)} < t < \frac{1}{8(2^n-1)} + \frac{1}{2}$, it is in T_1; if it possesses external angles $\frac{1}{8(2^n-1)}$ or $\frac{1}{8(2^n-1)} + \frac{1}{2}$, it is in $\star$; otherwise it is in T_0.

For this particular map, we have that $c_k = \gamma_{\frac{1}{4(2^n-1)}}(\frac{2^k}{8(2^n-1)})$ for nonnegative k, thus $\{c_1, ..., c_{n+1}\} \subset T_1$, $c_{n+2} \in T_0$, and $c_{n+3} = c_3$. Thus, our function has itinerary given by $\underbrace{11\overline{1...110}}_{\text{n+2 digits}}$. By the aside mentioned in Section 3.2 regarding structure of Hubbard trees with kneading sequence a series of 1's followed by a 0, this admits a star-like Hubbard tree structure. Since the external angles of postcritical points are increasing as we iterate forward (at least until we hit c_{n+2}) and each postcritical point corresponds to an endpoint of the Hubbard tree, we have the embedding for $f_{\frac{1}{4(2^n-1)}}$ as given in Figure 3.7.

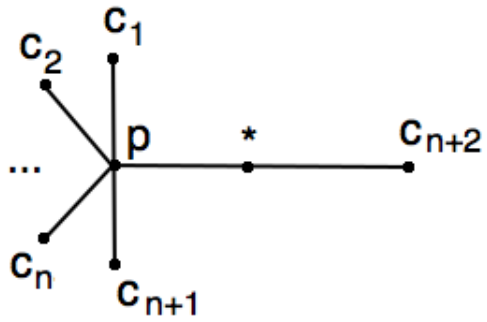

Figure 3.7: The embedded Hubbard tree for $f_{\frac{1}{4(2^n-1)}}$.

Similarly for $f_{\frac{-1}{8(2^n-1)}}$, we compute an itinerary to develop a Hubbard tree by using the regions T_1', T_0', and $\star'$ on the Hubbard tree of $f_{\frac{-1}{8(2^n-1)}}$. If a landing point has external angles t with $-\frac{1}{16(2^n-1)} - \frac{1}{2} < t < -\frac{1}{16(2^n-1)}$, it is in T_1'; if it possesses external angles $-\frac{1}{16(2^n-1)} - \frac{1}{2}$ or $-\frac{1}{16(2^n-1)}$, it is in $\star'$; otherwise it is in T_0'.

For this particular map, we have that $d_k = \gamma_{\frac{-1}{8(2^n-1)}}(-\frac{2^k}{16(2^n-1)})$ for nonnegative k, thus $\{d_1, ..., d_{n+2}\} \subset T_1'$, $d_{n+3} \in T_0'$, and $d_{n+4} = c_4 \in T_1'$. Thus our function has itinerary given by $\underbrace{1111\overline{...110}}_{\text{n+3 digits}}$.

As above,this admits a star-like Hubbard tree structure. Since the external angles of postcritical points are decreasing as we iterate forward (at least until we hit d_{n+3}) and each postcritical point corresponds to an endpoint of the Hubbard tree, we have the embedding of $f_{\frac{-1}{8(2^n-1)}}$ as given in Figure 3.8.

Now that we have developed a basic idea of the structure of $T_{\frac{1}{4(2^n-1)}}$ and $T_{-\frac{1}{8(2^n-1)}}$, we may focus more on the theorem's claim regarding their relationship. In showing that there is a Construction 3 type finite subdivision rule, we must prove that the number of nontriv-

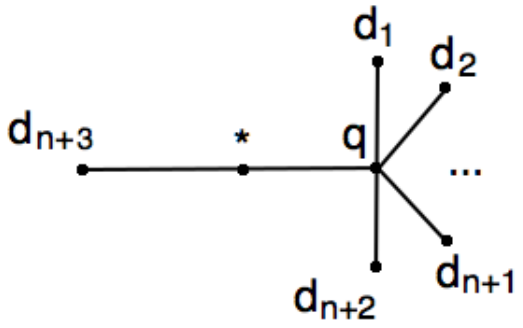

Figure 3.8: The embedded Hubbard tree for $f_{\frac{-1}{8(2^n-1)}}$.

ial equivalence classes of $\sim_{con3}$ for this mating is finite. This boils down to showing that there are a finite number of tree-to-tree identifications that map forward to a postcritical–to–postcritical identification for this map. We proceed by examining the postcritical–to–postcritical identifications and looking at their preimages. Since Hubbard trees map onto themselves, any place that we observe an off-tree–to–off-tree or tree–to–off-tree identification will be a dead end and not yield further tree-to-tree identifications. If we reach only these dead ends in iterating backwards, there are a finite number of nontrivial equivalence classes of $\sim_{con3}$, and there are Construction 3 based subdivision rules for our family of maps.

Since examining a particular set of preimages will be of utmost importance, we give notation for these points now: let $c_{-k}, k \in \mathbb{N}$ denote the iterated preimage of c_0 (under its associated map) with the itinerary $\underbrace{1...1}_{\text{k digits}} \star \underbrace{11\overline{1...10}}_{\text{n+2 digits}}$, and $d_{-k}, k \in \mathbb{N}$ denote the iterated preimage of d_0 (under its associated map) with the itinerary $\underbrace{1...1}_{\text{k digits}} \star \underbrace{111\overline{1...10}}_{\text{n+3 digits}}$. Further, let $c^*_{-k}, k \in \mathbb{N}$ denote the iterated preimage of c_0 (under its associated map) with the itinerary $\underbrace{01...1}_{\text{k digits}} \star \underbrace{11\overline{1...10}}_{\text{n+2 digits}}$, and $d^*_{-k}, k \in \mathbb{N}$ denote the iterated preimage of d_0 (under its associated map) with the itinerary $\underbrace{01...1}_{\text{k digits}} \star \underbrace{111\overline{1...10}}_{\text{n+3 digits}}$.

With our fundamental goal and necessary notation established, we continue by noting identifications that occur between $T_{\frac{1}{4(2^n-1)}}$ and $T_{-\frac{1}{8(2^n-1)}}$. A summary of tree-to-tree identifications for this mating is shown in Figure 3.9, and is supported by the following arguments.

By the previous notes on the external angles of postcritical points, we have that $c_k \sim_{degen} d_{k+1}$ for nonnegative k because the angles associated with these points are negative of each other. As all postcritical points are endpoints on both trees and not biaccessible, we've accounted for all tree-to-tree identifications that involve a pair of postcritical points. There is one postcritical to critical point identification noted by the above, given by $c_0 \sim_{degen} d_1$. Since c_0 is a critical point however, it is biaccessible. As "both" points of $(f_{\frac{1}{4(2^n-1)}})^{-1}(c_1)$ must pair off with the two points in $(f_{-\frac{1}{8(2^n-1)}})^{-1}(d_2)$, we have that c_0 identifies to both

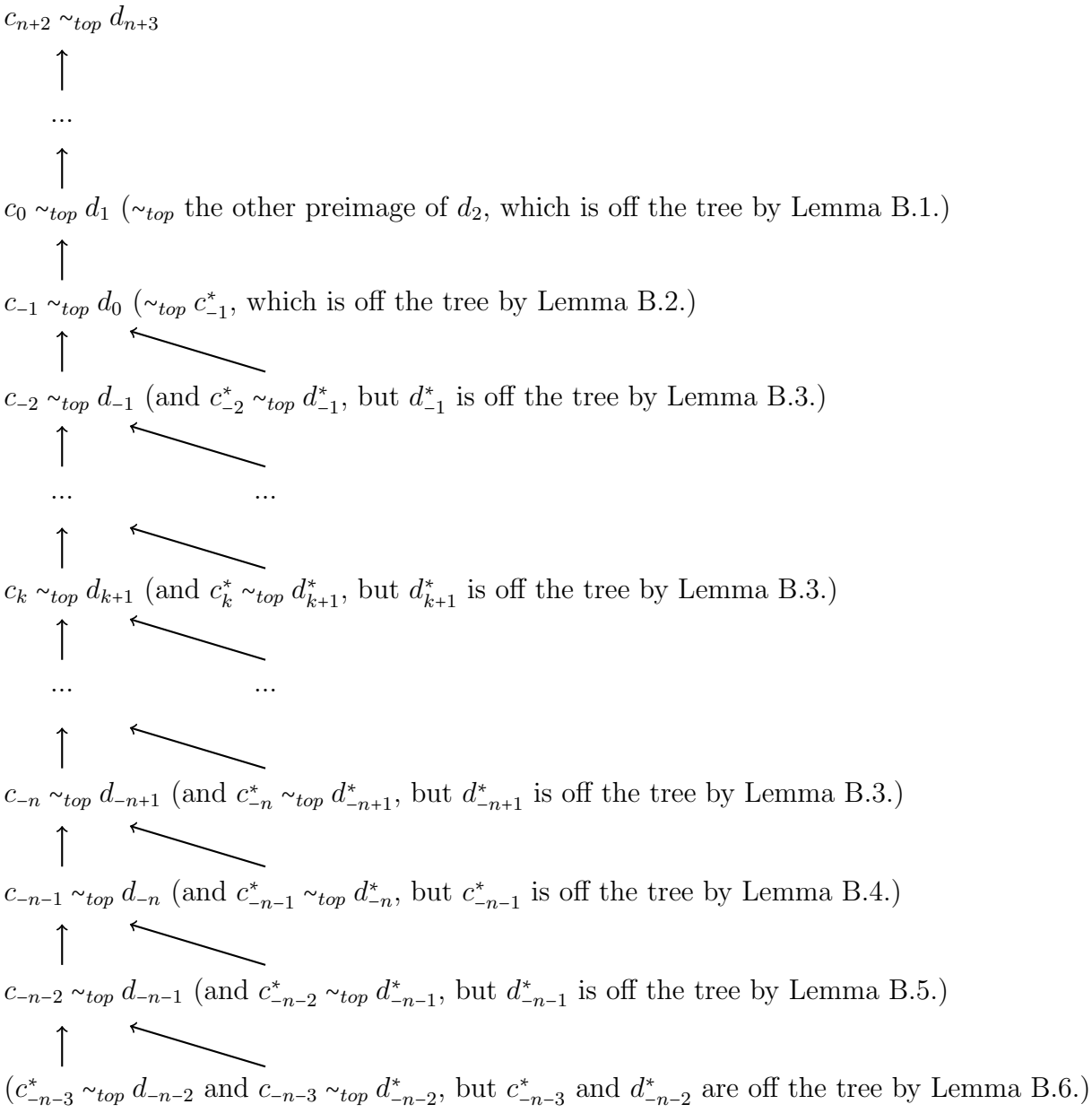

Figure 3.9: Preimages of points identified under $\sim_{degen}$. Arrows denote where the identified point pairing maps under the mating $f_{\frac{1}{4(2^n-1)}} \amalg_d f_{-\frac{1}{8(2^n-1)}}$.

preimages of d_2.

By Lemma B.1 of Appendix B, d_1 is the only preimage of d_2 contained in the Hubbard tree $T_{-\frac{1}{8(2^n-1)}}$. Thus, the only tree-to-tree identification whose preimages we need to concern ourselves with is c_0 to d_1.

Similarly, since d_0 is a critical point, it is also biaccessible. As the two points of $(f_{\frac{1}{4(2^n-1)}})^{-1}(c_0)$ must pair off with "both" points of $(f_{-\frac{1}{8(2^n-1)}})^{-1}(d_1)$, we have that both preimages of c_0 identify to d_0. By Lemma B.2 in Appendix B, c_{-1} is the only preimage of c_0 contained in the Hubbard tree $T_{\frac{1}{4(2^n-1)}}$. Thus, the only tree-to-tree identification whose preimages we must concern ourselves with at this point is c_{-1} to d_0.

At this point, it should be noted that c_{-k} can be computed to be $\frac{1}{2^{k-1}}(\frac{1}{16(2^n-1)}+\frac{1}{2})$ and d_{-k} can be computed to be $-\frac{1}{2^k}(\frac{1}{16(2^n-1)}+\frac{1}{2})$ for $1 \leq k \leq n+2$. (For $k = n+3$, angles of these forms land in T_0 and T_0' respectively.) Thus, $c_{-k} \sim_{top} d_{-k+1}$ for $2 \leq k \leq n+2$ (and also, $c_{-n-3} \sim_{top} d_{-n-2}$). By Lemma B.3 in Appendix B, we have that to avoid "dead ends" due to d_k which appear off-tree, we must follow the trail of c_{-k}'s and d_{-k+1}'s until we reach at least c_{-n} and d_{-n+1}. At this point, we are still concerned only with preimages of this pair which contain a point on either $T_{\frac{1}{4(2^n-1)}}$ or $T_{-\frac{1}{8(2^n-1)}}$.

The preimage groupings of c_{-n} and d_{-n+1} are c_{-n-1} and d_{-n} along with c^*_{-n-1} and d^*_{-n}. We can disregard the latter pair and its preimages as c^*_{-n-1} is off-tree by Lemma B.4 of Appendix B.

The preimage groupings of c_{-n-1} and d_{-n} are c_{-n-2} and d_{-n-1} along with c^*_{-n-2} and d^*_{-n-1}.We can disregard the latter pair and its preimages as c^*_{-n-1} is off-tree by Lemma B.5 of Appendix B.

Finally, the preimage groupings of c_{-n-2} and d_{-n-1} are c^*_{-n-3} and d_{-n-2} along with c_{-n-3} and d^*_{-n-2}. We can disregard *both* pairs, as c^*_{-n-3} and d^*_{-n-2} are both off-tree by Lemma B.6 of Appendix B.

Since we've run out of tree-to-tree identifications for the mating (and have thus explicitly spelled out all of the possible point groupings that fall into nontrivial equivalence classes of $\sim_{con3}$), there is a nonzero finite number of nontrivial equivalence classes of $\sim_{con3}$ for any mating in the family $f_{\frac{1}{4(2^n-1)}} \amalg_d f_{-\frac{1}{8(2^n-1)}}, n \geq 2$. By Theorem 2.18, the matings in this family admit a Construction 3 type subdivision rule. Further, since there are nontrivial equivalence classes of $\sim_{con3}$ which are not equivalence classes of $\sim_{degen}$, matings of this form fail to admit Construction 1 type finite subdivision rules. □

Even the simplest case of this family, $n = 2$, yields a somewhat messy-looking subdivision rule, as in Figure 3.10.

3.2.3 On a family failing Constructions 1 and 3

Theorem 3.4. *Matings of the form $f_{1/2^n} \amalg f_{-1/2^m}$ $(n \neq m; n, m \in \mathbb{N})$ do not admit a finite subdivision rule under Constructions 1 or 3.*

Here it should be noted that if we fail the Construction 3 method for finding a subdivision rule (i.e., our map forces too many identifications on the 1-skeleton), we will fail to obtain

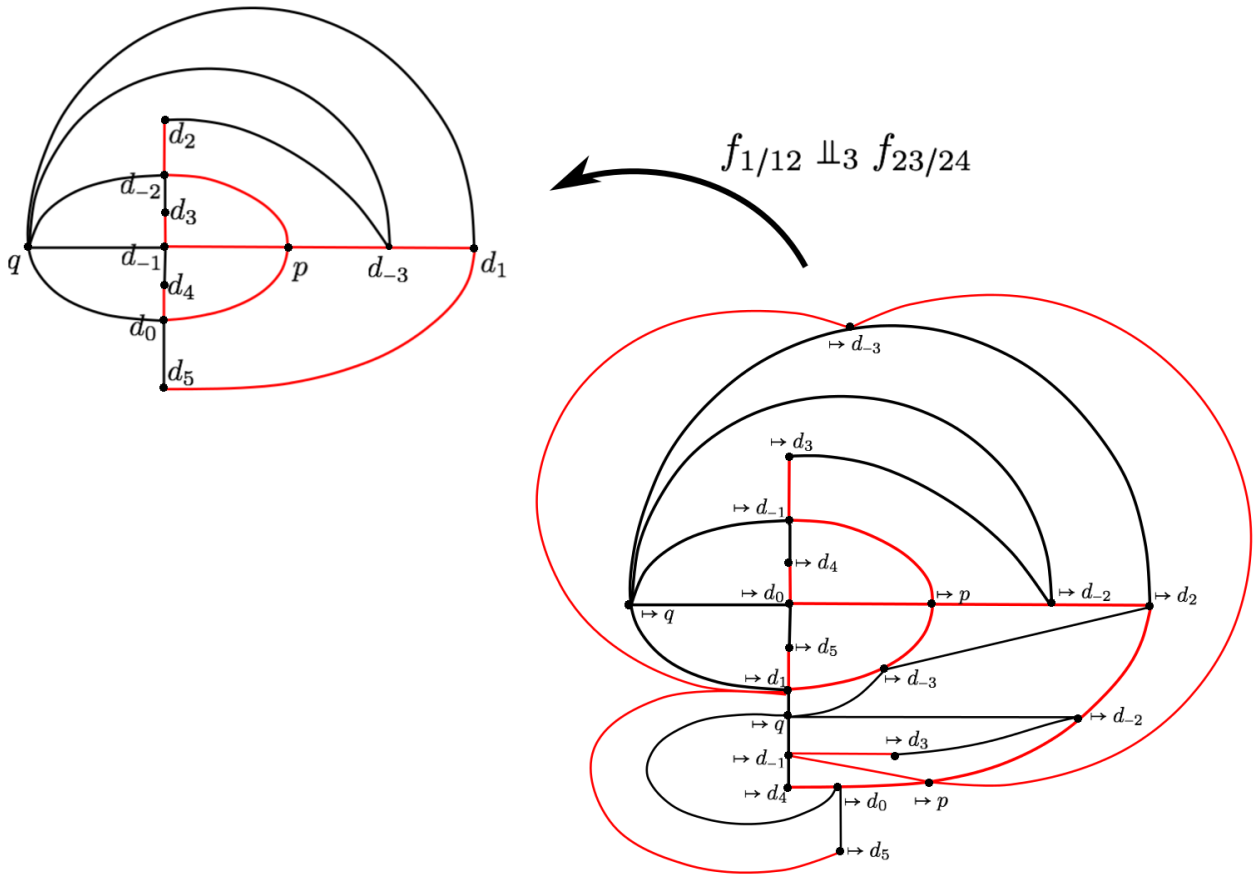

Figure 3.10: The mating $f_{1/12} \amalg_3 f_{-1/24}$. The Hubbard tree for $f_{1/12}$ is depicted in red; the Hubbard tree for $f_{-1/24}$ is depicted in black. The labels correspond to identified points of $T_{-1/24}$.

a Construction 1 type finite subdivision rule. Thus, we will focus on showing that there are an infinite number of identifications that are forced by the degenerate mating map, causing Construction 3 to fail.

Proof. To prove this, we will need to make an observation about the structure of the Hubbard tree for $f_{1/2^n}$: namely, that the landing points $\gamma(1/2^k), k > n$ lie on the body of the Hubbard tree.

The case $k = n+1$ is fairly simple: $\gamma(1/2^{n+1}) = c_0$ for the map $f_{1/2^n}$. What about the case $k > n+1$?

Here, with close attention the ranges of angles given for T_0 and T_1 in Section 3.2, we may note that the itinerary of $\gamma(1/2^k)$ is given by $\underbrace{0\ldots0}_{k' \text{ times}} \star \underbrace{1\ldots1}_{n \text{ times}} \overline{0}$ where $k' = k - n - 1$. For sake of maintaining our established notation in performing Bruin and Schleicher's test for degenerate/nondegenerate triods, we will refer to the point with this itinerary as $c_{-k'}$. Trying this test with $c_{-k'}$, the critical point, and c_{n+1} yields the following:

$[c_{-k'}, c_{n+1}, c_0]$ (Located respectively in $T_0, T_0, \star$)
$[c_{-k'+1}, c_{n+1}, c_1]$ (Located respectively in T_0, T_0, T_1. We must chop at the third coordinate.)
$[c_{-k'+1}, c_{n+1}, c_0]$ (Located respectively in $T_0, T_0, \star$)

Note that from the above, we will continue to sequentially iterate and truncate the third column until we reach the following:

$[c_{-1}, c_{n+1}, c_0]$ (Located respectively in $T_0, T_0, \star$)
$[c_0, c_{n+1}, c_1]$ (Located respectively in $\star, T_0, T_)$)

Since we end with a column representing each of the three components $\star$, T_0, and T_1, we have a degenerate triod. We may imagine the three initial marked points as lying on the Hubbard tree in such a way that we can form a path from c_0 to $c_{-k'}$ to c_{n+1}. Thus the landing points $\gamma(1/2^k), k > n$ are contained in the Hubbard tree for $f_{1/2^n}$.

Now that we have developed information on the structure of $f_{1/2^n}$, what about $f_{-1/2^m}$?

First note that the landing points of the θ and $-\theta$ parameter rays on the Mandelbrot set are at conjugate values. Second, note that just as the conjugate parameters $c, \overline{c} \in \mathbb{C}$ yield mirrored Julia sets for the function pair $f(z) = z^2 + c$ and $f(z) = z^2 + \overline{c}$, they similarly yield mirrored Hubbard trees for these functions. Thus, since we've already detailed the structure of Hubbard trees for the functions $f_{1/2^n}$, we've already completed most of the work of finding the Hubbard trees for the functions $f_{-1/2^n}$—we just mirror the previously found trees. In doing this, we can extend the previous result to state that the landing points $\gamma(-1/2^k), k > m$, are contained in the Hubbard tree for $f_{-1/2^m}$.

Comparing $f_{1/2^n} \amalg f_{-1/2^m}$ to the matings of Section 3.2, note that we increase the number of postcritical identifications by pairing these "mirrored" maps. (If $n < m$, all of the postcritical points of $f_{1/2^n}$ are identified to the body of the tree for $f_{-1/2^m}$, and vice versa.) Further, preimages of these identifications give us problems in performing Construction 1 to develop a finite subdivision rule. As noted in Subsection 2.4.2, identifications whose preimages yield unassigned tree-to-tree identifications give rise to tile pinching. This tile pinching can only be reconciled if the appropriate tree-to-tree identifications are assigned, and if there are only finitely many of them to be found upon taking preimages. Otherwise, the mating fails to take open tiles of the subdivision homeomorphically onto open tiles of the original tiling, and cannot be a subdivision map for a finite subdivision rule.

For any $N > \max\{n, m\}$, we have that the landing point of $\frac{1}{2^N}$ on the tree for $f_{1/2^n}$ will identify with the landing point of $-\frac{1}{2^N}$ on the tree for $f_{1/2^n}$. This forces an infinite number of tree-to-tree identifications which are preimages of postcritical identifications. This implies that we must construct an infinite number of tiles before reconciling all of our tree-to-tree identifications and having any chance that the mating $f_{1/2^n} \amalg f_{-1/2^m}$ will act as a subdivision map. This breaks the finiteness condition needed to obtain a finite subdivision rule, thus matings of the form $f_{1/2^n} \amalg f_{-1/2^m}$, $(n \neq m; n, m \in \mathbb{N})$ do *not* yield finite subdivision rules under Construction 1 or 3.

□

It should be noted that one of the simplest cases—$m = 3$ and $n = 2$, or $f_{1/4} \amalg_d f_{7/8}$–is an example of focus in Section 2.4.2 and Figure 2.24.

3.3 Topics for future study

As a look forward, there are several major topics that I would like to continue studying that relate finite subdivision rules and matings of polynomials. Function parameters have proven to be crucial in determining point-identification schemes under various refinements of the equivalence relation $\sim_{top}$. I thus believe that there is direct correlation between parameters and possible outcomes of finite subdivision rules. I would like to catalogue and investigate finite subdivision rules generated from quadratic function pairs in order to study this connection.

Once I've developed a stronger intuition regarding the direct relationship between quadratic parameters and the associated rules, I would like to examine matings for polynomials that are degree 3 and/or higher. Knowledge of how function parameters directly affect identification schemes in matings could be particularly useful in building rational maps with chosen postcritical mapping schemes at will.

I also wish to investigate further potential constructions for finite subdivision rules stemming from mating maps. In particular, are there any constructions that solve the "too many identifications" problem? Are there other utilizations of Hubbard trees as building blocks for forming finite subdivision rules on mating maps? If so, are there any that will work by default in all cases in some degenerate-like (i.e., with external rays collapsed to points on the 1-skeleton) setting? Is there a "canonical" choice of finite subdivision rule on the degenerate mating map, or can some examples just not be modeled by a finite structure?

Finally, I wish to investigate the connections between the rules generated here and current work being done in deconstructing iterates of rational maps as matings of two polynomials. How do each of my constructions relate to the two-tile subdivision rules used by Meyer to pry apart these rational maps? Is there any way that my constructions could potentially generate space-filling curves on the two-sphere, much like the 1-skeleton of his two-tile rule?

Hopefully the outcomes of any of the above work will lead to new insight into the dynamics of mated maps, and on the relationship between finite subdivision rules, matings, and rational maps.

Appendix A

Hubbard tree code

The following is code generated by the author in Mathematica 8 for obtaining Hubbard trees from appropriate kneading sequences. The tree structures asserted for all of the quadratic maps were verified using this code and [11]. The underlying algorithms driving this code are based on those given in [2]. (Note: the trees output by this program reflect topological structure of trees with a given itinerary, and not trees as embedded in the complex plane.)

```
(*Initialize the functions below. Instructions follow on how to use \
code to develop Hubbard trees based on appropriate kneading \
sequences.*)

ShortenRep[sequence_, period_] := (
   seq = sequence;
   test = False;
   While[test == False,
    If[Last[seq] == -1, test = True,(*it ends in a -1,
     it's a star periodic sequence.*)

     If[Length[seq] == period, test = True,
      If[seq[[-1]] == seq[[-period - 1]], seq = Drop[seq, -1],
       test = True]]]];
   {seq, period});
TestPeriod[sequence_, period_] :=
  (n = 1;
   norepeatsfound = True;
   per = period;
   If[Last[sequence] == -1, per = Length[sequence],
    While[(n <= period/2) && (norepeatsfound == True),
     If[Divisible[period, n],(*test to see if there are sequences,
      else increment n:*)
```

```
      If[Flatten[
         Table[Take[sequence, -n], {z, 1,
           period/n}]](*repeated end string*)==
        Take[sequence, -period],(*periodic part*)per = n;
       norepeatsfound = False, n++], n++]]];
   per);

SimplifySequence[sequence_, period_] :=
  ShortenRep[sequence, TestPeriod[sequence, period]];
(*For sequence_, input the itinerary in the form of a list; i.e. \
{1,0,1,1,1,0,-1}, with -1 denoting *. For period_, input the period \
of the sequence. For example, to check if the *-periodic sequence \
101* can be simplified, we would input it as \
SimplifySequence[{1,0,1,-1},4]*)

ShortenRep2[sequence_, period_] := (
   seq = sequence;
   test = False;
   While[test == False,
    If[Length[seq] == period, test = True,
     If[seq[[-1]] == seq[[-period - 1]], seq = Drop[seq, -1],
      test = True]]];
   {seq, period});
SimplifySequence2[sequence_, period_] :=
  ShortenRep2[sequence, TestPeriod2[sequence, period]];
TestPeriod2[sequence_, period_] :=
  (n = 1;
   norepeatsfound = True;
   per = period;
   While[(n <= period/2) && (norepeatsfound == True),
    If[Divisible[period, n],(*test to see if there are sequences,
     else increment n:*)
     If[Flatten[
        Table[Take[sequence, -n], {z, 1,
          period/n}]](*repeated end string*)==
       Take[sequence, -period],(*periodic part*)per = n;
      norepeatsfound = False, n++], n++]];
   per);

DoubleCheck[sequence_,
   period_] := (testset = SimplifySequence[sequence, period];
```

```
   If[Length[testset[[1]]] == testset[[2]] \[And]
     Last[sequence] != -1, Print["Periodic! Stop!"],
    If[First [sequence] == 0, Print["Sequence starts with 0! Stop!"],
     testset]];

Itinerary[number_, sequence_, period_] :=
  SimplifySequence2[
   Drop[Join[sequence, Take[sequence, -period]], number - 1], period];

FindT1[sequence_] := (T1 = Flatten[Position[sequence, 1]];
   T0 = Flatten[Position[sequence, 0]];);

ModOut[input_, sequencelength_, period_] := (
  If[IntegerQ[input],
   If[input <= sequencelength, input,
    Mod[input, period, sequencelength - period + 1]] ,
   If[input[[1]] <= Length[input[[2]]],
    input, {Mod[input[[1]], input[[3, 2]],
      Length[input[[2]]] - input[[3, 2]] + 1], input[[2]],
     input[[3]]} ]
   ]);(*returns a useful value that will refer to simplified versions \
of the sequence*)

ModOut2[input_, sequence_] :=
 If[IntegerQ[input] == False, input,
  If[input === 0, 0, If[sequence[[input]] === -1, 0, input]]];

AreTheseDifferent[input1_, input2_, input3_, sequencelength_,
   period_] :=
  If[Length[
     Union[Function[x, ModOut[x, sequencelength, period]] /@ {input1,
        input2, input3}]] == 3, True, False];

DegenTest[input1_, input2_, input3_, sequence_, period_] := (
   seq = sequence; seqlength = Length[seq]; per = period;
   in1 = ModOut2[ModOut[input1, seqlength, per], seq];
   in2 = ModOut2[ModOut[input2, seqlength, per], seq];
   in3 = ModOut2[ModOut[input3, seqlength, per], seq];
   QuittingTime = False; periodic = False;
   ListOfSequences = {{in1, in2, in3}};
   While[QuittingTime == False,
    If[AreTheseDifferent[in1, in2, in3, seqlength, per] ==
```

```
  False \[Or]
 Length[Union[seq[[{in1, in2, in3}]]   ]] ==
  3 \[Or] (MemberQ[seq[[{in1, in2, in3}]], -1] \[And]
   MemberQ[seq[[{in1, in2, in3}]], List]),
Degen = True;(*Print["Degenerate:
",ListOfSequences];*)QuittingTime = True,
chop = False;
If[MemberQ[seq[[{in1, in2, in3}]], -1] \[Or]
  MemberQ[seq[[{in1, in2, in3}]], List] \[Or]
  Length[Union[seq[[{in1, in2, in3}]]   ]] == 1,
 in1 = ModOut2[ModOut[in1 + 1, seqlength, per], seq];
 in2 = ModOut2[ModOut[in2 + 1, seqlength, per], seq];
 in3 = ModOut2[ModOut[in3 + 1, seqlength, per], seq];,
 If[seq[[ in1]] == seq[[in2]] \[And] in3 != 0, in3 = 0;
   chop = True,
   If[seq[[in1]] == seq[[in3]] \[And] in2 != 0, in2 = 0;
    chop = True,
    If[seq[[in2]] == seq[[in3]] \[And] in1 != 0, in1 = 0;
     chop = True]]];];
If[MemberQ[ListOfSequences, {in1, in2, in3}] == False \[And]
  chop == False, AppendTo[ListOfSequences, {in1, in2, in3}],
 If[MemberQ[ListOfSequences, {in1, in2, in3}] == False \[And]
   chop == True,
  ListOfSequences[[-1]] = {in1, in2, in3}; chop = False,
  If[chop == True, ListOfSequences[[-1]] = {in1, in2, in3},
   AppendTo[ListOfSequences, {in1, in2, in3}]];
  itinofbpt = (SimplifySequence[
     Flatten[Commonest /@
       Function[x, seq[[x]]] /@ ListOfSequences],
     Differences[
       Position[ListOfSequences, Last[ListOfSequences]]][[1,
      1]]]);(*Print["Periodic:
  ",ListOfSequences];*)(*Print["Itinerary of branched point = ",
  itinofbpt];*) periodic = True;
  If[(MemberQ[First /@ ListOfSequences, 0] \[Or]
      MemberQ[
       Table[sequence[[ListOfSequences[[i, 1]]]], {i, 1,
         Length[ListOfSequences]}], -1]) \[And] (MemberQ[
       Table[ListOfSequences[[i, 2]], {i, 1,
         Length[ListOfSequences]}], 0] \[Or]
      MemberQ[
       Table[sequence[[ListOfSequences[[i, 2]]]], {i, 1,
```

```
              Length[ListOfSequences]}], -1]) \[And] (MemberQ[
             Last /@ ListOfSequences, 0] \[Or]
            MemberQ[
             Table[sequence[[ListOfSequences[[i, 3]]]], {i, 1,
               Length[ListOfSequences]}], -1]), Degen = False(*...b/
        c it was a nondegenerate triod*), Degen = True];
       QuittingTime = True]]]]);

PartitionPoints[sequence_, period_] := (
   FindT1[sequence];
   ListOfItins =
    Table[Itinerary[i, sequence, period], {i, 1, Length[sequence]}];
   T1Branch = {}; a = 1; b = 2;
   While[a < Length[T1],
    While[b <= Length[T1],
     DegenTest[0, T1[[a]], T1[[b]], sequence, period];
     If[Degen == False \[And]
       itinofbpt != {Drop[
          sequence, (Length[sequence] - Length[itinofbpt[[1]]])],
         period},
      AppendTo[
       T1Branch, {1, Take[ListOfSequences, Length[itinofbpt[[1]]]],
        itinofbpt}]; b++, b++]]; a++; b = a + 1];
   a = 1; b = 2;
   While[a < Length[T1Branch],
    While[b <= Length[T1Branch],
     If[T1Branch[[a, 3]] == T1Branch[[b, 3]],
      T1Branch = Drop[T1Branch, {b}], b++]]; a++; b = a + 1];
   a = 1; While[a <= Length[T1Branch],
    If[MemberQ[ListOfItins, T1Branch[[a, 3]]],
     T1Branch = Drop[T1Branch, {a}], a++]];
   T1 = T1 \[Union] T1Branch;
   T0Branch = {}; a = 1; b = 2;
   While[a < Length[T0],
    While[b <= Length[T0],
     DegenTest[0, T0[[a]], T0[[b]], sequence, period];
     If[Degen == False \[And]
       itinofbpt != {Drop[
          sequence, (Length[sequence] - Length[itinofbpt[[1]]])],
         period},
      AppendTo[
       T0Branch, {1, Take[ListOfSequences, Length[itinofbpt[[1]]]],
```

```
        itinofbpt}]; b++, b++]]; a++; b = a + 1];
   a = 1; b = 2;
   While[a < Length[TOBranch],
    While[b <= Length[TOBranch],
     If[TOBranch[[a, 3]] == TOBranch[[b, 3]],
      TOBranch = Drop[TOBranch, {b}], b++]]; a++; b = a + 1];
   a = 1; While[a <= Length[TOBranch],
    If[MemberQ[ListOfItins, TOBranch[[a, 3]]],
     TOBranch = Drop[TOBranch, {a}], a++]];
   TO = TO \[Union] TOBranch;);

incrementelt[x_] :=
  If[IntegerQ[x],
   ModOut2[ModOut[x + 1, seqlength, per],
    seq], {ModOut2[ModOut[x[[1]] + 1, Length[x[[2]] ], x[[3, 2]]],
     seq], x[[2]], x[[3]]}];

location[x_] := If[IntegerQ[x], seq[[x]], x[[3, 1, x[[1]]]] ];

ChanceAtAdjacency[input1_, input2_, input3_, sequence_, period_] := (
   seq = sequence; seqlength = Length[seq]; per = period;
   in1 = ModOut2[ModOut[input1, seqlength, per], seq];
   in2 = ModOut2[ModOut[input2, seqlength, per], seq];
   in3 = ModOut2[ModOut[input3, seqlength, per], seq];
   QuittingTime = False;
   ListOfSequences = {Function[x, ModOut[x, seqlength, per]] /@ {in1,
       in2, in3}};
   adjacent = True;
   While[QuittingTime == False,
    If[AreTheseDifferent[in1, in2, in3, seqlength, per] ==
       False \[Or]
      Length[Union[location /@ {in1, in2, in3}  ]] ===
       3 \[Or] (MemberQ[location /@ {in1, in2, in3}, -1] \[And]
        MemberQ[location /@ {in1, in2, in3}, List]),
     (*AppendTo[ListOfSequences,incrementelt/@{in1,in2,
     in3}];*)(*Print["Degenerate"];*)
     If[Last[ListOfSequences][[3]] === 0, adjacent = False];
     QuittingTime = True,
     If[MemberQ[location /@ {in1, in2, in3}, -1] \[Or]
       MemberQ[location /@ {in1, in2, in3}, List] \[Or]
       Length[Union[location /@ {in1, in2, in3}   ]] == 1,
      {in1, in2, in3} = incrementelt /@ {in1, in2, in3},
```

```
      If[location[ in1] == location[in2], in3 = 0,
       If[location[in1] == location[in3], in2 = 0, in1 = 0]]];
     If[MemberQ[ListOfSequences, {in1, in2, in3}] == False,
      AppendTo[ListOfSequences, {in1, in2, in3}],
      AppendTo[ListOfSequences, {in1, in2, in3}];(*Print["periodic"];*)
            If[(MemberQ[First /@ ListOfSequences, 0] \[Or]
          MemberQ[Table[
            If[IntegerQ[ListOfSequences[[i, 1]]],
             sequence[[ListOfSequences[[i, 1]]]], 1], {i, 1,
             Length[ListOfSequences]}], -1]) \[And] (MemberQ[
           ListOfSequences[[1 ;; Length[ListOfSequences], 2]],
           0] \[Or]
          MemberQ[Table[
            If[IntegerQ[ListOfSequences[[i, 2]]],
             sequence[[ListOfSequences[[i, 2]]]], 1], {i, 1,
             Length[ListOfSequences]}], -1]) \[And] (MemberQ[
           Last /@ ListOfSequences, 0] \[Or]
          MemberQ[Table[
            If[IntegerQ[ListOfSequences[[i, 3]]],
             sequence[[ListOfSequences[[i, 3]]]], 1], {i, 1,
             Length[ListOfSequences]}], -1]), adjacent = False(*;
       Print["it's a nondegenerate triod, so adjacent is false"]*),
       If[(MemberQ[First /@ ListOfSequences, 0] \[Or]
           MemberQ[
            Table[If[IntegerQ[ListOfSequences[[i, 1]]],
              sequence[[ListOfSequences[[i, 1]]]], 1], {i, 1,
              Length[ListOfSequences]}], -1]) \[And] (MemberQ[
            ListOfSequences[[1 ;; Length[ListOfSequences], 2]],
            0] \[Or]
           MemberQ[
            Table[If[IntegerQ[ListOfSequences[[i, 2]]],
              sequence[[ListOfSequences[[i, 2]]]], 1], {i, 1,
              Length[ListOfSequences]}], -1]), adjacent = False(*;
        Print["the last term is never chopped, so it's between the \
first 2"]*), adjacent = True(*;Print[
        "it's degenerate, but the third vertex is not between the \
first two. the first two have a possibility of being adjacent"]*) ]];
      QuittingTime = True]]];
   adjacent);
(*RETURNS "False" IF THE LAST VERTEX SCREWS UP ADJACENCY OF THE FIRST \
TWO.*)
```

```
AreTheseAdjacent[test1_, test2_, freevertices_, sequence_,
   period_] := (
   a = 1; freevert = Complement[freevertices, {test1, test2}];
   seq = sequence; per = period;
   adjacent = True;
   While[a <= Length[freevert],
    If[ChanceAtAdjacency[test1, test2, freevert[[a]], sequence,
      period], a++, a = Length[freevert] + 1]]; adjacent);

DrawMeATree[sequence_, period_] := (
  itin = sequence;
  perd = period;
  PartitionPoints[itin, perd];
  Unplaced = T1;
  Unchecked = {0};
  HubbardTree = {};
  While[Unplaced != {},
   test = First[Unchecked];
   filler = 1;
   nonewmatches = True;
   While[filler <= Length[Unplaced],
    If[AreTheseAdjacent[test, Unplaced[[filler]], T1, itin, perd],
     nonewmatches = False;
     If[IntegerQ[Unplaced[[filler]]] \[And] IntegerQ[test],
      AppendTo[HubbardTree, test -> Unplaced[[filler]]],
      If[IntegerQ[test],
       AppendTo[HubbardTree, test -> Unplaced[[filler]][[2, 1]] ],
       If[IntegerQ[Unplaced[[filler]]],
        AppendTo[HubbardTree, test[[2, 1]] -> Unplaced[[filler]]],
        AppendTo[HubbardTree,
         test[[2, 1]] -> Unplaced[[filler]][[2, 1]]]]]];
     AppendTo[Unchecked, Unplaced[[filler]]];
     Unplaced = Drop[Unplaced, {filler}],
     filler++]];
   If[IntegerQ[test] == False \[And] nonewmatches == True,
    HubbardTree = DeleteCases[HubbardTree, (_ -> test[[2, 1]])]];
   Unchecked = Drop[Unchecked, 1]];
  Unplaced = T0;
  Unchecked = {0};
  While[Unplaced != {},
   test = First[Unchecked];
   filler = 1;
```

```
   nonewmatches = True;
   While[filler <= Length[Unplaced],
    If[AreTheseAdjacent[test, Unplaced[[filler]], T0, itin, perd],
     nonewmatches = False;
     If[IntegerQ[Unplaced[[filler]]] \[And] IntegerQ[test],
      AppendTo[HubbardTree, test -> Unplaced[[filler]]],
      If[IntegerQ[test],
       AppendTo[HubbardTree, test -> Unplaced[[filler]][[2, 1]] ],
       If[IntegerQ[Unplaced[[filler]]],
        AppendTo[HubbardTree, test[[2, 1]] -> Unplaced[[filler]]],
        AppendTo[HubbardTree,
         test[[2, 1]] -> Unplaced[[filler]][[2, 1]]]]]];
     AppendTo[Unchecked, Unplaced[[filler]]];
     Unplaced = Drop[Unplaced, {filler}],
     filler++]];
   If[IntegerQ[test] == False \[And] nonewmatches == True,
    HubbardTree = DeleteCases[HubbardTree, (_ -> test[[2, 1]])]];
   Unchecked = Drop[Unchecked, 1]];
  GraphPlot[HubbardTree, VertexLabeling -> True,
   Method -> SpringElectricalEmbedding])

(*****INSTRUCTIONS AND EXAMPLES BELOW*****)

(*Run DoubleCheck on the sequence to confirm whether or not the \
kneading sequence is in the right format and/or that it is an \
admissable sequence. Give itinerary in 1s, 0s, and -1s [where -1 \
represents *], followed by the period/preperiod of the sequence. \
DoubleCheck will tell you to stop if the sequence is inadmissible for \
a Hubbard tree, or will make an attempt at fixing the period on the \
given sequence to make it admissible.*)

DoubleCheck[{1, 0, 1, 0, 1, 0}, 2]
  (*Returns "Periodic! Stop!" This sequence is periodic, which \
implies * (or here, -1) should be on the periodic orbit. Since the \
sequence is not expressed in an appropriate format, it is \
inadmissible.*)

DoubleCheck[{0, 1, 1, 1, 0, 1}, 3]
(*Returns "Sequence starts with 0! Stop!" Per our naming \
scheme for T_ 0 and T_ 1, the first point after the critical point \
should fall in T_ 1 and thus should have first digit 1. Thus, the \
sequence is inadmissible.*)
```

```
DoubleCheck[{1, -1}, 34983]
(*Returns "{{1,-1},2}". Doublecheck \
simplifies sequences and their periods where possible.*)

DoubleCheck[{1, 1, 0, 1, 0, 1, 0, 1, 0, 1, 0, 1, 0}, 2]
(*Returns "{{1,1,0},2}". Again, DoubleCheck simplifies \
sequences and their periods where possible.*)

DrawMeATree[{1,1,0},2]
(*Once you run DoubleCheck, DrawMeATree takes similar input--the \
itinerary followed by it's period or preperiod. The above command \
yields following graphic.*)
```

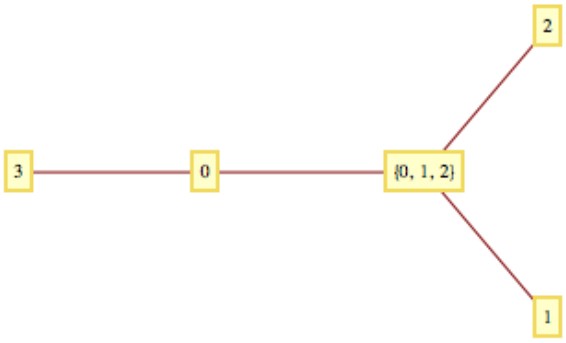

Figure A.1: The resulting output of DrawMeATree[{1,1,0},2].

Appendix B

Supporting claims for Subsection 3.2.2

The following require application of Bruin and Schleicher's degenerate triod test. Note that here, any coordinate labeled c_k refers to a point on the Hubbard tree for $f_{\frac{1}{4(2^n-1)}}$, and any coordinate labeled d_k refers to a point on the Hubbard tree for $f_{-\frac{1}{8(2^n-1)}}$, as defined in Section 3.2.2. These trees are determined in Section 3.2.2 to have a structure as given in Figure B.1. We will assume for the following lemmas that we work in the $n \geq 2$ case as proposed for the main theorem of Section 3.2.2.

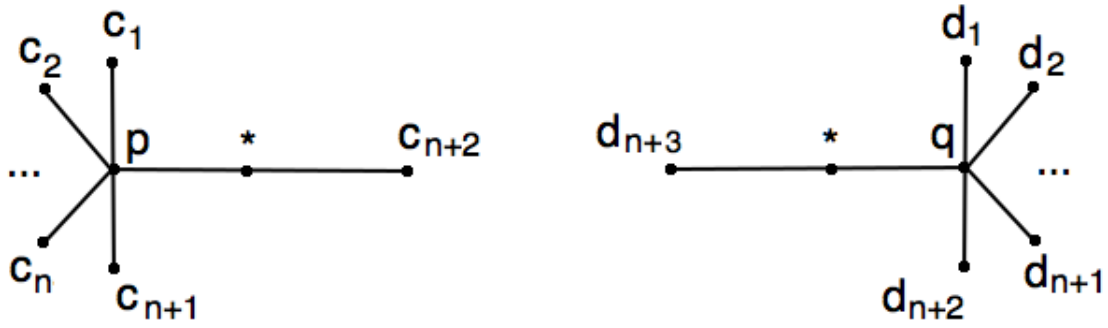

Figure B.1: The embedded Hubbard trees $T_{\frac{1}{4(2^n-1)}}$ (left) and $T_{-\frac{1}{8(2^n-1)}}$ (right).

Lemma B.1. *The non-postcritical preimage of d_2 is not contained in $T_{-\frac{1}{8(2^n-1)}}$.*

Proof. Per Figure B.1, we have that d_2 has itinerary $\underbrace{11\overline{1...10}}_{\text{n+2 digits}}$, and d_1 has itinerary $\underbrace{111\overline{1...10}}_{\text{n+3 digits}}$. Thus, the non-postcritical preimage of d_2 must have itinerary $\underbrace{011\overline{1...10}}_{\text{n+3 digits}}$. We will call this point d_1^*.

Since d_1^* has an itinerary starting with 0, it is contained in T_0'. We will test to see whether the critical point d_0, d_1^*, and d_{n+3} form a degenerate triod. (Since T_0' contains only degenerate triods, if we obtain a nondegenerate triod, d_1^* is not on the tree.)

$[d_0, d_1^*, d_{n+3}]$ (Located respectively in $\{\star'\}, T_0', T_0'$. We may iterate forward.)

$[d_1, d_2, d_4]$ (Located respectively in T_1', T_1', T_1'.)

Since $n \geq 2$, Figure B.1 shows that this triod is a nondegenerate triod in T_1'. Since we have mapped forward to a nondegenerate triod, $[d_0, d_1^*, d_{n+3}]$ must be nondegenerate. Thus, d_1^* is not on the Hubbard tree $T_{-\frac{1}{8(2^n-1)}}$. □

The following proofs follow an essentially similar structure in showing that the points in question form a nondegenerate triod with the critical point and postcritical point of T_0 or T_0'. Since T_0 and T_0' are degenerate subcomponents of $T_{\frac{1}{4(2^n-1)}}$ and $T_{-\frac{1}{8(2^n-1)}}$ respectively, this implies that the point in question is off-tree.

Lemma B.2. *The point c_{-1}^* with itinerary $0 \star \underbrace{11\overline{1...10}}_{n+2 \text{ digits}}$ on the Julia set of $f_{\frac{1}{4(2^n-1)}}$ is not contained in $T_{\frac{1}{4(2^n-1)}}$.*

Proof. Since c_{-1}^* has an itinerary starting with 0, it is contained in T_0. We will test to see whether c_{-1}^*, the critical point c_0, and c_{n+2} form a degenerate triod.

$[c_{-1}^*, c_0, c_{n+2}]$ (Located respectively in $T_0, \{\star\}, T_0$. We may iterate forward.)

$[c_0, c_1, c_3]$ (Located respectively in $\{\star\}, T_1, T_1$.

Since $n \geq 2$, Figure B.1 shows that this triod is a nondegenerate triod in T_1. Since we have mapped forward to a nondegenerate triod, the original triod must have been nondegenerate. Thus, c_{-1}^* is not on the Hubbard tree $T_{\frac{1}{4(2^n-1)}}$.

□

Lemma B.3. *The points $\{d_{-k-1}^*\}_{k=0}^{n-2}$ with itinerary $0 \underbrace{1...1}_{k \text{ digits}} \star \underbrace{111\overline{1...10}}_{n+3 \text{ digits}}$ on the Julia set of $f_{-\frac{1}{8(2^n-1)}}$ are not contained in $T_{-\frac{1}{8(2^n-1)}}$.*

Proof. Let $k \in \{0, ..., n-2\}$. Since d_{-k-1}^* has an itinerary starting with 0, it is contained in T_0'. We will test to see whether d_{-k-1}^*, the critical point d_0, and d_{n+3} form a degenerate triod.

$[d_{-k-1}^*, d_0, d_{n+3}]$ (Located respectively in $T_0', \{\star'\}, T_0'$. We may iterate forward.)

$[d_{-k}, d_1, d_4]$ (Located respectively in T_1', T_1', T_1'. We may iterate forward.)

...

$[d_{-1}, d_k, d_{k+3}]$ (Located respectively in T_1', T_1', T_1'. We may iterate forward.)

$[d_0, d_{k+1}, d_{k+4}]$ (Located respectively in $\{\star'\}, T_1', T_1'$.)

Since $k \in \{0, ..., n-2\}$, Figure B.1 shows that this triod is a nondegenerate triod in T_1'. Since we have mapped forward to a nondegenerate triod, the original triod must have been nondegenerate. Thus, d_{-k-1}^* is not on the Hubbard tree $T_{-\frac{1}{8(2^n-1)}}$. □

Lemma B.4. *The point c_{-n-1}^* with itinerary $0 \underbrace{1...1}_{n \text{ digits}} \star \underbrace{11\overline{1...10}}_{n+2 \text{ digits}}$ on the Julia set of $f_{\frac{1}{4(2^n-1)}}$ is not contained in $T_{\frac{1}{4(2^n-1)}}$.*

Proof. Since c^*_{-n-1} has an itinerary starting with 0, it is contained in T_0. We will test to see whether c^*_{-1}, the critical point c_0, and c_{n+2} form a degenerate triod.

$[c^*_{-n-1}, c_0, c_{n+2}]$ (Located respectively in $T_0, \{\star\}, T_0$. We may iterate forward.)

$[c_{-n}, c_1, c_3]$ (Located respectively in T_1, T_1, T_1. We may iterate forward.)

...

$[c_{-2}, c_{n-1}, c_{n+1}]$ (Located respectively in T_1, T_1, T_1. We may iterate forward.)

$[c_{-1}, c_n, c_{n+2}]$ (Located respectively in T_1, T_1, T_0. We must chop at the third coordinate.)

$[c_{-1}, c_n, c_0]$ (Located respectively in $T_1, T_1, \{\star\}$. We may iterate forward.)

$[c_0, c_{n+1}, c_1]$ (Located respectively in $\{\star\}, T_1, T_1$.)

Figure B.1 shows that this triod is nondegenerate in T_1. Since we have mapped forward to a nondegenerate triod, the original triod must have been nondegenerate. Thus, c^*_{-n-1} is not on the Hubbard tree $T_{\frac{1}{4(2^n-1)}}$.

□

Lemma B.5. *The point d^*_{-n-1} with itinerary $0\ \underbrace{1...1}_{n\ digits}\ \star\ \underbrace{111\overline{1...10}}_{n+3\ digits}$ on the Julia set of $f_{-\frac{1}{8(2^n-1)}}$ is not contained in $T_{-\frac{1}{8(2^n-1)}}$.*

Proof. Since d^*_{-n-1} has an itinerary starting with 0, it is contained in T'_0. We will test to see whether d^*_{-n-1}, the critical point d_0, and d_{n+3} form a degenerate triod.

$[d^*_{-n-1}, d_0, d_{n+3}]$ (Located respectively in $T'_0, \{\star'\}, T'_0$. We may iterate forward.)

$[d_{-n}, d_1, d_4]$ (Located respectively in T'_1, T'_1, T'_1. We may iterate forward.)

...

$[d_{-2}, d_{n-1}, d_{n+2}]$ (Located respectively in T'_1, T'_1, T'_1. We may iterate forward.)

$[d_{-1}, d_n, d_{n+3}]$ (Located respectively in T'_1, T'_1, T'_0. We must chop at the third coordinate.)

$[d_{-1}, d_n, d_0]$ (Located respectively in $T'_1, T'_1, \{\star'\}$. We may iterate forward.)

$[d_0, d_{n+1}, d_1]$ (Located respectively in $\{\star'\}, T'_1, T'_1$.)

Figure B.1 shows that this triod is a nondegenerate triod in T'_1. Since we have mapped forward to a nondegenerate triod, the original triod must have been nondegenerate. Thus, d^*_{-n-1} is not on the Hubbard tree $T_{-\frac{1}{8(2^n-1)}}$. □

Lemma B.6. *The point d^*_{-n-2} with itinerary $0\ \underbrace{1...1}_{n+1\ digits}\ \star\ \underbrace{111\overline{1...10}}_{n+3\ digits}$ on the Julia set of $f_{-\frac{1}{8(2^n-1)}}$ is not contained in $T_{-\frac{1}{8(2^n-1)}}$. Further, The point c^*_{-n-3} with itinerary $0\ \underbrace{1...1}_{n+2\ digits}\ \star\ \underbrace{11\overline{1...10}}_{n+2\ digits}$ on the Julia set of $T_{\frac{1}{4(2^n-1)}}$ is not contained in $T_{\frac{1}{4(2^n-1)}}$.*

Proof. First, we'll examine d^*_{-n-2} . Since d^*_{-n-2} has an itinerary starting with 0, it is contained in T'_0. We will test to see whether d^*_{-n-2} the critical point d_0, and d_{n+3} form a degenerate triod.

$[d^*_{-n-2}, d_0, d_{n+3}]$ (Located respectively in $T'_0, \{\star'\}, T'_0$. We may iterate forward.)

$[d_{-n-1}, d_1, d_4]$ (Located respectively in T'_1, T'_1, T'_1. We may iterate forward.)

...

$[d_{-3}, d_{n-1}, d_{n+2}]$ (Located respectively in T_1', T_1', T_1'. We may iterate forward.)
$[d_{-2}, d_n, d_{n+3}]$ (Located respectively in T_1', T_1', T_0'. We must chop at the third coordinate.)
$[d_{-2}, d_n, d_0]$ (Located respectively in $T_1', T_1', \{\star'\}$. We may iterate forward.)
$[d_{-1}, d_{n+1}, d_1]$ (Located respectively in T_1', T_1', T_1'. We may iterate forward.)
$[d_0, d_{n+2}, d_2]$ (Located respectively in $\{\star'\}, T_1', T_1'$.)

Figure B.1 shows that this triod is a nondegenerate triod in T_1'. Since we have mapped forward to a nondegenerate triod, the original triod must have been nondegenerate. Thus, d^*_{-n-2} is not on the Hubbard tree $T_{-\frac{1}{8(2^n-1)}}$.

Now, we may examine c^*_{-n-3}. Since c^*_{-n-3} has an itinerary starting with 0, it is contained in T_0. We will test to see whether c^*_{-n-3}, the critical point c_0, and c_{n+2} form a degenerate triod.

$[c^*_{-n-3}, c_0, c_{n+2}]$ (Located respectively in $T_0, \{\star\}, T_0$. We may iterate forward.)
$[c_{-n-2}, c_1, c_3]$ (Located respectively in T_1, T_1, T_1. We may iterate forward.)
...
$[c_{-4}, c_{n-1}, c_{n+1}]$ (Located respectively in T_1, T_1, T_1. We may iterate forward.)
$[c_{-3}, c_n, c_{n+2}]$ (Located respectively in T_1, T_1, T_0. We must chop at the third coordinate.)
$[c_{-3}, c_n, c_0]$ (Located respectively in $T_1, T_1, \{\star\}$. We may iterate forward.)
$[c_{-2}, c_{n+1}, c_1]$ (Located respectively in T_1, T_1, T_1. We may iterate forward.)
$[c_{-1}, c_{n+2}, c_2]$ (Located respectively in T_1, T_0, T_1. We must chop at the second coordinate.)
$[c_{-1}, c_0, c_2]$ (Located respectively in $T_1, \{\star\}, T_1$. We may iterate forward.)
$[c_0, c_1, c_3]$ (Located respectively in $\{\star\}, T_1, T_1$.)

Figure B.1 shows that this triod is nondegenerate in T_1. Since we have mapped forward to a nondegenerate triod, the original triod must have been nondegenerate. Thus, c^*_{-n-3} is not on the Hubbard tree $T_{\frac{1}{4(2^n-1)}}$.

□

Bibliography

[1] M. Bonk and D. Meyer, *Expanding Thurston Maps* preprint, 2010.

[2] H. Bruin and D. Schleicher, *Symbolic Dynamics of Quadratic Polynomials*, Institut Mittag-Leffler/The Royal Swedish Academy of Sciences, Report No. 7, 2001/2002.

[3] J. W. Cannon, W. J. Floyd, R. Kenyon, and W. R. Parry, *Constructing Rational Maps from Subdivision Rules*, Conformal Geometry and Dynamics, 7 (2003), 76-102.

[4] J. W. Cannon, W. J. Floyd, and W. R. Parry, *Finite Subdivision Rules*, Conformal Geometry and Dynamics, 5 (2001), 153-196 (electronic).

[5] J. W. Cannon, W. J. Floyd, and W. R. Parry, *Constructing Subdivision Rules from Rational Maps*, Conformal Geometry and Dynamics, 11 (2007), 128-136.

[6] A. Chéritat, *Accouplements de Polynomes*, videos, available from http://www.math.univ-toulouse.fr/ cheritat/MatMovies/

[7] A. Douady and J. H. Hubbard. *Exploring the Mandelbrot set. The Orsay notes.* available from http://www. math.cornell.edu/?hubbard/OrsayEnglish.pdf.

[8] Theodore Gamelin, *Complex Analysis*, Springer Science + Business Media, LLC, 2001.

[9] A. Hatcher, *Algebraic Topology*, Cambridge University Press, 2002.

[10] T. Lei, *Matings of Quadratic Polynomials*, Ergodic Theory and Dynamical Systems, 12 (1992), 589-620.

[11] W. Jung, Mandel 5.4, software, available from http://www.mndynamics.com

[12] A. Kameyama, *On Julia sets of postcritically finite branched coverings Part II—S^1-parametrization of Julia sets*, J. Math. Soc. Japan, 55, No. 2 (2003), 455-468.

[13] D. Meyer, *Expanding Thurston Maps as Quotients* 2009 preprint available from http://arxiv.org.

[14] D. Meyer, *Invariant Peano Curves of Expanding Thurston Maps*, 2009 preprint available from http://arxiv.org

[15] D. Meyer, *Unmating of rational maps, sufficient criteria and examples*, 2011 preprint available from http://arxiv.org

[16] J. Milnor, *Pasting Together Julia Sets: A Worked Out Example of Mating*, Experimental Mathematics, 13:1 (2004), 55-92 (electronic).

[17] J. Milnor, *Dynamics in One Complex Variable*, Annals of Mathematics Studies, Princeton University Press, 2006.

[18] R. Moore. *Concerning Upper Semi-continuous Collections of Continua*, Transactions of the American Mathematical Society, 27 (1925), 416?428.

[19] S. Nadler. *Continuum theory: an introduction*, Taylor & Francis, Inc., 2000.

[20] M. Rees. *A Partial Description of the Parameter Space of Rational Maps of Degree Two: Part 1*, Acta Math. 168 (1992), 11-87.

[21] M. Shishikura. *On a Theorem of M. Rees for Matings of Polynomials.* The Mandelbrot Set, Theme and Variations, London Mathematical Society Lecture Notes 274, edited by Tan Lei, pp. 289-305. Cambridge: Cambridge University Press, 2000.